2009

STRUCTURAL INTERACTIONS BETWEEN THE **A**3**B**1 INTEGRIN AND MMP-2: A POTENTIAL FUNCTIONAL ROLE IN CELL ADHESION

James Bowman
Virginia Commonwealth University

School of Medicine
Virginia Commonwealth University

This is to certify that the dissertation prepared by James Russell Bowman, III entitled STRUCTURAL INTERACTIONS BETWEEN THE A3B1 INTEGRIN AND MMP-2: A POTENTIAL FUNCTIONAL ROLE IN CELL ADHESION has been approved by his or her committee as satisfactory completion of the dissertation requirement for the degree of Doctor of Philosophy

David G. Simpson, Ph.D., School of Medicine

John W. Bigbee, Ph.D., School of Medicine

Robert F. Diegelmann, Ph.D School of Medicine

Helen Fillmore, Ph.D., School of Medicine

Babette Fuss, Ph.D., School of Medicine

John T. Povlishock, Ph.D., Department Chair, Department of Anatomy and Neurobiology

Jerome Strauss, M.D. Ph.D., Dean, School of Medicine

Dr. F. Douglas Boudinot, Dean of the Graduate School

July 16, 2009

STRUCTURAL INTERACTIONS BETWEEN THE A3B1 INTEGRIN AND MMP-2: A POTENTIAL FUNCTIONAL ROLE IN CELL ADHESION

A dissertation submitted in partial fulfillment of the requirements for the degree of Doctor of Philosophy at Virginia Commonwealth University.

by

JAMES RUSSELL BOWMAN, III
B.S., Hampden-Sydney College, 1998
M.S., Virginia Commonwealth University,

DIRECTOR: DAVID G. SIMPSON, PH.D.

Associate Professor, Department of Anatomy and Neurobiology

Virginia Commonwealth University
Richmond, Virginia
July, 2009

Acknowledgements

What we've got here is failure to communicate,
Some men you just can't reach,
So you get what we have here last week,
Which is the way he wants it,
Well, he gets it,
And I don't like it anymore than you men.
Cool Hand Luke, 1967

With that said, I want to thank my committee members, John Bigbee, Bob Diegelmann, Helen Fillmore, and Babette Fuss for their utmost patience and understanding as the years we have spent together have been, at times, arduous. Your consistent motivation and direction have shaped this project and my abilities. David, the words "thank you" fall short of describing the mentorship and guidance that you provided as "thank you" does not encompass the friendship or represent the selflessness by which have been there for me for nearly a decade.

Lastly, I thank my family for their never ending love and support.

Table of Contents

List of Tables

Page

List of Figures

Page

Abstract

STRUCTURAL INTERACTIONS BETWEEN THE $\alpha_3\beta_1$ INTEGRIN AND MMP-2: A POTENTIAL FUNCTIONAL ROLE IN CELL ADHESION.

By James Russell Bowman, III MS

A Dissertation submitted in partial fulfillment of the requirements for the degree of Doctor of Philosophy at Virginia Commonwealth University.

Virginia Commonwealth University, 2009

Major Director: David G Simpson, PhD
Assistant Professor, Anatomy and Neurobiology

During cardiac development and in cardiac disease changes in hemodynamic load initiate events leading to remodeling of the ECM. This study addresses the hypothesis that *interactions between Integrins and Metalloprotienases function to modulate cell adhesion in the cultured cardiac fibroblast*. The fibroblast is positioned to detect and respond to changes in the mechanical load on the heart. Functionally the cardiac fibroblast is the primary cell type responsible for the production, maintenance, and remodeling of the

cardiac interstitium. Matrix Metalloproteinases, specifically the Gelatinases, are expressed in concert during development and in disease with changes in the hemodynamic loading of the heart.

Our studies have identified by a complex on the surface of the cardiac fibroblast composed of the a3b1 integrin, MMP-2, and TIMP-2. Putatively, this complex is involved in the maturation of adhesions. Inhibition of MMP-2 was associated with a decrease in the strength of adhesion of cell plated on collagen and fibronectin. Confocal imaging and analysis indicate that a predominate interaction occurs between MMP-2 and the a3 integrin chain.

Taken together biochemical, functional, and microscopic data have identified a complex on the surface of the cardiac fibroblast that represents elements of mechanotransduction and matrix metabolism in a single site that functions in the maturation of adhesion

CHAPTER I

Introduction and Overview of Project

Cell adhesion is the process by which cells become adherent to various surfaces and is a necessary requirement for the existence multicellular organisms. In the most general sense, cell adhesion may be cellular or non-cellular in nature. The adhesion of cells to one another is commonly referred to as intercellular adhesion or cell-to-cell adhesion. Cell adhesion to non-cellular constituents present in the extracellular environment is denoted as cell-matrix adhesion. Adhesion events may be non-specific or specific in nature. In non-specific adhesion, cells can undergo attachment to one another or other surfaces as a consequence of physical entanglements or electrostatic interactions. These non-specific events often represent a preamble to the formation of a specific adhesion site. Specific adhesion processes are mediated through the interactions of cell surface receptors that recognize specific binding sites on adjacent cells and/or in the surrounding extracellular environment. While all adhesion events may induce a cascade of intracellular responses, the binding of cells to a specific site(s) provides an increased measure of control over intercellular signals and downstream processes.

The modulation of adhesion is central to the fundamental processes of cell migration during development, normal neonatal growth, the maintenance of normal homeostatic physiological states and at the onset of disease. The loss of normal cell-to-cell

or cell-matrix interactions during the critical early stages of development can lead to a nearly endless variety of congenital defects; many of these defects are lethal. For example, changes in adhesion underlie stem cell differentiation and the formation of the blastocyst [1], embryonic cell sorting and migration [2], tissue patterning [3] and the generation of organ and tissue architecture [4].

The pervasive role of cell adhesion is evident during many specific stages of development. Blocking the cell surface receptors that mediate the migration of epithelial cells in the apical ectodermal ridge disrupts the evolution of normal limb architecture [5]. The loss of normal neuronal cell-matrix interactions is believed to cause the X-linked, Kallmann syndrome, a defect characterized by hypogonadotrophic hypogonadism and anosmia [6]. Homozygous knockouts of the cell-matrix receptor α_4 integrin, prevents placentation and is associated with defects in the epicardium and coronary vessels that result in cardiac hemorrhage and embryonic death [7]. Cardiac looping and the subsequent stages of ventricular wall morphogenesis are mediated by homotypic and heterotypic cell-to-cell interactions driven by members of the Connexon and Cadherin families of receptors [8]. Signals generated through members of the integrin and cadherin families are both necessary for the apposition and closure of palatal shelves [9]. Blocking signals normally passed through E-Cadherin during early embryonic development results in dysgenesis and embryonic death in the Zebrafish [10]. This list of defects associated with the disruption of normal cell-to-matrix and cell-to-cell adhesion is by no means comprehensive.

In adult life changes in cell adhesion continue to play a persistent and central role in such diverse processes as clot formation during hemostasis [11], the modulation of

immune response [12], cell migration and targeting during wound healing, and cell motility during routine remodeling throughout the tissue compartments and organ systems [13].

Cell adhesion is a dynamic process. This dynamic aspect allows a cell to release from a specific site in response to various environmental conditions, undergo motility, and subsequently cease migration and establish stable long term, residency in a particular location. Non-specific and specific interactions may be disrupted by physical processes, electrostatic challenges, and or chemical insults. In addition to these general mechanisms of "control" (or perhaps lack there of), sites of specific cell-to-cell and cell-matrix adhesion are subject to more extensive regulation from the onset, by definition, this type of interaction is more "selective" in nature. At one level of control specific adhesion events are mediated by the structural characteristics of the receptor in question and the chemical identity, availability and tertiary structure of the target ligand. A cell may express any number of cell surface receptors; if, however, the target ligand is absent or otherwise masked there can be no specific adhesion event. At the other end of the spectrum, once specific adhesion has been established it may be lost in response to the global physiologically processes that underlie motile activity (*e.g.* de-adhesion) and/or though more subtle molecular events associated with the routine turnover of cell adhesion molecules.

The onset of specific cell adhesion is subject to regulation at several different sites. Beyond the notion that specific binding is regulated by receptor ligand interactions, specific adhesion can be subject to modulation by events initiated within the intracellular environment as well as through various external cofactors, including ions and/or other

peptides [14, 15, 16]. This study defines a potential role for proteases of the MMP family in the regulation of specific cell adhesion by the $\alpha_3\beta_1$ integrin to the ECM ligands, collagen and fibronectin. The present work developed from experiments designed to examine how adhesion to these ECM components and mechanical forces might regulate the expression of MMP-2 and MMP-9, extracellular proteases of the gelatinase family, in the cultured cardiac fibroblast [17, 18]. This preliminary work indicated that the expression of protease activity mediated by these enzymes in response to stretch was different when this cell type was plated onto collagen, laminin or fibronectin. Preliminary experimentation leading to the present document was conducted to extend these observations. These experiments were designed to use various molecular interventions to alter the relative number of specific integrins expressed by the cultured neonatal cardiac fibroblast. The aim of this approach was to determine if changes in MMP expression in response to stretch where more closely associated with the absolute number of integrins or the specific identity of the integrins present on the cell surface (*e.g.* more receptors = more binding sites = tighter adhesion = more response to strain: or, changes in receptor identity = changes in cellular response to stretch).

Technical and biological limitations limited interpretation of the data generated in these experiments; unfortunately, there was considerable noise in the experimental system ultimately used to test this hypothesis. However, in the course of these early experiments data was generated to suggest that MMPs may regulate integrin function to a greater extent than the opposite condition, notably, that integrins regulate MMP accumulation and activation in the cardiac fibroblast. The present study was developed as a consequence of

these observations. The overall objective of the present study is to test the hypothesis ***"that MMPs of the gelatinase family play an active role in modulating integrin mediated cell adhesion.*** To address this hypothesis four specific aims were developed:

1. Define the structural relationships that exist between specific integrin sub-types and members of the MMP family of gelatinases.
2. Optimize the binding conditions necessary to achieve maximal adhesion of neonatal rat cardiac fibroblasts to collagen, laminin and fibronectin using conventional adhesion assays.
3. Define the strength of adhesion that develops as the cells attach to different ECM substrates using centrifugal adhesion assays.
4. Define the functional relationships that link extracellular protease activity with the integrin mediated adhesion of cardiac fibroblasts to collagen, laminin and fibronectin.

CHAPTER II

Cell Adhesion Molecules

There is a broad spectrum of cell surface molecules that mediate cell adhesion. This discussion will focus on the cell adhesion molecules (CAMs) that mediate specific binding events. Principle members of the CAM family include, the Cadherins [19], the Immunoglobulin superfamily-like molecules (Igsf-CAM, I-CAM) [20], the Selectins [21], and the Integrins [22]. The CAMs can be further sub-divided into two main categories; those receptors that mediate intercellular (cell-to-cell) adhesion (ICAM) and those that mediate cell-ECM adhesion.

The Cadherins mediate calcium dependent cell-to-cell adhesion, most often through homotypic (cadherin-cadherin) interactions [23].This diverse class is composed of at least 80 different members that are differentially expressed during development and are present in a wide variety of different tissue types [24]. These ICAM molecules span the plasma membrane and typically exhibit an intracellular domain, a transmembrane domain and an extracellular domain. The intracellular domain can bind and signal though the catenin system [25, 26]. During development, signals propagated by the cadherins play a well documented, and prominent role in cell sorting during early embryogenesis [27] and in the formation of the extremities [28] and the digits [29] and in myogenesis [30]. In the central nervous system, N-Cadherin (neural cadherin) plays a role in growth cone mechanics and in the

interactions of neurites with glial cells and with glial cells interacting with each other [31]. In adult tissues, cadherins are prominently localized within the epithelial tissues [32]. These receptors are present in the adherens junctions of the keratinocytes. Adherens junctions form a nearly continuous band around the periphery of these cells and serve to anchor the lateral aspects of adjacent cells together. Within the intracellular space filaments of the actin-based cytoskeleton insert into the electron dense plaque that characterizes these junctions, providing a site for the distribution of mechanical forces across the cell population. Adhesion, at the molecular level, is mediated through homotypic bonds (cadherin-to-cadherin). Members of the cadherin family also are present within the desmosomes of the epithelium, these junctions, also called macula adherens junctions; appear as "spot-welds" between adjacent cells. Intermediate filaments insert into the cytoplasmic face of the desmosome.

Members of the Immunoglobulin superfamily-like CAM family comprise a second group of cell adhesion molecules. The transmembrane Ig-CAMs mediate cell-to-cell adhesion through homotypic and heterotypic interactions. These proteins are designated as part of the Immunoglobulin superfamily because they exhibit immunoglobulin like structural domain(s). Adhesion proteins of the Ig-CAM family have a wide tissue distribution. Representative of this Ig-CAM subfamily are Vascular Cell Adhesion Molecules (V-CAM), Intercellular Adhesion Molecules (I-CAM), and Neural Cell Adhesion Molecules (N-CAM) [33] and L1, a subset of the Ig-CAM family that functions in neuronal outgrowth, fasciculation and interneuronal adhesion [34]. Ig-like CAM heterotypic interactions often partner with a receptor of the integrin family of cell-matrix receptors.

For example, the heterotypic binding of VLA-4 ($\alpha_4\beta_1$ integrin) with VCAM-1 provides leukocytes with firm adhesion to the vascular wall in the process of diapedisis [35]. Heterotypic interactions between the Nectin class of Ig-like CAM and the cadherins also have been described [36].

Members of the Selectin family are concentrated in the endothelium and the leukocyte cohort of blood [37, 38]. These CAMs mediate adhesion to carbohydrate moieties through specific binding events; however, these cell-to-cell adhesions represent relatively low avidity (strength) contacts [39]. Selectins are type-1 transmembrane glycoproteins that display calcium dependant binding and, as the name implies, bind to selected polysaccharide residues. This group of CAMs is part of the C-type lectin family and subtypes are based on distribution and include; the L-(Leukocyte), the E-(Endothelial), and the P-(Platelet) selectins. Selectins function in the trafficking and accumulation of inflammatory cells in the vicinity of a wound [40]. In response to injury both selectins and selectin ligands are rapidly expressed, from intracellular granules, onto the surface of the endothelium. These molecules can then interact with the selectins and selectin ligands present on the surface of circulating leukocytes. Selectin-to-selectin interactions mediate the initial aspects of adhesion that allow leukocytes to roll along the luminal surface of blood vessels. This low affinity adhesion process, which is reversible, represents a preamble to the subsequent formation of more "mature", stable adhesions that are mediated by integrins.

Integrins comprise the last major family of CAMs. These receptors are widely expressed and are present in nearly all cell types. These transmembrane heterodimeric

glycoproteins bind to a broad spectrum of ECM components [41]. Integrin dependent events take place throughout life from the earliest stages of embryogenesis. The receptors of this family represent integral components of the cellular machinery that mediates motility [42] . Loss of integrin mediated adhesion frequently results in apoptosis or more specifically anikosis [43]. The binding properties of the Integrins are subject to considerable regulation from intrinsic and extrinsic factors, this study describes results suggesting that these proteins interact in a unique fashion of members of the MMP family of proteases. This interaction has potential consequences in the regulation of integrin biology during cardiac development and at the onset of disease in this organ. The biology of the integrin family will be considered in more detail in the subsequent chapters.

CHAPTER III

Integrin Biology

Integrin fine structure.

The functional integrin receptor is composed of an α and a β chain, the specific complement of subunits that are present within a given integrin receptor define its binding specificity. At least 18 α and 8 β subunits have been described and in all at least 26 different functional heterodimers have been identified. Splice variants of the β chain inflate the actual number of functional receptors to a small degree. Each transmembrane glycoprotein chain that makes up the integrin complex is expressed from a unique gene sequence; the subunits are linked in a non-covalent fashion with one another and arrive on the cell surface as an intact receptor [44].

The integrins can be grouped into a series of subcategories based on the identity of the β chain. For example, the β_1 family of integrins is composed of all the α chains that can combine with this subunit to form a functional receptor (α_1-α_{11}). The β_2 family combines with the αL, αM, αX, and the αD subunits. Integrin families based on the β_3, β_4, β_5, β_6, β_7, and β_8 chains have been described.

Each integrin chain displays an intracellular, a transmembrane and an extracellular domain. The intracellular domain, or cytoplasmic tail, of the prototypic β chain is composed of 20-50 amino acid residues, this domain represents a target for intracellular

regulatory factors and ultimately, as a docking site for cytoskeletal proteins and signal molecules. Integrin binding events are believed to be initiated by the interaction of Talin, a cytoskeletal associated protein, with the cytoplasmic tail of the β chain. This ***intracellular*** binding event, called integrin activation, promotes a conformational change in the receptor that leads to increased adhesion avidity for target substrates in the ***extracellular*** environment [45]. In cells of hematopoietic origin talin function can be replaced by kindlin-3 [46]. The cytoplasmic tail of the β chain also is a target for tyrosine phosphorylation. The addition of phosphates to this domain may be a component element of the signal transduction pathway that destabilizes the association of the integrin complex with the actin based cytoskeleton, thereby facilitating the onset of motility [47]. The α chain cytoplasmic domain is variable, but typically very limited in length. This domain participates in the interactions that ultimately generate the functional integrin complex [48].

The helical transmembrane domains of the α and β chains function to localize, and anchor, the receptor in the plasma membrane [49]. Interactions of these domains orchestrate the assembly of the non-covalently linked α and β heterodimer and participate in the formation of higher order interactions between other integrin complexes (clustering).

In the extracellular space the integrin chains extend from the surface of the cell through a series of domains that exhibit structural, regulatory, cation binding, or ECM binding activity. The extracellular domains of the β chain exhibit several epidermal growth factor-like (EGF) repeats, a plexin, a semphorin, and integrin (PSI) domain, a hybrid domain, and a terminal β-A domain [44]. The prototypical α integrin extends from the cell

surface and contains a "calf" domain, a "thigh" domain, a β propeller, and a variable α-A domain inserted in the β propeller. Integrin α chains can be further subclassified based on the presence of the A-α domain, this sequence helps to define ligand binding [50].

The structural/functional properties of the A-α domain are dependent upon the binding of metal ions to adjacent domains in the α chain. The $\alpha_v\beta_3$ integrin binds to fibronectin in an RGD dependent fashion. For this binding event to take place metal ions must be present in three adjacent domains; the MIDAS (Metal Ion Dependant Adhesion Site) domain, the adjacent MIDAS (ADMIDAS) domain, and in the neighboring LIMBS (Ligand associated metal binding site) domain of A-α sequence [51]. The occupation of these metal ion binding sites stabilizes the tertiary structure and architecture of the ligand binding pocket. Crystallographic analysis of the $\alpha_v\beta_3$ integrin demonstrates that ligand binding occurs within the groove that is present between the α and β chains, providing a structural correlate to explain how the complement of integrin subunits present in a given receptor can define binding specificity.

Integrin activation.

There is evidence that the functional integrin complex exists in 3 distinct structural states [52]. Each of these states, the folded closed state, the folded open state and the extended open state, exhibits unique binding properties against the target substrate. In the folded closed state, or non-activated state, the integrin resides on the cell surface in a somewhat folded conformation that exhibits low binding affinity. In this folded

conformation the calf and thigh of the α chain exist in a "knees" bent state and the PSI domain of the β chain is folded in a fashion thought to sequester the binding domains from ECM ligation [53]. During activation the entire integrin complex is believed to undergo a conformational change that is initiated by the binding of talin to the cytoplasmic tail of the β chain [45]. This binding event leads to the extension of the entire molecule; a transformation that is marked by a marked increase in the binding affinity of the receptor for the target ligand. The conformation that is intermediate to the folded state and the extended fully activated state is transitory in nature; however, it does appear to exhibit intermediate binding properties.

Integrin activation can occur through "outside-in" and "inside-out" mediated events. Outside-in activation occurs in response to cues, such as structural motifs, that exist in the surrounding ECM [54]. However, the final pathway to integrin activation ultimately involves the binding of talin (or the analog kindlin) to the intracellular domain of the β chain. Talin, itself, exists in at least 2 states, a masked, auto-inhibited and an unmasked, active state [55]. In the masked state talin exists in a cytoplasmic compartment and does not interact with the integrin. At unmasking, talin binds to the integrin and initiates the conformational change associated with activation. It is not known how the binding of talin to the cytoplasmic tail of the β chain might induce structural changes in the extracellular domain of the integrin.

Talin represents a pivotal regulator protein for integrin activation. This small peptide is directed to the plasma membrane by Rap1-GTP-interacting adaptor molecule, (RIAM) mediated linking of Rap 1, a ras GTPase that serves as a targeting sequence [56].

This complex places RIAM as an intermediary for the docking of Talin between the plasma membrane and integrins. Typically RIAM is distributed throughout the cytosol and is focused to the plasma membrane by Rap1. The physiological basis for the unmasking of talin remains unclear; however, this process can be driven by increased phosphatidylinositol 4,5-bisphosphate [55]. *In vitro,* the proteolytic processing of the extended talin molecule with the enzyme calpain II dissociates the head from the tail of talin, allowing it to bind to the β integrin chain. Phosphorylation also appears to regulate the stability of the association of the talin head domain with β chain and the overall stability of focal adhesions [57]. Beyond the effects on integrin activation, the tail section of talin serves as a mechanically sensitive site for the incremental accumulation of the actin binding protein vinculin [58].

Integrin binding properties.

As a family, Integrin binding activity can be unique towards a specific moiety in the ECM; however, different integrins may exhibit considerable overlap in binding specificity. Multiple integrins exhibit binding activity against the same ECM protein and a given ECM target may be recognized by more than one integrin subtype. In addition, selected integrin subtypes are highly promiscuous and may bind to a variety of different ECM substrates. Integrin binding to a target may be mediated by specific amino acid sequences or by the presentation of a defined tertiary structure in the target molecule. See table 1 for representative binding properties of specific integrins

Integrin chains and Classic Binding Partners

Table 1			
	Integrin β chain	**Integrin α chain**	**Classic binding partner**
	β_1 Family (VLA)	α_1, α_2	Collagen, laminin
		α_3	Collagen, laminin and fibronectin
		α_4	VCAM-1
		α_5	Fibronectin, RGD sequence
		α_6, α_7	Laminin
		α_8	RGD sequence
		α_9	Tenascin
		α_{10}, α_{11}	Collagen
	β_2 Family (LFA)	αL,αM,αX,αD	Leukocyte specific receptors
	β_3 Family	αII_b	RGD sequence, highly promiscuous
	β_4 Family	α_4	Plaque proteins and plectin
		α_6	Laminin
	β_7 Family	αE	Leukocyte specific receptor
		α_4	Lymphocyte trafficking, VCAM-1
	Other		
	β_1, β_3, β_5, β_6, β_8	α_V	RGD Sequence

This discussion will focus on the binding properties of the $\alpha_1\beta_1$, $\alpha_2\beta_1$, $\alpha_3\beta_1$, and the $\alpha_5\beta_1$. These receptors represent the principle integrins expressed in the neonatal rat myocardium [59]. The $\alpha_1\beta_1$ and $\alpha_2\beta_1$ integrins both bind to collagen and laminin. The $\alpha_3\beta_1$ is highly promiscuous and exhibits binding activity against collagen, laminin and fibronectin. The $\alpha_5\beta_1$ integrin is highly specific to fibronectin. These receptors of the β_1 family are expressed in a developmental pattern and the profile of integrins present in the adult rat heart undergoes a shift during ventricular wall hypertrophy [60]. The expression of the $\alpha_1\beta_1$ and the $\alpha_3\beta_1$ integrins are low in fetal life and increase with age, both are prominently expressed in neonatal life. The $\alpha_2\beta_1$ is not detectable by immunoprecipitation in fetal life and is expressed at relatively modest levels later in development. The $\alpha_5\beta_1$ is expressed at substantial levels throughout life. In sedentary adults and during the onset of pressure overload hypertrophy $\alpha_1\beta_1$ expression is depressed, $\alpha_3\beta_1$ expression is regulated in a nearly opposite fashion under these conditions.

The $\alpha_1\beta_1$ and $\alpha_2\beta_1$ integrin both exhibit binding activity against Type I collagen [61] and EHS laminin [62, 63]. However, these integrins recognize distinctly different binding sites within these ECM molecules [64]. The $\alpha_1\beta_1$ integrin exhibits a lower affinity to collagen than the $\alpha_2\beta_1$ integrin [65]. This integrin ($\alpha_1\beta_1$) binds to type I collagen in an RGD independent manner sites that is dependant upon the topography of the triple-helical conformation of the collagen molecule [66,67]. In contrast, $\alpha_2\beta_1$ integrin binds to a specific peptide sequence (GFOGER) that is present in the α_1(I) chain of type I collagen [68]. Laminin is comprised of an alpha, beta, and gamma chain arranged in a cruciform shape.

Proteolytic dissection of the laminin molecule indicates that $\alpha_1\beta_1$ and $\alpha_2\beta_1$ bind to different domains within this basement membrane protein [69]. Further, the binding of the $\alpha_2\beta_1$ integrin to laminin-1 is dependent on the extended open conformation and the activation state of the integrin [70].

The $\alpha_3\beta_1$ integrin exhibits binding properties that are described as promiscuous because it participates in the adhesion of cells to collagen, laminin, and fibronectin. The binding of the $\alpha_3\beta_1$ integrin to each of these ECM substrates exhibits varying sensitivity to cations and challenge with RGD antagonists [71]. Binding appears to be mediated by RGD dependent and RGD independent events. While this integrin is described as promiscuous in its binding properties with respect to collagen, laminin and fibronectin the $\alpha_3\beta_1$ integrin certainly does not exhibit pan ECM adhesion properties. Over expression of the $\alpha_3\beta_1$ integrin enhances cell adhesion to the RGD motif present in entactin but does enhance the RGD dependent adhesion of cells to fibronectin [72]. One possible explanation for the unique binding properties of this integrin, the $\alpha_3\beta_1$ molecule may not mediate the ***initial*** events of adhesion to ECM target substrates. Rather, this integrin may become secondarily localized to developing focal adhesion sites in association with other integrins [73]. Intracellular signals induced by this integrin complex play a role in regulating the expression of pericellular matrix constituents, a reasonably common theme in integrin biology [72].

The $\alpha_5\beta_1$ integrin is an example of an integrin that exhibits unique binding activity against a target ligand. This receptor mediates specific and high affinity binding to the glycoprotein fibronectin [74]; this binding event enhances fibronectin expression and the

assembly of this protein into fibers in the vicinity of the cell surface [75,76]. The specificity of the $\alpha_5\beta_1$ integrin for fibronectin is derived from a target RGD sequence as well as the conformation of this ECM molecule. Fibronectin is a dimeric protein that contains three distinct, and repeating, structural modules, type I, type II and type III. All three modules contain anti-parallel β sheets, the type I and type II domains are stabilized by disulfide bonds [77]. The integrin RGD target sequence resides within the ninth fibronectin type III repeat ($FNIII_9$). The $FNIII_{10}$ repeat site contains a sequence called the synergy site (PSHRN). The initial binding of the $\alpha_5\beta_1$ integrin to the fibronectin molecule is driven primarily by an interaction between the β_1 chain and the RGD sequence; full engagement of the integrin can only occur if the synergy site is present in an accessible conformation. This synergy site can be exposed by strain induced changes in fibronectin conformation [78]. Proteolytic processing of fibronectin increases the number of available RGD sites [79].

Chapter IV.

Cell Adhesion

Cell adhesion is an umbrella term that encompasses a variety of concepts and in reality the term has a number of working definitions. Typically, the term cell adhesion refers to the attachment of a cell to a surface, usually one that is coated with an ECM protein, a carbohydrate moiety and/or other candidate molecule, under controlled conditions in the tissue culture environment. However, cell adhesion routinely takes place *in vivo.* Regardless, cell adhesion is a process that is subject to a variety of checkpoints. These checkpoints "allow" cells that are "designed" to be mobile to remain mobile. At the same time the regulation of cell adhesion enables a cell that is resident to a particular place to form stable, long term adhesions (both cell-cell and cell-matrix), allowing that cell to remain in place for extended periods of time.

As a working definition of adhesion for this discussion, cell adhesion represents the specific adhesion of neonatal rat cardiac fibroblasts to a 2D surface coated with collagen, laminin, or fibronectin in tissue culture at 37^0C. This working definition requires yet more refinement as cell adhesion is a dynamic process that takes place in time, the nature of the interaction between cells and the surrounding environment changes rather dramatically

over a 1-2 hour interval [80], the time frame used in this study. When applied to a surface, cells initially interact with the surrounding micro-environment through physical entanglements and/or charge-based interactions. These non-specific interactions represent a prelude to adhesion events driven by CAMs. Once specific adhesion events have taken place many cell types spread out over a 2D surface and assume a highly flattened and spread morphology. Subsequently, cells typically undergo some degree of motility once they have reached "a spread equilibrium" with their surroundings.

For integrin-mediated events that take place in tissue culture the process of specific cell adhesion is initially marked by the formation of the focal contact (complex). This structure represents the transition from non-specific adhesion interactions to an event associated with the talin-initiated activation and ligation of an integrin with a target ligand [81]. During the initial phases of contact with a surface in 2D culture these structures are scattered over the basal surface of the cells in a punctate pattern. Over time, and given the appropriate circumstances, this structure evolves into the much more elaborate focal adhesion site. The classical focal adhesion exhibits a much larger surface area than the focal contact and generally has a triangular-like shape. This structure is composed of a population of integrins packed into a defined area on the cell surface. It is essential to recognize the equally important role of de-adhesion in the regulation of cell adhesion. Without this aspect of the process cells could not change shape and/or undergo motile activity.

The transition from the focal contact to the focal adhesion begins with the accumulation and clustering of integrin receptors with one another into a higher order

structure [82]. A pool of integrins that is freely mobile within the plane of the plasma membrane (lateral diffusion) is recruited to the developing focal adhesion [83]. This recruitment process requires a minimal threshold of mechanical loading in the guise of strain (stretch), this loading may originate from intracellular or extracellular sources [84]. The disruption of the actin based cytoskeleton with drugs such as cytochalasin b [81] or latrunculin [85] suppresses the maturation process. This occurs, presumably, because the actin based cytoskeletal network generates the internal tension necessary to promote focal adhesion assembly. Similar effects are observed when actin mediated contraction is suppressed [86]. Models of assembly predict that strain literally pulls the integrins into clusters, leading to the formation of the focal adhesion site. Early models were based on the assumption that actin was polymerized into cables from the forming focal adhesion; however, with the advent of more sophisticated imaging techniques it has become clear that the actin fibers exist prior to the adhesion site [87].

In parallel with integrin clustering there is a marked up-regulation of intracellular signal cascades and a continuing reorganization of the cytoskeleton, these events result in assembly of the multi-molecular complex that typifies the focal adhesion site. In the fully mature adhesion site, large scale actin bundles approach and terminate into an electron-dense, sub-plasmalemma plaque. This plaque contains structural proteins, including, talin, vinculin, and α-actinin [88, 89] as well as signal molecules including FAK, Paxillin and ILK (integrin linked kinase) [90, 91]. The strength of the focal contact is weak in the prototypic cell-substrate interaction and increases in strength as cells develop mature focal adhesions [92].

The maturation of initial contacts into the mature focal adhesion is intertwined with the process of cell spreading. In turn, cell spreading encompasses many of the events that take place during cell motility. During cell spreading, nascent focal contacts present at the cell periphery provide traction for the protrusion of lamellapodia. The formation of these membrane processes is driven by the polymerization of actin fibers in the core of the lamellapodia [94]. The focal contacts present at the protruding margin of the cell are "pulled" centripetally under the motive force of actin "tread milling", an action that generates the internal strain necessary to induce integrin clustering and the elaboration of the prototypical triangular focal adhesion site [85]. The assembly and contraction of the actin based cytoskeleton is regulated through the Rac/Rho signal transduction pathway [94]. RAC, a small GTPase, induces actin polymerization. Subsequently, RHO drives the accumulation of smaller actin-based fibers into stress fibers through ROCK, a downstream kinase that promotes actin contractility [95].

Cell migration can be viewed as an extension of the cell spreading phenomena. In the case of motility, adhesion sites, spreading and the release of adhesions must be sequentially regulated to enable the cell to undergo movement. The rates at which adhesion sites are lost are believed to represent the rate limiting step in cell motility [96]. The disassembly of integrin mediated adhesions is a distinct process and it is not a simple reversal of the assembly process. Determining the events, and signal molecules that regulate the disassembly of adhesion sites has proved difficult, these factors are in continual flux between the cytosolic compartment and the existing adhesion sites. However, experimental evidence points to a microtubule-based process. Blocking the

formation of microtubules with Nocodazole promotes the formation of extensive focal adhesions under the direction of Rho. Upon subsequent washout of this agent, focal adhesions are disassembled in concert, and in parallel, with the formation and growth of microtubules [97]. The disassembly of the existing focal adhesions is not affected by changes in Rho GTPases activity, rather, the disassembly process is sensitive to the formation of a FAK: dynamin: Grb2 complex. Based on these findings and morphological data, it appears that focal adhesion disassembly is dependant upon endocytosis [97, 98, 99]. Consistent with this model of regulation there is an increased concentration of integrins within endocytic compartments when dynamin becomes associated with FAK [100].

Grossly, the nature of the adhesions that cells make in tissue culture and the strength of these adhesions are dependent upon several variables. First, if the adhesion process is to transition beyond the initial contact stages that are non-specific in nature, the cells under consideration must express the appropriate complement of receptors to the candidate substrate. The target ligand must be present, and accessible, in sufficient density to support cell spreading. Next, metabolic activity (*i.e.* viable, living cells) must be utilized to re-organize the cytoskeleton and enable cell spreading to take place. Lastly, mechanical signals, originating from the cytoskeleton or from the external environment, are needed to drive the elaboration of the fully mature adhesion site [101]. A variety of different techniques and model systems have been used to define the processes and events that lead to cell adhesion and the assembly of the focal adhesion. Each of these paradigms has its own attendant strengths and weaknesses. Some assays are designed to look at population

dynamics while others are more subtle and are designed to examine specific events at the level of the single cell.

Conventional adhesion assays

In a classical approach, often denoted as the ***conventional adhesion assay***, a tissue culture dish is coated with a substrate of interest [102]. In this study these assays were conducted to define the baseline kinetics and binding characteristics of the cultured neonatal cardiac fibroblast to different ECM substrates. For these experiments a suspension of cells is applied to a surface of interest for a defined interval of time, usually 30 to 60 minutes. This time interval, for many cell types, encompasses the critical time period where cell adhesion is transitioning from non-specific processes to events that are mediated by specific, receptor-driven interactions. At the conclusion of the plating interval the culture plate is inverted and the cells are "dumped", adherent cells are retained, stained and quantified in some fashion. One aspect of this assay that remains an art form is the dumping phase. The amount of force that is used to invert and displace non-adherent cells can vary considerably from one investigator to another and as a result this phase of the experiment can be subject to variability from one lab to the next. However, in practice, and with experience, individual investigators can conduct this type of assay with remarkable consistency. By varying the plating interval used, the rate at which cells become adherent to the candidate substrates can be evaluated on a population wide basis.

The conventional adhesion assay is a very effective approach to study population dynamics and characterize the basic rate at which cells undergo adhesion to different types

of surfaces. However, given that integrin binding can be redundant and overlapping (with other integrins and even other CAMs) it can be difficult to ascribe a result to a specific receptor subtype. This limitation can be circumvented to some degree by using a cell line that is engineered to express a limited repertoire of receptors [103] or by examining how adhesion is effected when specific receptors are blocked. This later condition can be achieved through the use of antagonistic peptides like cyclic RGD peptides [104]and/or through the use of function blocking antibodies [105]. By eliminating one class of receptors and then evaluating the rate of cell adhesion, it is possible to extrapolate the contributions that the inhibited receptor might have in the outcome of the experiment. Alternatively, cells also can be transfected to express increased (or decreased) levels of receptors or other components of the cell adhesion machinery. From a functional prospective, the relatively brief interval between the initial adhesion events and the elaboration of the fully mature focal adhesion site results in a highly synchronized population of cells. This characteristic can be exploited to examine the biochemical correlates of the various events of adhesion.

ECIS assays

Conventional adhesion assays essentially take a snap shot of information at defined intervals of time, however, attachment and spreading can be continually monitored in a cell population with an ***ECIS*** (Electric Cell-Impedance Sensing) device[106]. This platform is fabricated on a microscope slide and consists of a series of miniature tissue culture wells (the volume of each well in this device is on the order of the volume found in an individual well in 96 well plate). At the floor of these miniature tissue culture wells is a conductive

grid that is linked through a circuit to a detector. This grid surface can be coated with ECM proteins, or other materials, prior to cell plating. When cells are applied to the wells they settle out onto the grids and there is a change in the electrical impedance that is present across the circuit [107]. Over time, the impedance decreases as the cells spread out over the surface of the grid, essentially insulating the surface and changing the conductive properties of the circuit as a consequence. By adding various reagents, for example drugs that inhibit components of the cytoskeleton and/or specific signal molecules, the ECIS assay makes it possible to evaluate the dynamics of cell attachment and subsequent cell spreading.

Centrifugal adhesion assays

Conventional adhesion assays have limited utility at defining the absolute strength of adhesion that takes place between the cell and the target substrate. As noted there is too much variability in the "dump phase" in this type of assay. This limitation can be circumvented through the use of the ***centrifugal adhesion assay***. In this application, cells are usually labeled with a vital dye (often a fluorescent metabolic reagent that is taken up and retained by live cells) and plated out onto a substrate of interest for a defined interval of time. At some point in the assay after the metabolic labeling has been completed an initial reading is taken of the plate to generate an estimate of cell number. The plates are then sealed and placed in an inverted position within a centrifuge equipped with a swinging arm rotor and an appropriate carrier for the culture plate and spun for a specific time and rotation per minute (RPM.) By knowing the radius of the rotor arm the actual

force experienced by the cultures can be estimated. At the completion of the centrifugation interval the plates are gently rinsed and a final determination of adherent cells is determined. A comparison of the initial cell number before and after centrifugation provides a measure of adhesion.

Molecular adhesion

"Adhesion" has been examined at the "***molecular level"*** using atomic force microscopy and magnetic twisting. These experiments for the most part are designed to examine the forces that are present at the interface of the integrin and ECM (atomic force) or at the interface of the integrin and the cytoskeleton (magnetic twisting). In atomic force microscopy beads coated with various peptides are linked to the cantilever arm of the microscope. As the cantilever arm is brought into contact with the cell surface binding events are initiated, the physical nature of this interaction is then characterized by determining the amount of force that is necessary to deflect the cantilever [108] . A similar approach has been used to characterize the association of specific integrins with the actin based cytoskeleton. In these experiments a magnetic bead can be coated with various peptides that will bind to a given class of integrins and allowed to interact with the cell surface. When these experiments are conducted in the presence of drugs that alter actin stability the amount of force necessary to twist the bead is substantially decreased with respect to untreated samples [109] (Wang 1999); a result that demonstrates the physical association of actin fibrils and the cytoplasmic domain of the integrin receptor.

Morphological Assessment of Cell Adhesion.

The principal strength of the conventional adhesion assay is in its simplicity and utility at generating adhesion data for a large population of cells to a defined surface over a defined interval of time. This assay and the related centrifugal adhesion assay are not particularly effective at examining the dynamics of adhesion, the processes that underlie cell spreading, or the relative distribution of different proteins with respect to one another. High resolution light or fluorescence microscopy designed to examine these events in single cells are more appropriate for this type of analysis. In early experimentation, this work was conducted on fixed samples, cells were plated for varying lengths of time and processed for microscopic examination [110]. Occasionally, transmission and scanning electron microscopy techniques have been applied to study cytoskeletal organization [111,112]. Considerable insight has been provided by this strategy concerning how cell structure changes over time during cell adhesion and spreading. These experiments essentially generated a static map of cytoskeletal changes (and signal cascades) associated with the different steps in the adhesion process.

The actual site of cell-substratum interaction can be unambiguously defined by the technique of interference reflection microscopy. This form of light microscopy uses a high numerical aperture lens constructed with strain free optics. When light is passed through a cell and focused on a cover glass the light is reflected off the surface of the substratum, a fraction of this light passes back along the original light path. When the optics are focused on the cover glass the maximal amount of light is passed back to the detector (eye, camera,

photo-detector etc.). At sites where a cell is in contact with the cover glass the amount of light that is reflected back into the detector is decreased, the extent to which the light reflection is decreased is proportional to the distance the intervening structure is from the glass reflecting surface [113]. In practice a cover glass produces a bright reflection, focal contacts will appear as punctate spots that are somewhat gray. A fully mature focal adhesion site appears as a much darker structure. Within a given cell the darker the area associated with the contact the more intimately applied that structure is to the underlying surface. This technique can be used in living or fixed samples. However, for live cell imaging the heating effects of the illuminating light must be minimized, fixation tends to collapse the cell to a degree.

Real-time observations of living cells with high resolution optics make it possible to study the dynamics of adhesion and cell spreading. This method can be coupled with the micro-injection of mutant or fluorescently labeled proteins that target different elements of the cytoskeleton or the focal adhesion complex [114]. The true dynamics of protein turnover in these structures has been evaluated with the technique of fluorescence recovery after photobleaching (FRAP). Once an injected fluorescently labeled protein has been allowed to come to equilibrium within the cell, the fluorescent tag present in a specific domain of the cell is bleached with a pulse of light [115]. The site of bleaching is then monitored over time as the bleached proteins are replaced with tagged proteins. This turnover is a reflection of the stability of the structure under investigation, the bleached and unbleached proteins exchange with one another from the structural compartment and the cytosol.

Chapter V.

The Matrix Metalloprotienases

While there are clear homologies, the binding events and processes that underlie cell motility *in vivo* are different than the binding events that take place in the simplified 2D microenvironment of tissue culture. *In vivo* the cell is enmeshed within a 3D microenvironment consisting of cells and the ECM. This complex matrix is composed of a heterogeneous array of interconnected fibrous proteins and other macromolecules that define tissue architecture. This heterogeneous mixture of proteins and proteoglycans provide the cellular compartment with a diverse variety of potential binding sites. Unique cell-matrix interactions between a single cell surface receptor subtype and a single unique moiety are rarely, if ever, encountered within intact tissues.

Like the cell:ECM interaction *in vitro*, the cell:ECM interaction *in vivo* is highly dynamic. In both environments there is evidence of two-way regulation across the plasma membrane (*i.e.* inside-out as well as outside-in signaling) on a local, as well as a global scale. The chemical identity, and physical arrangement, of the ECM interact to regulate the function of the resident cellular population. In turn changes in the steady state physiology of the cellular compartment can lead to changes in the composition and organization of the ECM.

Under steady state conditions an external signal or other change in the status quo must ordinarily alter the balance of information passing between from the cellular and extracellular compartments. Signals that initiate or modulate this two-way pattern of signaling often originate from soluble factors present in the local microenvironment. These signals can have direct consequences on the expression and/or deposition of specific ECM constituents [116]. Sustained changes in mechanical load can also impact the cell:ECM interaction and thereby alter the steady state conditions. These forces can be detected directly in the cellular compartment and transduced into intracellular signal cascades that modulate cell phenotype and/or ECM metabolism [117, 118].

In native tissues many cell types express a variety of integrin subtypes (and other CAMs). Within this complex 3D environment any given cell can be linked to a variety of different binding moieties, providing several different potential conduits for the transmission of information across the plasma membrane. For integrin-based binding events it is unclear how or if a cell discriminates between these different signals. The observation that different integrin:ECM interactions exhibit different binding constants (*e.g.* strength of adhesion), suggests that information concerning the local mechanical environment might be detected in a biased fashion [64]. For example, an integrin with a high avidity interaction with a target molecule can be expected to transduce mechanical information in a different pattern than an integrin that is weakly linked to the surrounding environment. Ultimately, the physiological status of the cell must be the sum of the individual binding events; cell adhesion does not take place in a vacuum. Preliminary experimentation conducted for this study was designed to determine if the absolute number

of a specific integrin subtype or the identity of integrins present on the cell surface dictated cellular response to strain and the expression of the gelatinases, MMP-2 and MMP-9. As noted in the introductory remarks of this study the results of these experiments suggested that MMP-mediated protease activity modulated cell adhesion to a greater extent than the converse circumstance (cell adhesion modulating MMP expression).

The characteristic specificity of MMP-2 and MMP-9 for ECM proteins suggests that these proteases might impact cell adhesion by altering the structure and/or availability of cell binding sites in the surrounding matrix. Native proteins can contain adhesion sites that are sequestered and not presented to the cellular compartment in an orientation that is available for binding activity. These sites, called cryptic sites, can be unmasked by changes in mechanical loading and/or through the proteolytic processing of ECM components. For example, increased mechanical loading can act to uncoil or otherwise alter the tertiary structure of the protein(s) under consideration, thereby exposing these hidden binding sites [78]. While changes in strain are often associated with an increase in mechanical load, the converse circumstance, a decrease in mechanical load, can also induce changes in protein structure that result in the exposure of previously unavailable binding sites. This unmasking process is undoubtedly facilitated by the highly interconnected nature of the ECM and cellular compartments.

Proteolytic processing of ECM components or the denaturation of proteins through physical, chemical or through radiation can directly alter protein structure and unmask cryptic sites contained within individual proteins. Such degradative events also can unmask hidden sites indirectly by altering the degree of strain that is present across an

individual protein[119] or even across a relatively large volume of tissue [120]. In dermal burn injuries, native collagen fibrils are physically damaged, this serves to unmask specific integrin binding sites that are not ordinarily available [121, 122]. Once these sites become available the keratinocyte population begins to shift in phenotype to mediate the re-epithelialization of the wound bed. A variety of proteolytic enzymes can mediate the processing of ECM proteins, not surprisingly; these degradative events are subject to a considerable degree of regulation. Relevant to this study are the extracellular enzymes of the Matrix Metalloprotienase Family.

The Matrix Metalloprotienases

The Matrix Metalloprotienases (MMP) is a family of zinc dependant enzymes that collectively degrade most ECM proteins. These extracellular proteases are expressed broadly in the animal kingdom. First identified in the tail of the metamorphosing frog these enzymes play a central role in regulating the turnover and remodeling of the ECM in development [123], normal homeostasis and in disease [124]. Subsequent to this initial identification 28 different MMP have been identified. A defining feature of this class of endopeptidases is the Zn^{+2} ion that is an integral component of the active enzyme. Members of this family are classified into subfamilies based on functional and structural criteria. Substrate specificity serves as a functional criteria; the primary and tertiary structure of the peptide define the structural characteristics. The MMP subfamilies include; (i) the Collagenases, (ii) the Stromelysins, (iii) the Gelatinases, (iv) other MMP, and (v) the Membrane-type MMPs.

Structural domains present in MMPs underlie the functional differences used to define the subfamilies. Common to all MMP is the Zn^{+2} cation that is necessary for the function of the catalytic domain. Other divalent cations such as Ca^{+2} serve to stabilize the tertiary structure of the enzymes. The molecular weight of these proteases can vary considerably; the actual mass of each MMP is determined by the number of functional domains that are present in the enzyme [17] For example, the smallest protease of the family, MMP-7 or Matrilysin (28 kD, classified as an "other MMP"), is a soluble enzyme that is composed a signal domain, a pro-domain, and a catalytic domain. In contrast, MMP-9, also a soluble protease, is considerably larger (92kDa). In addition to a signal domain, a pro-domain and the catalytic domain this protease contains a fibronectin type II repeat that is typical, and diagnostic, of the gelatinase family of MMPs. MT1-MMP (54-64 kDa-depending upon activation state) is a Membrane-type protease that contains a transmembrane domain that functions in part to anchor the enzyme to the plasma membrane.

Typically the prototypic, soluble MMP is expressed in a latent, zymogenic state (non-active) into the extracellular compartment. Intracellular processing by furin represents an alternate site for enzyme activation. These enzymes may be stored in the extracellular environment in this state for variable intervals of time and then activated in response to an environmental signal. Activation is regulated through the pro-domain, this portion of the molecule acts as a physical constraint on the structure of the enzymatic domain. Within the 80 amino acid sequence of the pro-domain there is a conserved region, PRCG(V/N)PD, that contains a cysteine residue that forms a coordination complex with the Zn^{+2} cation that

resides within the catalytic domain. This bond confers latency to the enzyme and has given rise to the concept of a "cysteine switch" [125]. The nature of this bond makes these enzymes susceptible to a host of chemical, mechanical, and physiologic events that can lead to activation. A family of peptides, the **T**issue **I**nhibitor(s) of **M**etallo**p**rotienase (TIMP), modulate the activation cascades that ultimately regulates the enzymatic activity of these proteases. There are 4 described TIMPs, these small (~24 kDa MW) peptides bind to various sites on the enzymes and act to suppress activation and/or localize specific MMPs to different extracellular compartments.

The Gelatinases: MMP-2 and MMP-9

Representative of the Gelatinase family of MMPs are MMP-2 and MMP-9. These proteases are of particular interest to this study as these enzymes are active in the myocardium during embryonic growth and during episodes of ventricular wall remodeling in adult life [126, 127]. These enzymes represent the primary MMPs expressed by the cardiac fibroblast in the rodent [128]. Historically the nomenclature designating these enzymes has been based on substrate specificity, molecular weight and/or the order of discovery. MMP-2 has been variously identified as Gelatinase A and/or the 72 kDa type IV collagenase (and MMP-2). MMP-9 has been known as Gelatinase B and/or the 92 kDa type IV collagenase (and MMP-9). The designations of MMP-2 and MMP-9 for these gelatinases reflect a naming convention that is based on the order of discovery and these terms are widely used to describe these two proteases.

For most MMPs, non-catalytic interactions with ECM proteins occur through the C-terminal, hemopexin domain. However, unique to MMP-2 and MMP-9 are the fibronectin Type II-like domain repeats that are present within the N-terminal catalytic domain of these enzymes. These domains mediate the unique N-terminal binding interactions of these proteases with collagenous components of the ECM [129]. Note, MMP-2 and MMP-9 are both expressed and deposited into the ECM as inactive enzymes that are subsequently activated in response to environmental signals. Essentially, the fibronectin Type-II repeats function to tether these inactive enzymes to components of the 3D scaffolding that surrounds the fibroblasts of the heart (and most other tissues).

Substrate specificity of the gelatinases is fairly broad. MMP-2 and MMP-9 both have demonstrated activity against such diverse proteins as elastin, vitronectin, laminin, SPARC, aggrecan, decorin, Link Protein and MBP [18]. MMP-2 can cleave collagen Type I, III, IV, VII, X and XI. MMP-2 also has unique activity against the non-collagenous proteins, fibronectin and various laminins. MMP-9 has activity against the collagen Types IV, V, XI, and XIV. Enzymatic activity of MMP-2 and MMP-9 against the target substrate proteins has largely been defined *in vitro,* resulting in some degree of controversy, and uncertainty, as to the targets that might be degraded *in vivo* by these proteases (defining this type of activity in the complex *in vivo* environment is not a trivial task). Nevertheless, MMP-2 binds and can cleave native type I collagen into fragments in a fashion typically assigned to the interstitial collagenases [130, 131]. In contrast, MMP-9 exhibits only binding activity against this ECM protein and does not appear to cleave Type I collagen [132].

The activation of MMP-2 and MMP-9 is regulated at a number of different sites; the uncontrolled activation of these proteases would clearly have deleterious consequences on the structural integrity of the ECM [133]. Under most circumstances MMP-2 is expressed constitutively into the extracellular environment in the inactive, pro-form and stored as a zymogen within the ECM. MMP-9 is more often expressed into the extracellular environment in response to specific environmental signals. As with MMP-2, MMP-9 is typically deposited into the ECM in the inactive, pro-form. The conversion of these pro-forms of these enzymes into the active state is subject to a multi-tiered pattern of regulation.

The regulatory schemes controlling the activation state of MMP-2 and MMP-9 vary to some degree. As noted, MMP-2 is usually expressed in a constitutive manner; however, this does not mean that the enzyme is expressed in a haphazard, unregulated manner. The over-expression (and dysregulation) of this protease occurs in some cancers and is associated with enhanced cell migration and the spread of metastatic disease [134, 135]. The principle pathway for the activation of pro-MMP-2 involves the cell surface bound MT1-MMP and the regulatory peptide, TIMP-2 [136, 137]. When MMP-2 and TIMP-2 are present at equimolar concentrations in the extracellular environment, the conversion of pro-MMP-2 to the active MMP-2 isoform is inhibited. As the concentration of TIMP-2 is increased, the TIMP-2 molecule binds to MT1-MMP. When a critical concentration of TIMP-2 is reached, TIMP-2 can be bound simultaneously to a pro-MMP-2 and to a MT1-MMP, forming a ternary complex at the cell surface. This complex positions the pro-MMP-2 in proximity to an adjacent "free" MT1-MMP leading to the proteolytic processing of the

pro-MMP-2 molecule to the active MMP-2 state. If very high concentrations of TIMP-2 are present with respect to pro-MMP-2 and MT1-MMP these "enzymatic" compartments become saturated; effectively blocking the formation of the ternary complex and quenching the activation cascade. Alternate pathways leading to the formation of the MT1-MMP:TIMP-2:MMP-2 complex and/or the activation of pro-MMP-2 are limited. The pro-MMP-2 enzyme is highly resistant to many endoproteases, which limits the activation process through spurious cleavage events [138]. However, pro-MMP-2 can undergo a process of self cleavage and subsequent autoactivation under conditions in which the enzyme is present in very high concentrations [139].

The regulation of MMP-9 is perhaps in some ways more elaborate as it is not expressed constitutively [140]. MMP-9 expression is regulated by growth factors, cytokines, cell-cell interactions, and cell-ECM interactions and events that alter cell shape [141]. In a model of cyclic stretch MMP-9 was detected only at moderate degrees of stretch whereas MMP-2 was detected at baseline, moderate and high degrees of stretch [142]. The proteolytic activation cascade that regulates the processing of pro-MMP-9 to active MMP-9 is subject to TIMP-dependant regulation in a pattern similar to MMP-2. TIMP-1 (a peptide related to TIMP-2) and TIMP-2 can both bind and suppress the conversion of pro-MMP-9 to the active state. The relative contributions of TIMP-1 and TIMP-2 in the regulatory cascade remain ill-defined [143], although TIMP-1 dependant regulation of MMP-9 appears to be the predominate regulatory pathway in the control of pro-MMP-9 [144]. Adding additional support to this conclusion, TIMP-1 and pro-MMP-9 are expressed in a highly coordinated fashion. In an analogous axis of control that regulates the activation of pro-MMP-2, the

activation of pro-MMP-9 is mediated by the disruption of the cysteine/ Zn^{+2} coordination bond. TIMP-1: pro-MMP-9: MMP-3 (Stromelysin-1) form a ternary complex that results in the formation of active MMP-9 [145]. MMP-3 and a plasmin dependant pathway effectively process the pro-peptide yielding the active MMP-9 [146,147]. Plasmin has two fold effects on the activation cascade, first, this protease can directly active MMP-9, second plasmin can increase MMP-3 mediated processing of MMP-9 [148].

Functional Consequences of MMP-2 and MMP-9

Changes in MMP-2 and MMP-9 activity are closely associated with disease states and developmental processes (events in which the balance of signals between the intracellular and extracellular environments have been perturbed, leading to a change in the steady state condition) and that lead to alterations in ECM architecture and function. The role of these gelatinases in matrix remodeling is particularly striking in arthritis and in a variety of cancers. For example, increased gelatinase activity parallels the onset of the osteoid and rheumatoid types of arthritis [149,150]. Increased levels of Activated Protein C process and cleave PAR-2 (protease activated receptor-2) in osteoarthritic cartilage; this enzymatic activity leads to increased activation of MMP-2 and MMP-9 [151]. This pathway is not observed to be active in normal cartilage. Symptomatic of osteoarthritis is the accumulation of high levels of collagen breakdown products, this diagnostic feature of the disease can be blocked by treatment with broad spectrum MMP inhibitors [152]. In rheumatoid arthritis, the invasion of the cartilage matrix by migrating synovial fibroblast occurs in a MT1-MMP dependent process that is susceptible to the application of TIMP-2

(to block activation processes) and other pharmacologic agents that disrupt MMP-2 activation. The invasive process also can be blocked by the over expression of a dominant negative MT1-MMP that is inactive and cannot activate MMP-2 [153].

The dysregulation of gelatinases (and other MMPs) has devastating effects in the progression of cancers. The breakdown of the basement membrane and the loss of compartment integrity is often a prelude to the dissemination of cancer cells in tumor invasion and metastases [134]. For example, the loss of basement membrane type IV collagen paralleled elevation in MMP-2 and MMP-9 activity in the progression of colorectal tumors in human [154]. For migration and direct invasion of cancer cells, the native ECM forms a barrier that is overcome by the proteolytic events that compromise its structural (and functional) integrity. MMP-2 specific protease activity mediates the processing of ECM proteins during the attachment and migration of ovarian tumor cells within the peritoneum [155]. Critical to the growth of solid tumors is the process of angiogenesis, an event that can be initiated by the migration, in the absence of proliferation, of the existing of endothelial cells [156]. The gelatinases can drive the process of vessel formation by inducing the release of VEGF [157]. Alteration in the levels of MMP activity are associated with a poor outcome in many cancer types. A representative but by no means comprehensive list highlights the many cancer types that involve deregulated MMP.

- The expression of MMP-2, MMP-9 and MT1-MMP was associated with disseminated, advanced disease and correlated with shorter disease specific survival in ovarian carcinoma [158].

- In prostate cancer a major problem diagnostically is the lack of markers that delineate clearly the disease state. Traditionally PSA levels along with clinical impression were the mainstay in this determination. In a comparison of men with normal, benign hypertrophic, organ confined and metastatic prostate adenocarcinoma the levels of plasma activity of MMP-2 and-9 were highest in men with disseminated disease [159].
- In a range of severity of astrocytic tumors MMP-2 and MMP-9 expression levels were not correlated with survival rates [160]. The lack of difference in the survival rates is likely a reflection of the high degree of infiltration of astrocyomas which is correlated with the level of MMP-2 activity [161].
- Levels of gelatinases and TIMP were correlated with established prognostic criteria in breast cancer it was seen that alteration on the MMP-2/ TIMP-2 ratio was indicative disease that had spread and was positive for nodal involvement.
- MMP involvement is also a determinant in the growth of more "cellular" tumors as Hodgkin's lymphoma[162]. In CLL (chronic lymphocytic leukemia) MMP-9 is involved in the invasion and migration of this B-cell cancer [163].

The changes in MMP mediated proteolytic activity observed in parallel with the growth of so many different types of transformed cells has lead to the increased interest

and use of inhibitor based therapies that are designed to limit cell migration [164]. The recurrent theme in the interplay between cancer and MMP is that MMP degrade ECM components, which serve as a barrier to constrain cells. Additionally, MMP are responsible for the release of cryptic site and for the processing and release of growth factors from the ECM. In this context the ECM can be though of as 1) the substrate that provides structure to tissue and 2) the series of tissue interfaces created by basement membranes that define compartments. The breakdown of both of these components is evidenced in disseminated diseases. In cancer invasion within the local tissue environment requires migration that is dependant on the action of MMP. Differences in levels of TIMP-2 regulate the activation of MMP-2 by MT1-MMP and underlie the invasive potential of melanoma [165]. Basement membrane demarcates tissue compartments and is enriched in type IV collagen. Gelatinases are relevant as type IV collagenases.

MMPs in the Heart in Development

During embryonic and fetal development in mammals the forming body and individual organ systems undergo dramatic changes in topology (shape) and size. These processes are mediated by events that take place on a local cellular scale that transpire in a coordinated fashion, ultimately resulting in the formation of the adult body plan. Organs of the gut, the lungs, the central nervous system, urogenital system are initially expressed in one form during embyrogeneis and then during subsequent development are completely remodeled to achieve the final adult form (and function). Synthetic and degradative processes must be precisely regulated to achieve normal development.

The changes in tissue architecture that mark normal development are clearly apparent in cardiac development and growth. At the onset of organogenesis mesenchymal stem cells emerge from the primitive streak, congregate, undergo differentiation and establish the cardiogenic zones [166]. As development precedes this cell population is recruited to form the solid, paired cylindrical heart tubes parallel to the midline of the body axis. The tubes condense to form a single hollow heart tube and that will undergo erosion to form the internal lumen that will become portions of the ventricular and atrial chambers. Initially the heart tube is nearly straight, as growth continues it elongates and this primordial structure begins to loop to form the basis for the four chambered architecture of the mammalian heart. At this point the developing heart is structurally simple with an outer layer of differentiating myocytes, a proteoglycan rich connective tissue, cardiac jelly, and the innermost layer of endocardium [167].

The biological events that drive formation of the four chambered mammalian heart take place in a complex regulatory environment. Signals from multiple sources modulate the looping process, although, hemodynamic signals do appear to play an absolutely central role in the formation of the four chambered myocardium [168]. In the rat, changes in load alter the differentiation patterns of myocytes and selectively promote the maturation of myofibrillar arrays in a regional pattern [169]. These changes in cytoskeletal organization may serve to limit the extensibility of the ventricular wall and thereby direct the looping process by stiffening (strengthening) aspects of the muscle wall. In this model of development, the less stiff domains undergo the looping process. Protease mediated events also are critical to normal development. In the context of these events, the suppression of

MMP-2 mediated proteolytic activity results in gross defects in cardiac looping and varying degrees of cardia bifida [170]. Presumably, proteolytic events facilitate cardiac looping by reducing the structural integrity of the ventricular ECM, thereby allowing the gross movements in the ventricular wall that must take place during looping. The embryonic period from E-12 to E-21 is dominated by MMP-2 mediated proteolytic activity, with a peak of activity around E-16. In contrast, MMP-9 has much lower level of activity during this window of development with a peak around E-16 [126]. This interval of development is associated with the formation of valvular structures.

A recurring theme in cardiac physiology is the notion that changes in hemodynamic load promote the elaboration and accumulation of the ECM throughout the heart proper as well as in the outflow tracks and valve structures [128]. Changes in MMP expression typically track with the events that promote the accumulation of nascent ECM proteins during these developmental processes. For example, MMP-2 activity is contemporaneous with migration of mesenchymal cells and the expression of this enzyme parallels the differentiation of cardiac valves [171]. The migration of non-resident, neural crest cells into the developing heart during septation is spatially and functionally associated with changes in MMP-2 expression; suppressing MMP mediated migration of neural crest cell results in severe cardiac defects as persistent truncus arteriosus, double outlet right ventricle and the tetrology of Fallot [172].

MMPs in the Heart in Adult Life

Sustained changes in mechanical loading in the adult heart initiate well documented remodeling events [173]. Within the myocardial compartment elevated peripheral vascular resistance results in increased mechanical load and the onset of hypertrophic cardiac growth. During the compensatory stage of the disease the heart exhibits increased contractility and improved performance (output). Overtime the heart begins to decompensate as remodeling events alter the ECM composition and the myocardial compartment begins to fail [174,175]. In long standing hypertension the progression into congestive heart failure is hallmarked by left ventricular dilation. This transition involves a thinning of the myocardial wall and a dilatation of the ventricular lumen. In rodent models of hypertrophy expression of MMP-2 and MMP-9 are markedly elevated during when compensation or decompensation [127]. Moreover, inhibition of MMP activity can directly attenuate this process [176]. Experimentally induced expression of MMP-2 in the heart can, independently of hemodynamic load, induce marked ventricular wall remodeling and the onset of systolic dysfunction [177].

In experimental myocardial infarction the suppression of MMP mediated processes acts to preserve ventricular architecture. Notably, Ramipril, an Angiotensin Converting Enzyme (ACE) inhibitor, prevents left ventricular dilation following a coronary artery occlusion induced infarct in the spontaneously hypertensive rat. This treatment is associated with a depression in MMP-2 activity [178]. The positive effects of ACE inhibitor treatment in lowering MMP-2 activity, in the A-V shunt (High output failure) model, were detected with a reduction of the intendant cardiac hypertrophy that develops in untreated

control animals [179]. Lower levels of MMP-2 activity decrease the remodeling of the existing cardiac interstitium that is a prelude to the development of hypertrophy. Of patients with controlled hypertension, only patients with left ventricular hypertrophy and congestive heart failure had high serum levels of TIMP-1[180]. The high level of TIMP-1 was related to the extent of left ventricular remodeling. These data are mentioned to reiterate the importance of balance in the turnover of ECM components in the heart as being effected by the not only the activity(amounts) of MMP, but also the regulatory peptides that control activation of these proteases.

MMP Interactions with Integrins

In the classic view of MMP-2 and MMP-9 these proteases are found bound to constituents of the extracellular matrix. The enzymes are then processed into an active state and function to degrade elements of the surrounding environment. It is unclear how enzymes that are bound to the ECM are transitioned into a more or less soluble state for processing into the active protease. These processes are clearly regulated as enzyme activity increases and decreases in response to various environmental signals.

Another factor in the biology of these systems concerns the extent to which the positioning and the degree to which the actual enzymatic processing of target substrates is regulated. Developing evidence has pointed to binding interactions between specific integrin subtypes and selected MMP molecules. This type of interaction results in a

complex on the cell surface that theoretically can target small, and highly relevant domains (to the cell) for processing.

The association of pro-MMP-1 collagenase with the $\alpha_2\beta_1$ integrin in keratinocytes represents a profound, and elegant, example of the functional consequences of the formation of this type of complex. In dermal burns (and other forms of full thickness injuries to the dermis) the keratinocytes at the periphery of the wound site undergo a phenotypic shift. At least 4 distinct sub-populations, based on various molecular markers, can be described, including the ***differentiated, proliferative, motile*** and ***differentiating*** phenotypes [181]. Each cell type appears to "evolve" from cells that existed in a previous phenotypic state. Differentiated basal keratinocytes represent the cell population that resides at the base of the epithelial layer in normal skin. Within hours of injury rates of cell division increase, marking the appearance of proliferative keratinocytes. During this phase of wound healing there increased expression of MMP-3[182]. The motile phenotype is composed of the keratinocytes that migrate out over the provisional wound matrix to form the epithelial tongue [183]. Differentiating keratinocytes appear as contiguous sheets of cells form on the wound.

The migration process for the motile phenotype of keritinocytes on native collagen is absolutely dependent upon the expression of functional $\alpha_2\beta_1$ integrins and the MMP-1 protease [122, 184]. Demonstrating this association were a series of experiments that blocked the function of MMP-1 with either pharmacological, physiological (TIMP-1), immunological, also blocked the migration of keritinocytes on native collagen. Moreover, keritinocyte migration was inhibited by collagenase resistant collagen. Specific blocking of

$\alpha_2\beta_1$ blocked migration on type 1 collagen and the expression of MMP-1. These functional (observations) of keritinocyte migration suggests a physical association of proMMP-1 and $\alpha_2\beta_1$ integrin. This association was vetted by microscopic demonstration of the colocalization of these proteins on the surface of migratory keritinocytes and the coimmunoprecipitation these antigens. Disrupting the association by the exogenous application of active MMP-1 or antibodies directed against the I-domain of the α_2 chain demonstrate the interaction to be constrained to the linker and hemopexin domain of MMP-1 with the I- domain of the α_2 chain. The specific interaction of the I-domain and MMP-1 was delineated with a series of binding assays of purified α_2 I-domain to native and chimeric MMP-1 [185]. This complex appears to direct proteolytic activity to domains that must be remodeled in the ECM in order for migration to take place [184].

Several other examples of integrins linked to MMPs also exist. In **angiogenic blood vessels** MMP-2 colocalizes with the $\alpha_v\beta_3$ integrin on the endothelium. This interaction is mediated through the C-terminal domain of the MMP-2 molecule with the $\alpha_v\beta_3$ integrin. It is thought that this interaction is based on homology of the C-domain with the established $\alpha_v\beta_3$ integrin ligand vitronectin. In this topological arrangement the N-terminal catalytic domain of the MMP is free to mediate proteolysis [186]. The fibronectin Type II like repeats of the MMP-2 molecule have also been implicated in linking this protease to the cell surface. In this instance, a pericellular collagen peptide acts as a bridge between the β_1 integrin subunit and the MMP-2 protease [187]. One aspect of this particular relationship that remains to be more fully explored concerns the observation that the

MMP-2 recovered from this complex is resistant to cellular activation. It has been theorized that this resistance may be a reflection of this pool of MMP-2 being positioned as "reserve" of readily available latent gelatinase that can be secreted in the inactive pro-form without intersecting the MT1-MMP activation pathway.

Several lines of evidence indicate that specific interactions between selected MMPs and other cell surface molecules exist in a variety of systems. MMP proteases have been detected in association with CD44, ICAM-1, and Caveolin-1 [188]. The formation of these complexes appears to allow the cell to specifically direct and control proteolytic activity within its immediate vicinity. In the heart, changes in MMP expression and activation occur during periods of active ventricular wall remodeling. Given this observation and the emerging literature that MMPs are specifically tethered to the cell surface in many tissue types this study was undertaken to test the hypothesis that MMP mediated proteolytic activity is spatially regulated in the rat cardiac fibroblast by members of the integrin family. The specific aims of this study were to:

1. Define the structural relationships that exist between specific integrin sub-types and members of the MMP family of gelatinases.
2. Optimize the binding conditions necessary to achieve maximal adhesion of neonatal rat cardiac fibroblasts to collagen, laminin and fibronectin using conventional adhesion assays.
3. Define the strength of adhesion that develops as the cells attach to different ECM substrates using centrifugal adhesion assays.
4. Define the functional relationships that link extracellular protease activity with the integrin mediated adhesion of cardiac fibroblasts to collagen, laminin and

fibronectin.

The results of this study demonstrate that MMP-2, and not MMP-9, is linked specifically to the $\alpha_3\beta_1$ integrin in a complex that also contains TIMP-2. Evidence in support of this conclusion is derived from co-immuno-precipitation experiments designed to alternately pull down the α_3, the β_1, or the MMP-2 molecule from a cell extract isolated from 3-5 day old neonatal rat cardiac fibroblasts. The recovered material was then assayed for the presence of α_3, the β_1, MMP-2, MMP-9, TIMP-1 and TIMP-2. MMP-2 immuno-reactivity was present in material recovered from immuno-precipitations against α_3 and β_1. Assays of material recovered by immuno-precipitations directed against MMP-2 indicated that these integrin subunits represented the predominate site of attachment. There was no immuno-reactivity against α_1 α_2 or α_5 integrin when MMP-2 was targeted for immuno-precipitation. Quantitative scanning confocal microscopic observations were used to confirm these results. Functionally, adhesion assays suggest that MMP mediated protease activity promotes the attachment and or maturation of adhesion sites in cells plated onto collagen and fibronectin, but not laminin or poly-l-lysine.

CHAPTER VI.

Methods

Cell Culture

Cell Isolation. Cardiac fibroblasts were isolated from postnatal, three to five day old (P3 to P5) Sprague-Dawley rat pups. (IUCAC 0204-3058) Pups were decapitated and subjected to a mid-line thoracotomy. Skin was folded back from the thorax and the pressure applied to the dorsum of the pup during this procedure causes the heart to move to the anterior surface of the thorax and through the thoracotomy where it was clipped from the attached vasculature. Hearts were collected and placed into PBS in a 50 ml centrifuge tube. Any floating or suspended debris was decanted and discarded. Hearts were rinsed with PBS until clear of blood. Hearts were transferred to a sterile 30 ml beaker (Pyrex No. 1000) and minced with iris scissors into 1 mm^2 pieces. This preparation was rinsed in fresh PBS until clear of blood.

Using a 30 ml syringe (BD Falcon) fitted with a #14 gauge x 6 in stainless steel cannula (Popper), the minced heart tissue was transferred to a sterile 50 ml Erlenmeyer flask (Pyrex No. 4980) for enzymatic dissociation. Liquid contents were aspirated and discarded using the syringe and cannula. A 10 ml aliquot of collagenase solution was introduced into the vessel. Collagenase was prepared fresh in PBS (Collagenase type I, 250

u/mg, Worthington Biochemical Corporation; Lakewood, NJ), diluted to 120 units of enzymatic activity/ml and filtered through a 0.2 μm syringe filter. The flask containing the heart tissue and collagenase solution was placed into a shaking water bath set to agitate at 100 cycles/min at 37˚C (Precision; Winchester, VA) for 10 min. The supernatant was aspirated and discarded. A fresh 10 ml aliquot of collagenase solution was added to the tissue, followed by gentle cannulation (4x) to mechanically disrupt the tissue. The flask was returned to the water bath for a 10-15 min digestion cycle. Supernatant was collected and strained (100 μm cell strainer, BD Falcon) to remove large debris into a 50 ml centrifuge tube. The addition of collagenase, the digestion incubation, and collection procedure was repeated, without additional mechanical cannulation, until the tissue was fully digested.

The pooled cell supernatant was pelleted by centrifugation at 800 x G for 8 min (ALC International, Milano, Italy). The recovered cell pellet was suspended in 5 ml of Complete Media (DMEM/F-12 supplemented with 5% Horse Serum, Sigma H1138, 2.5% Fetal Bovine Serum, Heat Inactivated, Invitrogen 10437-028, 1.2% Sodium Bicarbonate, Invitrogen 25080, and 1.2% Antibiotic/Antimycotic, Invitrogen 15240).

Differential adhesion was used to partially purify viable cardiac fibroblasts from the crude digest. The suspended cell pellet was divided into three 150 mm^2 tissue culture flasks (Corning), each having a total final volume of 20 ml, for each litter of pups (assuming 8-10 animals per litter). Flasks were incubated in a 5% CO_2 incubator at 37˚C for 5 hours. At the conclusion of this interval the media was decanted and the flask was rinsed briefly with PBS. Complete Media was added to a final volume of 25 ml. At best, a

nominal number of cardiac myocytes will adhere to tissue culture dishes under these conditions. Any surviving myocytes are lost during subsequent cell passages.

Culture Maintenance. Cultures of neonatal rat cardiac fibroblasts were routinely maintained in 150 mm^2 culture flasks supplemented with 25 ml of Complete Media in a 5% CO_2 incubator at 37˚C. Media was changed every 3-5 days. Cultures were assessed by microscopic examination. When cultures were 90% confluent, the cells were split 1:2 into fresh culture vessels. For cell passage, media was decanted, plates were rinsed with PBS and supplemented with 10 ml of 0.25% Trypsin/EDTA (Invitrogen, 25200) prepared in DMEM and incubated for 10 min at room temperature. The release of cells was visually confirmed. Cells were collected in 50 ml centrifuge tubes, flasks were rinsed with 10 ml of complete media which was collected and added to the 50 ml tube containing the released cells. The number of 50 ml tubes needed for each passage was determined by the number of culture flasks that were to be split; typically 3 flasks can be accommodated by one 50 centrifuge ml tube. Cells were brought to pellet by centrifugation (800 x G for 8 min). The cell pellet was suspended in a small volume of complete media (~ 5-10 ml per flask) mixed and then distributed into twice the number of starting flasks. Complete media was added as needed to bring the total volume of media to 25 ml per flask. Fibroblasts were used for experimentation after 3 and no more than 8 passages.

Culture Media Formulation. Media formulations that were used during these experiments are as listed. All reagents from Gibco/Invitrogen unless noted. Formulations included:

1) "Complete Media" as already described-used for routine culture maintenance: DMEM F-12 supplemented with 5% Horse Serum (Heat Inactivated: Sigma), 2.5% Fetal Bovine Serum (Heat Inactivated; Sigma), 1.0% Sodium Bicarbonate, and 1.0% Anti-biotic/anti-mycotic (penicillin G, streptomycin, and amphotericin).
2) "ITS Media"- DMEM F-12 supplemented with; 1.0% Insulin Transferrin, Selenium (ITS+1; Sigma), 1.0% Sodium Bicarbonate, 1.0% Anti-biotic/anti-mycotic (penicillin G, streptomycin, and amphotericin).
3) "Depleted Media"- used for selected experimentation: DMEM F-12 supplemented with 0.1% Gelatinase depleted FBS, 1.0% Insulin Transferrin Selenium (ITS+1; Sigma), 1.0% Sodium Bicarbonate, 1.0% Anti-biotic/anti-mycotic (penicillin G, streptomycin, and amphotericin). Gelatinase depleted media was prepared by incubating FBS overnight at 4º C against a 1% Gelatin/ PBS slab polymerized in a 150 cm^2 culture flask (proteases of the MMP family that reside in serum adhere to the gelatin slab). Following recovery, the depleted FBS was passed through a 0.2 μm syringe filter. Depletion of endogenous gelatinase activity in this media formulation was verified by 10% gelatin zymography. This

media formulation was selected for use to minimize the effects of serum proteases in the experimental paradigms.

Adhesion Assays

Conventional Adhesion assays. Conventional adhesion assays were conducted on surfaces coated with different extracellular proteins. These experiments are designed to examine the initial stages of cell adhesion. Conventional adhesion assays were subsequently used in conjunction with various MMP inhibitors to investigate how this family of enzymes might modulate initial adhesion.

In preliminary conventional adhesion experiments, 96 well flat bottom culture plates (Immunolon HB2, ThermoForma) were coated with various concentrations (0, 1, 5, 10, 25, or 100 μg protein/ml of PBS in 250μl) of Type I collagen (Vitrogen 100, Palo Alto, CA), laminin (EHS, Sigma), or fibronectin (Human Plasma, Sigma) or poly-l-lysine (0.01% 70k-150k in 250μl, Sigma) overnight at 4˚C. The protein concentrations translate into surface densities of 0.007 μg protein/mm^2, 0.035μg/mm^2, 0.07 μg/mm^2, 0.21μg/mm^2, and 0.7μg/mm^2, respectively. This range of extracellular protein concentrations (ECM) was selected to produce 2D surfaces that exhibit an incremental increase in the number of available ECM sites for specific adhesion. After coating all wells were blocked with 2% BSA (1 hour) and rinsed with PBS prior to experimentation.

Trypsin released cells were counted and plated onto the different surfaces in 100μl of depleted media or ITS media for varying time points from 30 min to 4 hours. Non-adhering or floating cells were removed by blotting the plate upside down on lint-free

towels and a single gentle rinse with PBS. This rinse was done by tilting the dishes to approximately 45^0 angle and allowing the rinse solution to flow slowly across the bottom of the dishes. Adherent cells were stained and fixed with 100 µl of 0.5% (w/v) Methylene Blue (Fisher Scientific) prepared in 50/50 ethanol/ water for 30 min at room temperature. Excess stain was removed by 3x flooding with ddH_2O and aspiration. The retained dye was solubilized with 100 µl of 1% Sodium Dodecyl Sulphate prepared in ddH_2O. Absorbance at 620 nm was read after 1 hour in a Molecular Devices SpectramaxPlus spectrophotometer [189].

In 30 minute adhesion assays the absolute cell number present on the dishes at the conclusion of the experimental interval was determined by extrapolation against a standard curve of cells seeded onto plates coated with 100 µg/ml Type I collagen. Data sets were screened by one-way ANOVA, absolute cell numbers that were adherent to the different surfaces were compared by pairwise multiple comparison using the Holm-Sidak method. In 60 minute adhesion assays the numbers of cells present on each ECM substrate was expressed as a percentage of cells present on poly-l-lysine. Once again these data sets were screened by one-way ANOVA, the Holm-Sidak method was used for multiple pairwise multiple comparisons.

Centrifugal adhesion assays. The strength of adhesion of CF to different surfaces was tested using a centrifugal adhesion assay. In this assay cells are allowed to adhere to a given surface for a defined interval of time and then subjected to a controlled centrifugal force that is oriented perpendicular to the plating surface (*i.e.* the plates are centrifuged

upside down). See [189] for additional discussion. These assays were conducted in Immunolon HB2 96 well plates (ThermoForma) that had been coated overnight at 4˚C with 10 μg/ml of Collagen type I (Vitrogen 100), Fibronectin (Human Plasma) (Sigma Aldrich), EHS Laminin (Sigma Aldrich) or Poly-L-Lysine (Sigma Aldrich, 100 μl 0.01% 70k-150k) prepared in PBS. The plates were rinsed with PBS and blocked for 1 hour at room temperature with 1% BSA in PBS.

Cells were trypsinized with 0.25% Trypsin/EDTA (Invitrogen) from 150 mm^2 tissue culture flasks. Complete Media was used to quench any residual trypsin activity. Cells were recovered by centrifugation (800 x G for 8 min) for cell plating and suspended in ITS media. The cells were counted and diluted to the target stock concentration desired for a particular experimental protocol (1.0×10^6 or 5×10^4 cells/ml) using ITS media. These stock concentrations were used to deliver 2,000 to 40,000 cells per tissue culture well, depending upon the nature of the specific experiment or the concentration of cells needed in the assay (*e.g.* sparse vs. dense cell cultures).

Statistical evaluation of the centrifugal adhesion assays was conducted in 2 steps. At the conclusion of the initial 1 hour plating interval the number of cells present on each surface was expressed as a percent present on poly-l-lysine. At this stage of the experiment the data sets are equivalent to the data sets generated by a conventional 1 hour adhesion assay. These data sets were screened by one-way ANOVA, the Holm-Sidak method was used for multiple pairwise comparisons. The objective of the centrifugation paradigm is to examine how the controlled force applied by centrifugation impacts cell adhesion as a function of ECM substrate. Cell number at this juncture of the experiment was expressed

as a percent of cells present on each matched substrate at the conclusion of the 1 hour initial adhesion interval. For example, at the conclusion of the experiment the number of cells present on collagen after centrifugation was expressed as a percentage of the number of cells present on collagen after 1 hour of adhesion. Data sets were screened by one-way ANOVA, the Holm-Sidak method of pairwise multiple comparison was used for multiple pairwise comparisons.

Enzyme Inhibition.

The use of pharmacological inhibitors was employed to inhibit the activity of extracellular proteases to test the hypothesis that enzymes of the MMP family play a role in the processes that control the adhesion of CF to specific substrates. The broad spectrum collagenase inhibitor GM6001 (Ilomastat; Chemicon, CC1010) [191,192,193] and the gelatinase MMP specific inhibitor, SB-3CT (Chemicon, CC1500) were used in these experiments [194,195,196]. In cultured cells the typical working dosage of GM6001 is 10-25μM with inhibition coverage for MMP-1 (K*i* = 4 nM), MMP-2 (0.5 nM), MMP-3 (27 nM), MMP-8 (0.1nM) and MMP-9 (0.2nM) [197]. SB-3CT is more selective and inhibits the activity of MMP-2 (K*i* = 0.0139 +/- 0.0004 μM) and MMP-9 (K*i* = 0.6 +/- 0.2 μM) [198]. Cells were diluted for experimentation from a starting stock concentration of 5 x 10^4cells/ml.

GM-6001. For experiments using GM-6001, the stock concentration (2.5 mM) was prepared to a working stock (100μM) in PBS and diluted as necessary to achieve the desired working concentrations. Dilutions that were used during experimentation include;

5, 10, 25 μM. Vehicle control (DMSO) was prepared following this same dilution format. The preparation of sample groups is depicted in the table below.

GM-6001 (μM)	Cell Volume	Inhibitor/Vehicle	Media	Total Volume
0 μM	1600 μl	0	2.4 ml	4 ml
5 μM	1600 μl	200 μl	2.2 ml	4 ml
10 μM	1600 μl	400 μl	2.0 ml	4 ml
25 μM	1600 μl	1000 μl	1.4 ml	4 ml

SB-3CT. A stock solution of 20 mM was prepared and diluted 1:20 in Buffer R (50 mM HEPES pH 7.5, 150 mM NaCl, 5 mM $CaCl_2$, 0.01% Brij-35, and 50% DMSO) to a final concentration of 1 mM. This stock solution was then diluted to 200 μM in ITS media. Vehicle control dilution was made based on this dilution. Final doses used in experimentation included; 1, 5, 10, 25 μM. In table format, experiments conducted with 2000 cells per well on a 96 well plate in a well volume of 100 μl would have the following culture tubes prepared for plating.

SB-3CT (μM)	Cell Volume	Inhibitor/Vehicle	Media	Total Volume
0 μM	1200 μl	0 μl	1.800 ml	3 ml
1 μM	1200 μl	15 μl	1.785 ml	3 ml
5 μM	1200 μl	75 μl	1.725 ml	3 ml
10 μM	1200 μl	150 μl	1.650 ml	3 ml
25 μM	1200 μl	375 μl	1.425 ml	3 ml

Adhesion experimentation with protease inhibitors. The proper volume of cell solution was added to the media/ inhibitor solution to generate the desired plating number. This mixture was gently swirled to ensure an even distribution of cells with inhibitor and was incubated with intermittent swirling for 30 min prior to plating onto different ECM coated surfaces. During the protease inhibitor incubation, a standard curve of CF that had been serially diluted over a five point range (A=4000 cells/well, B=2000 cells/well, C=1500 cells/well, D=1000 cells/well, E=500 cells/well) were plated onto tissue culture wells coated with 10 μg/ml type I collagen (Type I acid soluble collagen, Vitrogen).

Following the 30 min protease inhibitor incubation interval, 100 μl of cell suspension was plated in triplicate on each of the substrates Collagen type I (0.07 μg protein/mm^2), Fibronectin (0.07 μg protein/mm^2), Laminin (0.07 μg protein/mm^2), and Poly-l-Lysine (100 μl 0.01% 70k-150k) to be examined and incubated for 1-4 hour at 37˚C. At the conclusion of the adhesion interval media was carefully aspirated and replaced with 100 μl of media supplemented with of Calcein AM solution (2 μM in PBS-D) and allowed to incubate for 15 min at room temperature. Following this interval, non-adhering cells were removed by blotting the plate upside down on lint-free towels. The wells were filled with 200 μl of PBS-D (1x PBS, 1% Sodium Bicarbonate, 200 mM Dextrose) and an initial fluorescence measurement was conducted at 485 nm excitation/520 nm emission using a BMG Labtechnologies FLUOstar. This measurement provides a baseline for comparison and standardization and represents the relative number of cells that are retained on each substrate at the onset of centrifugation. The wells were

then filled completely with PBS-D and sealed. The plate was placed upside down in a custom plate carrier (ThermoForma, 5785) and centrifuged for 1 min at 51rcf in a (ThermoForma 5682 GP8R) centrifuge. With the plate remaining upside down, the sealing tape was removed and the contents blotted to remove any non-adhering cells. Wells were filled with 200 µl of PBS-D and a final absorbance measurement was taken to determine the relative number of cells remaining on the plates after centrifugation.

In preliminary experiments the timing of the Calcein AM labeling was varied to test for possible global metabolic effects that protease inhibitors or carrier solvents might induce on the cultures. If one or another of these agents were to adversely and or selectively effect the uptake of the Calcein AM the relative number of cells present in a culture may be under (or over) estimated due to a metabolic effect (poor uptake or stimulated uptake of the Calcein AM). For these experiments freshly suspended cells were allowed to recover from trypsin digest for 10-15 min and exposed to Calcein AM labeling. Cells were rinsed by centrifugation (800 x G, 8 min) and processed with inhibitors as described in the centrifugation adhesion experiments. This approach makes it possible to ensure that all cells are exposed to the same pool of Calcein AM. However, this strategy increases the length of time that a particular cell population is maintained in suspension, a condition that appears to non-specifically reduce the absolute number of cells that will adhere to the ECM substrates. In summary, the results of these experiments, in conjunction with cell viability assays, indicate that there is no measurable impact of the enzyme inhibitors or carrier solvents on the accumulation of the Calcein AM indicator. As a result

of these preliminary observations, the experiments documented in this study were conducted by labeling plated cells with Calcein AM.

Statistical analysis of the adhesion data generated from the centrifugal assays was conducted in two separate steps. In the first analysis the number of cells present at the conclusion of the initial plating interval (as estimated from Calcein AM labeling) was expressed as a percent of the cells present on poly-l-lysine. A 2-way ANOVA was used to screen data sets for the impact of substrate composition (Factor 1: collagen, laminin, fibronectin or poly-l-lysine) and the impact of drug dose (Factor 2: drug dose) on cell adhesion (Data). The Holm-Sidek method was used in multiple pairwise comparisons. Second, after the centrifugation interval the number of cells present on each substrate was expressed as a percent of the number of cells present on each specific substrate at the onset of centrifugation. These data also screened by two-way ANOVA, where, once again Factor 1=substrate (collagen, laminin, fibronectin or poly-l-lysine) and Factor 2= (drug dose) and the data was the percentage of cells present on each surface. The Holm-Sidek method was used for multiple pairwise comparisons.

Viability assays. The use of viability assays occurred in parallel with the design and in defining the parameters used in our adhesion assays. Assays were conducted to verify that cell viability remains constant under the conditions used to define cell adhesion. The selective loss of cells (for any reason) from this type of an assay manifests itself as a reduction in total cell adhesion. As such, many of these assays were conducted on CF that had been plated and allowed to adhere for a defined time interval prior to the cultures being supplemented with drug or vehicle. These assays were designed to parallel the cell number

used for plating in adhesion assays (2k and 40k/ per well/ 96 well plate.) Viability was assessed by routine microscopy, and with two metabolic based measures; the WST-1 assay and with Calcein AM. The WST-1 assay is typically used as an assay to measure cell proliferation; in this study we utilize this assay to determine the potential toxicity of the inhibitors (GM-6001 and SB-3CT) used in conventional and centrifugal adhesion assays. This colorimetric assay relies on the conversion by mitochondrial dehydrogenases of the WST-1 tetrazolium salt to formazan. The accumulated formazan can be measured at an absorbance at ~450nm. Calcein AM is metabolically dependant as well; however, it is the metabolic cleavage of this dye that 1) converts Calcein AM to Calcein, the fluorescently active species of the dye, and 2) decreases the membrane permeability of the dye thereby "trapping" the dye in the cell and providing a "direct" measure of cell number. Accumulated Calcein was measured at 480ex/520em. As stated, theses assays were conducted in concert with the process of determining the parameters; the type of inhibitor (GM 6001 / SB-3CT), the concentration of that inhibitor, and the density at which CF were plated. These assays function to validate the adhesion data and suggest a cell number/density dependant response to treatment with MMP inhibitors. As the scope of adhesion assays narrowed, viability testing became more focused and was tailored to encompass the relevant inhibitor concentrations and cell density.

Viability was assessed on collagen, laminin, and fibronectin under the following sets of conditions;

Inhibitor	Assay	Cells Per well	Dose/ Vehicle	Timing of dose	Incubation time
GM-6001	WST-1	40k	0, 10, 25μM	After 30min	4hr
SB-3CT	WST-1	40k	0,1,5,10,25μM	At plating	4hr
SB-3CT	WST-1	40k	0,1,5,10,25μM	At plating	24hr
SB-3CT	WST-1	2k	0,1,5,10,25μM	At plating	24hrs
SB-3CT	CalceinAM	2k	0,1,5,10,25μM	At plating	24hrs
SB-3CT	WST-2	2k	0,1,5,10,25μM	At 24, 26, 28hr post plating	6hr,4hr,2hr

Data from viability assays on SB-3CT was expressed as the percent of activity detected in the untreated, substrate matched control. Data from each plating substrate was treated with one-way ANOVA (P=<0.001) and followed with pairwise multiple comparison using the Holm-Sidak method with an overall significance level of 0.05.

Microscopy

Hoffmann Modulation Contrast. The morphology of live cardiac fibroblasts was examined using a Nikon Eclipse TE 300 microscope equipped with Hoffman modulation optics and Nikon DXM 1200 digital camera. Culture plates were coated with various ECM substrates or poly-l-lysine as described at a rate of 0.07 μg protein/mm^2 (optimized ECM density that supports maximal adhesion for each of the surfaces assayed). Cells were plated at a rate of approximately 55 cells per mm^2, a density equivalent to that used in adhesion assays. Cells were plated in depleted media and cultured for 4 hours. Non-

adherent cells were rinsed from the wells by PBS rinsing, and the cultures were re-fed with depleted media. Imaging was conducted with a 40x objective at the 4 hour time point and again at 24 hours post plating.

A similar approach was used to examine the effects of GM 6001 on cell morphology. These experiments were run in parallel with the adhesion assays. Cells were incubated with inhibitor (10 and 25 μM) and plated onto plates coated with 0.07 μg protein/mm^2 with collagen, laminin, fibronectin, or Poly-l-lysine (100 μl 0.01% 70k-150k). Cells were imaged at the time of plating or following a 30 min and a 4 hour interval of culture.

Given observations concerning the effects of gelatinase inhibition on cell adhesion, the morphological impact of SB-3CT was documented by time lapse microphotography in cultures plated onto different ECM substrates. CF were plated onto collagen, laminin, fibronectin (all at 0.07 μg protein/mm^2) or poly-l-lysine in the presence or absence of 10 μM SB-3CT or vehicle control (Buffer R) in ITS Media . Over the next 60 min images were captured at 2 min intervals; data files (.TIFF) were compiled and converted to a Windows Media File format. For presentation in this document selected time points (0, 10, 30, 40, 50, 60min) for each data set are presented in graphical format for side-by side comparisons. In a similar set of experiments, CF were plated onto laminin in the presence or absence of 25 μM SB-3CT. Times series were taken for the one hour interval following plating, and for one hour following the addition of inhibitor to cells that had been plated for 24 hours. This dose was abandoned due to overt toxicity issues.

Colocalization experiments: Quantitative scanning confocal microscopy. To document the spatial relationships between specific integrins, MMP-2 and MT-MMP1 co-localization experiments were conducted. Coverglass slides, #1.5 were acid etched (100% Nitric acid) and rinsed extensively in PBS and distilled water and autoclaved. The glass coverslips were allowed to air dry and coated at a rate of 0.07 μg protein/mm^2 with collagen, laminin, fibronectin or poly-l-lysine (100 μl 0.01% 70k-150k) overnight at 4^0C. Surfaces were blocked for 1 hour with 1% BSA prepared in PBS; CF were then plated onto each surface for 1 hour at 37^0C. At the conclusion of the plating interval cultures were rinsed in PBS, fixed in 4% para-formaldehyde for 5 min rinsed 3x with fresh PBS and blocked for 2 hours with 500 μl normal serum at 4^0C.

Members of the integrin family that were imaged in these experiments include the β_1 integrin (AB1952, Chemicon), the α_1 chain (AB1934, Chemicon), the α_2 chain (AB1936, Chemicon), the α_3 chain (AB1920, Chemicon) and the α_5 chain (AB1952, Chemicon) all in rabbit polyclonal format. Based on previous work these represent the principle integrins expressed by the rat neonatal cardiac fibroblast (Kanekar, 1998). A monoclonal mouse anti-MMP-2 was used to image this protease (IM51, Calbiochem). A monoclonal rabbit isolate was used to detect MMP-MT1 (Ab51074, Abcam). DAPI was routinely used to image the nuclei of the cells. Secondary antibodies used for detection included goat anti-rabbit 488 (A11034, Invitrogen), and goat anti-mouse Texas Red (T862, Invitrogen.)

Images for co-localization analysis were captured on a Leica DMIRE2 confocal microscope using a 63x oil immersion lens with a N.A. of 1.4, x-y resolution of 0.1394 μm, x-z resolution of 0.2358 μm. Images were captured at 400Hz with a line average setting of 4 and formatted at 1024 x 1024 pixel dimensions. With this optical setup and pixel dimensions a minimum zoom of 3.37X is necessary to achieve Nyquist sampling parameters and a voxel size of 69.03nm x 69.03nm. PMT settings were set within the dynamic range of the collectors and maintained constant during the capture of images from different slides. Sequential scanning was used to collect all data in the "between lines" mode for image capture. Three separate PMTs were used; the first PMT was set up for interference reflection to direct and verify the plane of focus was at the cell-coverslip interface, the second PMT was set to capture a narrow bandwidth in the vicinity of 520 nm, and the third PMT was set to capture wavelengths in the vicinity of 615 nm. During the initial set up for each experiment all instrumentation settings were optimized to eliminate chromophore bleed through between PMTs 1-3.

JACoP (Just Another Colocalization Plugin) in the NIH Image J software package (http://rsb.info.nih.gov/ij/) was used for image analysis. Data generated from this software include; 1) Pearson's Correlation Coefficient, 2) the Overlap coefficient and, 3) Mander's coefficient.

Pearson's Correlation Coefficient looks at the overall relationship between two channels. This analysis effectively determines the "strength" of the relationship that might exist between images. This method determines the correlation of fluorochrome association given by linear regression. For example, the position of each antigen site in 1 channel is

plotted against the position of each antigen site in channel 2 in a scatterplot. When these values are most coincident, a single straight line with positive slope is generated. If this line is positive in slope there is (+1) perfect colocalization; however, if this line is negative in slope (-1) there is perfect inverse correlation. A slope of (0) represents that the channels are not correlated. The tighter the distribution of points in channel 1 are with the points in channel 2, the closer to (1) is the correlation between these channels. Partial correlation occurs when not all of the molecules imaged in channel 1 are coincident with the molecules imaged in channel 2. The plotting of the point to point position of channel 1 with channel 2 then deviates from perfect correlation and a single straight line, and graphically has a wider distribution.

In Overlap analysis, the correlation coefficient ranges in value from 0 to 1 and provides an indication of the overlap that exists between two channels of interest without sensitivity to variations in signal intensity. The relative insensitivity to variations in signal intensity originates in the calculation of the Overlap coefficient. In the equation for calculating the overlap coefficient, the mean pixel intensities for each channel are not subtracted from the original pixel intensities. This is the primary difference between Overlap and Pearson's Coefficient an analysis where the mean channel intensity is subtracted. By not subtracting the mean channel intensity the result is a correlation coefficient that reflects the "raw" overlap between channel 1 and channel 2. Addressing the issue of differences in intensity of the channels are the component coefficients, k(1) and k(2). Briefly, k(1) is dependant on the values of intensity of Channel 2 whereas k(2) is

dependant on the values of intensity in Channel 1, and the product of these component coefficients is equal to the square of the Overlap. When there is greater variation in the intensity of Channel 1 as compared to Channel 2, the value of k(2) will be higher than the value of k(1).

Mander's coefficients indicate the percentage of each antigen that is present in one channel that is co-incident with another molecule present in the second channel. For example, given M1, this data represents the percentage of the molecules present in channel 1 that are participating in overlap with a molecule imaged in channel 2. The data might look at 100 sites of M1 and ask how many of these sites are coincident with M2. Then the analysis takes the converse circumstances and asks the question "for 100 M2 molecules present in channel 2 how many of these are coincident with M1 in channel 1?" It follows from this discussion that it is possible for 100% of the molecules in channel 1 to be coincident with molecules present in channel 2. However, if the molecules present in channel 2 far out number the molecules present in channel 1 the converse circumstances will not be true. Substantially less than 100 of the molecules in channel 2 may be associated with molecules in channel 1 under these circumstances. This condition was detected in the analysis of Mander's coefficient for the association of MMP-2 ("channel 1 in this example") with the α_2 integrin ("channel 2").

Interference Reflection Microscopy.(IRM) In this imaging mode the focal plane at the cell/ substratum interface produces a maximal amount of reflection off the sample (*i.e.* the image background is dark when the imaged focal plane is not at the cell-substratum

interface and becomes progressively brighter as the interface is approached). At the cell substratum interface the sites where cell processes are most tightly linked (closest) to the underlying substratum appear dark, sites of contact just distal to the actual contact sites appear grayer in the final image [113]. IRM approach unambiguously identifies the sites where cells and the surface of the coverslip are in contact with one another.

Interference reflection microscopy was used to characterize focal adhesion structure with respect to protein markers of these structures. Number 1.5, 22 mm x 60 mm cover slips (Fisher) were etched with nitric acid for 15 min, neutralized with PBS, rinsed with ddH_2O and autoclaved prior to substrate coating. Coverslips were coated with collagen, laminin, fibronectin (0.07 μg protein/mm^2), or poly-l-lysine (100 μl 0.01% 70k-150k) overnight at 4^0C, rinsed with PBS, and blocked with 1% BSA for 1 hour. Cells were plated for varying lengths of time depending upon the nature of experimentation. All cultures were rinsed gently with PBS and fixed in 3% paraformaldhyde for 10 minutes. Cultures were permeabilized with 0.1% Triton X-100 prepared in PBS, rinsed in PBS and blocked (3% BSA, 10% Normal Goat Serum, 0.1% Tween 20 in PBS or as otherwise noted in specific experiments using interference reflection microscopy as a method to identify the cell substratum interface) for 30 min at room temperature.

Mouse monoclonal anti-talin (T3287, Sigma) antibodies were applied at 1:40 overnight at 4ºC. Samples were counter stained with Texas Red goat anti-mouse (1:200, Invitrogen) and with 2 units fluorescein phallodin for 1 hour at room temperature. Selected cultures were stained with DAPI to detect nuclei. Coverslips were mounted with anti-fade mounting media (Vector) and sealed with nail polish. Confocal images were taken with a

63x objective using a 6x zoom setting with a Leica DRE2 scanning laser scanning confocal microscope.

Gelatinase Labeling

To conduct localization and competition experiments in live cells MMP-2/ MMP-9 gelatinase zymography standards (Chemicon, gelatinase standard, CC073) were labeled with rhodamine. Briefly, the EZ-Label Rhodamine Protein labeling kit (Pierce 53002) was used according to the manufactures protocol for the labeling of gelatinase standard. In this reaction, 50 µl of stock gelatinase standard (Chemicon) was labeled with 1 µl of NHS-Rhodamine. Labeled MMP was dialyzed against PBS to remove un-incorporated rhodamine. The rhodamine labeled gelatinase (RLG) standard was frozen at -70˚C in 5 µl aliquots. RLP was run separated by SDS gel electrophoresis and processed for gelatin zymography to verify that the labeling procedure did not overtly alter protein structure or cause the formation of multimeric complexes.

Titration of Gelatinase label. Experiments utilizing confocal microscopy were conducted to determine the localization of exogenously applied RLG protein as well as to optimize the amount of labeled gelatinase needed for use in future experimentation. CF were incubated in suspension (20k cells/ml) in ITS media supplemented with a 1000 fold range of RLG. Serial dilutions were made as follows:

A) 5 µl of RLG stock solution to 20 ml ITS media (solution A)
B) 1 ml of solution A added to 9 ml ITS media (Solution B=10X dilution of A)
C) 1 ml of solution B added to 9 ml ITS media (Solution C= 100X dilution of A)
D) 1 ml of solution C added to 9 ml ITS media (Solution D=1000X dilution of A)

Cardiac Fibroblast were incubated in RLG formulations for 30 minutes and centrifuged for 8 min at 800 x G, media was decanted and cells were suspended in 10 ml of fresh ITS media. Cells were pipetted into 4-well Lab-Tek II Chambered slides that were coated at a rate of 0.07 µg Type I collagen/mm^2 and allowed to adhere for 1 hour at 37^0C. Chamber wells were rinsed with PBS and then fixed with 3% paraformaldhyde for 15 min. Cultures were rinsed 3x with PBS and permeablizied with the addition of 500 µl of 0.01% Triton X-100 prepared in PBS for 5 min. Cultures were rinsed 3x with PBS. In the final rinse, 2 units of fluorescein phallodin were added to each well for the visualization of F-actin. After 15 min, the samples were rinsed with PBS, and mounted in anti-fade media (Vector Laboratories). Samples were imaged by laser scanning confocal microscopy as described.

Results from preliminary dilution experiments using various concentrations of the RLG indicated that dilution "D" described in the previous discussion provides more than adequate signal for the detection of surface associated gelatinase. Next, unlabelled "cold" gelatinase (ULG) was added to the experimental paradigm over the 1000 fold range used in the initial RLG experiments. The objective of this approach was to determine if it is possible to chase off the labeled gelatinase in manner analogous to a radio immune assay. In these experiments varying concentrations of ULG were added to a constant

concentration of RLG and mixed. Control (ITS supplemented with 10 μg/ml BSA) and ITS media containing no additional gelatinase were used to determine the non-specific effects of adding protein or fresh media to the cultured cells. Each media formulation was added to an equal density of cells and gently mixed. Replicate cultures were incubated at 4^0C (cold) or at 37^0C (warm) for 1 hour in solution. At the conclusion of this incubation interval the suspended cells were pelleted by centrifugation (800 x G for 10 min), re-suspended in 200 μl of PBS and plated by centrifugation (51rcf x 5 min) onto coverslips coated with collagen (0.07 μg/mm^2). This plating procedure was used to minimize the potential impact that adhesion processes might have on the distribution of surface associated MMPs. Cultures were fixed with 3% paraformaldhyde for 15 min, rinsed with PBS 3x, and stained with fluorescein phallodin.

Evaluation of SB-3CT effects on cell surface associated MMPs. Experiments were conducted to determine if the distribution of cell surface associated MMP-2 gelatinase in the living state is effected by the SB-3CT inhibitor. These experiments, while largely unsuccessful (in the sense that the inhibitor did not displace the MMP-2 molecule), provided indirect evidence that the integrin MMP-2 complex is structurally stable in the face of challenge by protease inhibition. A series of 4-well Lab-Tek II Chambered (#1.5 Borosilicate Coverglass; NalgeNunc) were coated at a rate of 0.07 μg protein/mm^2 with collagen type I (adhesion is sensitive to MMP inhibition) or with EHS Laminin (adhesion to this surface is not sensitive to MMP inhibition) overnight at 4^0C and then blocked for 1

hr with 1% BSA prepared in PBS. Cells in suspension were treated to one of the following interventions:

1) Exogenous RLG (5 ul/20ml ITS media)
2) Exogenous RLG (5 ul/20ml ITS media) + SB-3CT
3) Exogenous RLG and vehicle (DMSO)
4) Baseline controls, no treatment.

Cells were incubated for 30 min in each of the conditions as described. Cells were then plated at 55 cell mm^2 as per conventional adhesion experiments for 1 hour and then rinsed 3x with 500 µl of PBS. Cultures were fixed in 3% para-formaldehyde for 10 min, rinsed 3x with fresh PBS and blocked for 2 hours with 500 µl Normal Goat serum at 4^0C. Primary monoclonal mouse-anti MMP-2 antibody (Ab-4, Oncogene) was applied at a rate of 5 µl per well in 200 µl of blocking buffer for 1 hour at room temperature. In this application, blocking buffer is formulated in PBS supplemented with 3% BSA, 10% Normal Goat Serum, and 0.1% Tween 20. Chambers were rinsed 3x for 15 min with blocking buffer on a rotating table at room temperature. Primary antibodies were imaged with a Texas Red conjugated goat anti-mouse antibody (Molecular Probes, Eugene OR, 1:200) diluted into blocking buffer for 1 hour at room temperature. The chambers were then rinsed 3x with PBS + 0.1% Tween 20 for 15 min intervals. These antibody complexes were then fixed with 3% paraformaldhyde and rinsed 3x for 15 min with PBS + Tween 20. The chambers were then incubated overnight at 4^0C with 500 µl of blocking buffer.

For β_1 integrin staining, 250 µl of Rabbit anti-β_1 (1:500, Chemicon, AB1952) was prepared in blocking buffer and added to each well for 1 hour at room temperature. Cultures were incubated with blocking buffer 3x for 15 min. Alexa 488 conjugated goat anti-rabbit antibody (Molecular Probes) was used for detection at a dilution of 1:200 in blocking buffer. The secondary antibody solutions were supplemented with 2 µl of DAPI for the detection of DNA. Chambers were rinsed 3x with PBS + 0.01% Tween 20. A final brief rinse with ddH_20 was used to reduce salt contamination. One drop of medium set anti-fade mounting media (Vector Laboratories) was delivered to each well. Images were captured using a Leica DMIRE2 scanning laser confocal microscope.

Immunoprecipitation

A variety of different immunoprecipitation (IP) strategies were used to characterize the structural relationships that exist between members of the integrin family and MMP-2. This section will describe the methods used to immunoprecipitate antigens from cell lysates. Experiments in which immunoprecipitation was used to evaluate specific events will be described in sub-sections that are experiment specific.

Routine immunoprecipitation. Cells were plated on 100 mm x 15 mm Falcon Petri dishes for 1 hour at 37^0C, media was decanted and the plates were rinsed 3 X with 10 ml sterile PBS. Cultures extracted in 1 ml ice-cold, modified RIPA buffer (50 mM Tris-HCl, 150 mM NaCl, 1% Triton X-100, pH 7.4). In selected experiments this buffer was

supplemented with protease inhibitors (Roche, 11 836 145 001). On ice, cells were removed from the plate with a cell scraper (Falcon), the lysate was quantitatively recovered and transferred to a 1.5 ml microcentrifuge tube. Cell lysates were placed on ice for 30 min with occasional mixing and centrifuged at 10 G for 15 min at 4^0C (Eppendorf, 5804 R). Supernatant was decanted, without disturbing the pellet, and transferred to a clean 1.5 ml centrifuge tube.

Cell lysates were pre-cleared using normal serum appropriate to the primary antibody used in the IP. A 20 µl aliquot of normal serum (2 mg/ml normal serum; Rabbit or Mouse, Pierce Immunopure) was added to each lysate sample and allowed to incubate at 4^0C for 30 min on a shaker. Next, 50 µl of protein A/G agarose beads (Santa Cruz, SC-2003) was added to each solution, samples were incubated for 60 min on ice and centrifuged at 10 x G for 10 min at 4^0C. Supernatant was decanted, without disturbing beads and transferred into a clean centrifuge tube (if beads were disturbed, samples were spun again and transferred to a new tube). Each pre-cleared cell lysate was supplemented with 5 µl of the primary (precipitating) antibody and incubated on ice for 2-8 hour at 4^0C on a shaker. Following this interval, 50 µl of protein A/G agarose beads was added and incubated at 4^0C on a shaker for 60 min. Tubes were then spun at 10 x G for 1 min at 4^0C. Without disturbing the pellet, the supernatant was decanted, and the beads were washed with 500 µl of ice-cold, modified RIPA buffer. The wash, centrifugation cycle, and aspiration cycle was repeated 3-5 times. Following the final wash, 80 µl of 1x Laemmli buffer (Bio-Rad, Cat # 161-0737) was added to the bead pellet. Samples were placed in a

pre-heated (95^0C) dri-bath for 3-5 min (Thermolyne, Type 16500 Dri-Bath). Samples were once again centrifuged at 10G for 5 min and the supernatant was recovered for analysis.

Antibodies used in these experiments include:

- Anti β_1 integrin, Chemicon
- Anti MMP-2, IM51 Calbiochem
- Anti MMP-9, IM73 Oncogene

Samples were immediately separated by SDS-PAGE (25 µl per sample) or gelatin zymography. Selected material recovered by IP was frozen until needed at -20°C.

Crosslinking of cell surface Except were noted, the bulk of the experimentation presented in this document was conducted with cells with a "native" plasma membrane. However, during early experimentation cell surface associated proteins were crosslinked to stabilize protein-protein interactions using DTSSP (21578, Pierce). This reagent has an effective cross linking distance of 12 Å. In these experiments CF were plated out onto poly-l-lysine coated 6 well dishes in ITS media. Following one hour of plating, cultures were rinsed 2x with PBS, cultures were then supplemented to a final concentration of crosslinker at 1 mM in PBS and allowed to incubate for 30 min at room temperature. The reaction was quenched with the addition of sufficient Tris (stock solution 1 M, pH 7.5) to bring the final Tris concentration to 15 mM for 15 minute incubation. At this point cultures were treated with cell lysis buffer in preparation for SDS-PAGE. Parallel cultures without the use of crosslinker were processed for SDS-PAGE.

Seize IP. By definition conventional IP experimentation recovers the primary antibodies used to identify (capture) an antigen of interest. When this type of material is processed for Western blot analysis the primary antibodies can be dislodged from the protein A/G agarose beads used to initially recover the antigen complex. Subsequently, these primary antibodies can and clearly do appear as a component element in the analysis of the antigen complex. This condition can introduce artifacts into the analysis of the recovered material; this is especially a consideration when Western blot analysis is conducted. The primary or secondary antibodies used to probe the recovered antigens may react with the contaminating precipitating antibodies that have been dislodged from the agarose beads. The presence of this contaminating antibody restricts the species of antibodies that can be used to probe the blot, can cause interference and ambiguity if the molecular weight of the antigen of interest overlaps with the contaminating antibody, and or limits the selection of antibodies that can be used in the Western blot analysis (due to cross-reactivity and or poor specificity of the secondary detection antibodies).

To validate the conventional IP experiments, IPs were also routinely conducted with primary antibodies cross-linked to the surface of agarose beads using a Seize primary IP kit (Pierce, 45335). Cross-linking the primary antibody of interest to the agarose beads negates the need for the protein A/G interaction for the capture of the antibody/antigen complex and eliminates the risk of antibody contamination in the eluted antigen fraction. This method is identical in the preparation of cell lysate as described above under "routine immunoprecipitation." The seize IP method was used in experiments designed to test the

the interaction of β_1 integrin and MMP-2, to identify the α integrin chain(s) involved, and to determine the interaction of TIMP-1 and TIMP-2 with the $\alpha_3\beta_1$: mmp-2 complex.

Primary antibodies of interest were coupled to agarose beads supplied by the manufacturer as per AminoLink Plus Coupling Gel recommendations. The process of coupling the antibody to the beads involved "activation" (using the buffers supplied by the kit) of the beads, over-night incubation at 4°C with mixing, and a series of rinsing and washing steps to remove any uncoupled antibody present on the beads. The reactions using this kit take place in a spin cup placed in the top of a 2 ml centrifuge tube which allows for ease of rinsing and elimination of possible bead contamination during the elution of antigen. In brief, approximately 2 million cells were prepared as cell lysate either from suspension or following one hour of plating in ITS media in 1 ml of modified RIPA buffer by a 30 minute 4°C extraction with agitation. Lysate was then centrifuged for 30 minutes 4°C at 14 K rpm to remove debris. Prepared lysate (333uL) was added to the antibody conjugated beads or frozen at -20°C for future analysis. Conjugated beads and lysate were incubated with end-over-end mixing overnight at 4°C. Column was then spun to remove flow through and washed (3X) to clear any nonspecifically bound material on the beads. Antigen complexes were eluted in a series of three repetitive elution steps by lowering the pH with the supplied elution buffer. The fractions were kept separate for analysis by Western blot. For Western blotting, eluted material was mixed at a ratio of 20ul:5 ul of 5X sample buffer, heated to 65°C for 5 min, allowed to cool, and loaded at a rate of 25 ul per gel well for 10% SDS-PAGE. When reduction of sample was necessary, samples were prepared to a final concentration of 5% 2-mercaptoethanol, and heated to 95°C for 5

minutes. The Seize IP format was used for the pull down of antigen complexes recognized by the following antibodies (coupled to beads) and these antibodies were used in antigen detection as primary antibodies in Western blotting.

Primary antibodies used in these assays include:

- Anti- α_1 integrin, Rbt polyclonal (AB1934, Chemicon)
- Anti- α_2 integrin, Rbt polyclonal (AB1936, Chemicon)
- Anti- α_3 integrin, Rbt polyclonal (AB1920, Chemicon)
- Anti- α_5 integrin , Rbt polyclonal (AB1946, Chemicon)
- Anti- β_1 integrin, Rbt polyclonal (AB1952, Chemicon)
- Anti- TIMP-2, Rbt polyclonal (ab38973, Abcam)
- Anti-TIMP-1, Rbt polyclonal (AB800), Chemicon)
- Anti- MMP-2, Ms Monoclonal (IM51, Calbiochem)
- Normal Mouse IgG, (12-371, Upstate)

Secondary Antibodies;

- HRP labeled Anti- Rabbit, Goat (H+L)(PI-1000, Vector)
- HRP labeled Anti- Mouse, Horse (H+L)(PI-2000, Vector)

Immunoprecipitation and gelatin zymography. Gelatin zymography was conducted on samples recovered by IP against β_1 Integrin. Material recovered by IP was first separated

by conventional SDS gel electrophoresis on a 10% slab gel and transferred to PVDF for Western blot analysis against β_1 and/or MMP-2 (AB1952, Chemicon; IM51, Calbiochem, respectively.) Representative fractions of the IPs were then subjected to gelatin zymography.

Zymography. Equal volumes of whole cell lysate or protein fractions purified by IP were mixed with Laemmli buffer and separated on a SDS 10% polyacrylamide gel supplemented with 1.0% gelatin. Gelatinase standards (Chemicon) were loaded (20 µl of stock solutions that had been diluted 1:200) were used as positive controls to identify MMP-9 and MMP-2 enzymatic activity. In experiments that focused on MMP-2, pro-MMP-2 (Calbiochem, PF037) was used as the positive control (20 µl of a 1:200 dilution of the stock solution). Following electrophoretic separation at 120V (constant voltage), gels were incubated in renaturation buffer (BioRad) for 1 hour and then transferred into development buffer (Bio-Rad) for 18 hour at 37ºC. Gels were fixed (20% Methanol, 10% Glacial Acetic Acid, 70% distilled de-ionized H_2O) and stained with Coomassie Blue, G-250 (Bio-Rad). De-stained gels were imaged (Gel Doc 2000, BioRad) and analyzed by densitometry (Quantity One, BioRad) to characterize gelatinolytic activity.

Following development and documentation, the gelatin zymograms were transferred to PVDF for Western Blot analysis against MMP-2. The preparation of these samples was done in the absence of exogenous protease inhibitors (to allow protease activity associated with IP material to function and degrade the gelatin present in the zymograms). Lanes were loaded with a whole cell lysate prepared from a CF cell

suspension, an IP to β_1 (AB1952, Chemicon), or recombinant human MMP-2 pro-enzyme standard (PF037, Calbiochem). The anti-MMP-2 antibody used in these experiments recognizes the 72 kDa latent and 66 kDa active species of MMP-2.

*Western Blotting***.** Following protein separation by SDS-PAGE, gels were incubated in Towbin buffer (Tris-Glycine, 20% MeOH) for 30 min to equilibrate and remove residual SDS. Simultaneously, PVDF Membranes (BioRad) was activated by a brief incubation in 100% methanol and then equilibrated in Towbin Buffer. Transfer cassettes were loaded and placed into a Criterion Blotting chamber (Biorad) for the transfer of proteins from gels to PVDF membranes, transfer was effected at 125 mA for a total of 1250 mA/hour at 4^0C. Following the transfer interval, the appearance of the molecular weight standard on the PVDF was used to visually verify the transfer process. PVDF was blocked in 5% Non-Fat Dry Milk prepared in PBS/0.01% Tween-20 for a minimum of 30 min. To reduce "spotting" artifacts blocking buffer was made at least 1-2 hour prior to use to ensure the milk was fully dissolved when applied to the PVDF membranes. Primary antibodies were applied overnight at 4^0C or for 1 hour at room temperature with constant agitation. Antibodies were applied to the blots in 10 ml of Blocking buffer per 7 cm x 8.4 cm sheet of PVDF. Specific dilutions included:

- Rb anti-α_1 1:1000 (Chemicon, AB1934),
- Rb anti-α_2 1:1000 (Chemicon, AB1936),
- Rb anti-α_5 1:500 (Chemicon, AB1949),
- Rb anti-β_1 1:1000 (Chemicon, AB1952),

- Rb anti-TIMP-2 1:1000 (Abcam, ab38973)
- Ms anti-MMP2 1:5000 (EMD, IM51),
- Ms anti-MMP-9 1:5000 (EMD, IM73).

Following incubation with primary antibodies the PVDF membranes were rinsed extensively with PBS-0.1% Tween 20 (5 rinses for 15 min/ rinse) under constant agitation. Prior to the application of secondary horse radish peroxidase labeled antibodies, blots were placed in blocking buffer for additional 30 min incubation. This step was found to further reduce non-specific background staining. Again, 10 ml of antibody solution was used per sheet with secondary antibody concentrations of 1:20,000, in blocking buffer, of either Goat anti-Rabbit (Vector, PI-1000) or Horse anti-Mouse (Vector, PI-2000) as appropriate for a 1 hour incubation at room temp. PVDF was rinsed, as previously described, and then treated for 5 min with ECL Plus Western Blot detection reagent (GE Healthcare, RPN 2132). Excess chemiluminescence solution was wicked from the PVDF, the PVDF membranes were wrapped in plastic and then secured in an 8 x 10 inch Spectroline radiographic cassette (Spectronics Corporation, Westbury, New York.). In the dark, radiographic film (Kodak BioMax MR, Rochester, New York) was placed for detection of Chemiluminescence signal. Film was developed on an automatic processor (Futura 2000K, Fischer Industries Inc, Geneva, IL). Exposure time was adjusted to optimize the signal intensity over a linear range. Developed film was then returned to the cassette and molecular weight ladder indication and blot orientation was made with indelible ink.

To verify the specificity of primary and secondary antibodies used in conventional IP and seize IP based experiments, sera were separated by SDS and transferred to PVDF as described. To test the specificity of secondary rabbit antibodies blots were stained with Goat anti-rabbit or Horse anti-mouse antibodies. If these blots remained devoid of staining the samples were stripped (100mM 2-mercaptoethanol, 2% SDS, 62.5mM Tris-HCL pH 6.7) and restained with Horse anti-mouse or Goat anti-rabbit to verify the presence of the primary antibodies on the blot and verify the specificity of the matched primary and secondary antibody interaction.

CHAPTER VII.

Identification of a MMP-2/Integrin/TIMP-2 Complex in the Cultured Neonatal Cardiac Fibroblast.

INTRODUCTION

In this chapter the structural association of MMP-2 and the $\alpha_3\beta_1$ integrin is documented in pull down assays. These experiments were conducted with freshly prepared suspensions of neonatal cardiac fibroblasts isolated from 3-5 day old pups and cultured for 2-3 passages. In several sites in the following chapters supportive evidence for various observations or experimental techniques are referenced to Appended materials. This approach was used to provide the reader with additional information with minimal interruption to the primary data presented in this chapter (which has been designed to be submitted as a manuscript in support of this thesis).

RESULTS

Immunoprecipitation from cell suspensions. The gelatinases MMP-2 and MMP-9 are expressed at elevated levels during ventricular wall remodeling in development [128] and at the onset of cardiac hypertrophy in the adult [127]. Given the association of selected

integrins with selected members of the broader MMP family, pull down assays were conducted to evaluate the possible structural relationships that might exist between these receptors and MMP-2 and MMP-9 in the rat neonatal cardiac fibroblast. Beginning with a suspension of cells in ITS Media, β_1 integrin or MMP-2 was first recovered by immunoprecipitation (IP) using Seize IP kits (ThermoScientific). The enriched material recovered by IP was eluted in 3 separate fractions from the antibody columns; each fraction was then separated by SDS gel electrophoresis under non-reducing conditions and probed by Western blot for β_1 integrin, MMP-2, or MMP-9. The Seize IP kits were used in these experiments to avoid cross-contamination/cross-reactivity of the primary antibodies with antibodies used in the Western Blot analysis (see also Appendix 1, for examples).

Western blot analysis of an IP against β_1 integrin for β_1 integrin reveals 3-5 prominent bands, depending upon the elution fraction, running at 210-220 kDa, 180 kDa, 110-120 kDa, 60 kDa and 40 kDa (Figure 1A, lanes 1-3). The lower molecular weight β_1 immunoreactivity represents intracellular domain containing fragments [113]. Blotting this same isolate for MMP-2 revealed a single band in each of the 3 fractions recovered from the antibody columns running at 210-220 kDa (1A, lanes 4-6). Immuno-reactive MMP-9 was not detectable in this same assay or in a raw cell pellet fraction of cardiac fibroblasts plated for 1 hour in ITS Media. However, MMP-9 was detectable by zymography in the soluble media fraction recovered from CF plated for 1hour (see also Appendix 2 for this data).

In the converse series of experiments, Western blot analysis of an IP against MMP-2 for MMP-2 detected 2-3 bands (again, depending on the elution fraction examined).

Elution fraction 1 exhibited a single prominent band running at 210 kDa. Elution fractions 2 and 3 exhibited 3 bands, running at 220 kDa, 210 kDa and 180 kDa (Figure 1B, lanes 1-3). Blotting material recovered by an IP against MMP-2 for β_1 integrin revealed a single distinct band running at 210-220 kDa (Figure 1B, lanes 4-6).

Given these results, zymographic analysis was conducted to confirm the presence of gelatinolytic activity in material recovered by an IP against the β_1 integrin subunit. In these experiments, protease activity was only detected in IPs directed against β_1 that were recovered in the presence of the gelatinase specific inhibitor SB-3CT (Figure 1C). This protease activity was present on the gels in association with a 200+kDa protein that appears to correspond to the complex detected by the initial IP experiments. This result is somewhat counterintuitive; however, it is possible that MMP-2 protease activity is at such a high concentration in material recovered by IP that the enzyme is subject to some degree of auto-proteolytic degradation during processing under baseline conditions [139]. Consistent with this conclusion gelatinase activity was present near the base of each gel lane; this low molecular weight material was present even in samples treated with SB-3CT gelatinase inhibitor. The gelatinolytic activity present in lanes treated with SB-3CT is probably a reflection of the method used to assay gelatinase activity; this drug does not completely suppress all MMP-2 proteolytic activity in this type of analysis (see Appendix 3, Figure 1). As judged by zymography, SB-3CT suppresses approximately 50% of the MMP-2 associated gelatinase activity present in this type of analysis.

FIGURE 1

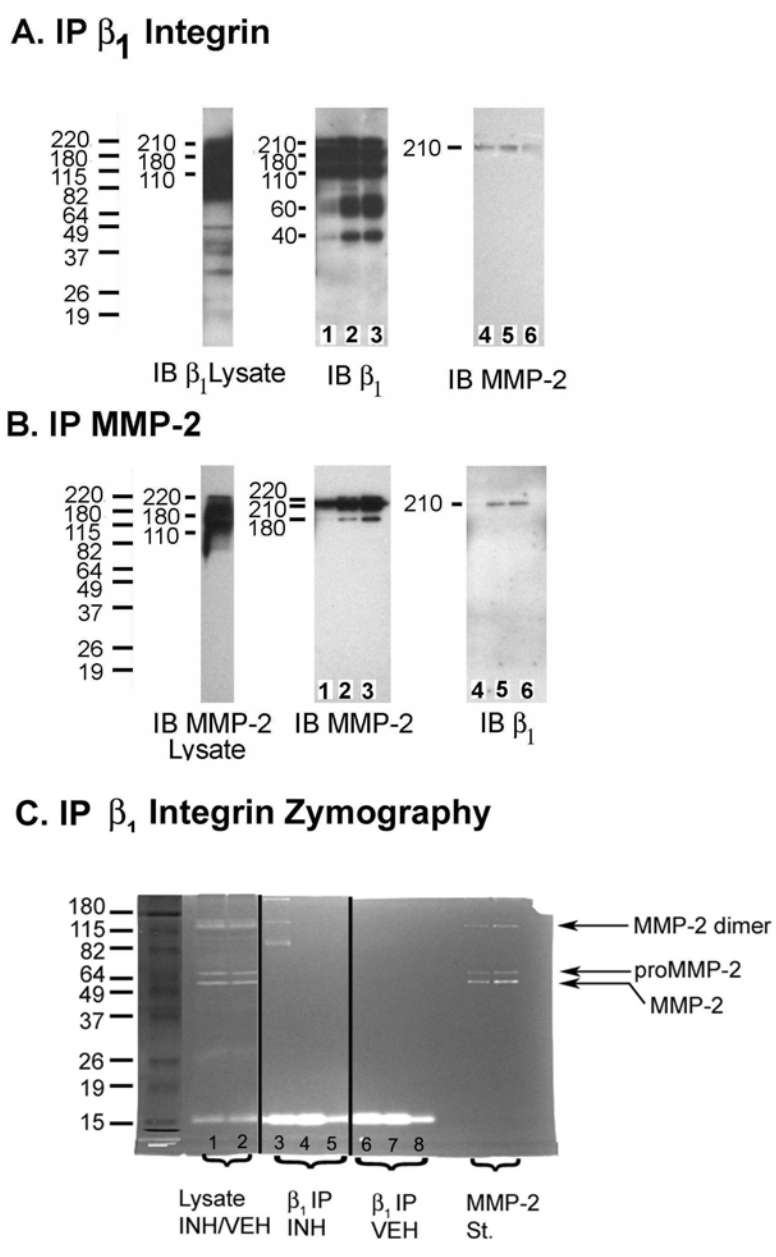

Figure 1

Figure 1. *Immunoprecipitation (IP) experiments; Identification of a complex of β_1 integrin and MMP-2.* Panel (A) represents various fractions recovered from cardiac fibroblasts subjected to immunoblotting (IB). IP against β_1 integrin blotted for β_1 reveals proteins running at 210-220 kDa, 180 kDa, 110-120 kDa, 60 kDa and 40 kDa (A, lanes 1-3). MMP-2 immunoreactivity is present in association with the 210-220 kDa protein band (A, lanes 4-6). Panel (B) represents the analysis of an IP against MMP-2. Western blot analysis of this IP against MMP-2 reveals 3 bands running at 220, 210 and 180 kDa (B, lanes 1-3). β_1 integrin immunoreactivity is present in association with the 210 kDa band (B, lanes 4-6). Panel (C) represents zymographic analysis of IP to β_1 integrin with Gelatinase inhibition. Lanes 1 and 2 represent raw lysate from cells in suspension treated with 10μM SB-3CT or vehicle. Eluted fractions (Lanes 3-5) from IP to β_1 with 10μM SB-3CT or fractions (Lanes 6-8) from IP to β_1 with vehicle were processed for zymography. Zymographic analysis of an IP against β_1 integrin in the presence of SB-3CT revealed distinct bands of gelatinolytic activity (Panel C, Lane 3) at 210-220 kDa, 148 kDa and 94 kDa, representative of the intact complex, dimeric MMP-2, and pro-MMP-2 with TIMP-2, respectively. To verify the identity of the material recovered by IP selected samples were processed for zymography and then transferred for Western blot analysis and the detection of MMP-2 (see Appendix 4).(See also Appendix 2 , Figure 1 for documentation of SB-3CT inhibitory effects on MMP-2 activity).

To determine if MMP-2 is associated with a specific integrin complex an IP against MMP-2 was conducted and then probed by Western blot for β_1, or α_1, α_2, α_3, or α_5, the principle α integrin chains present in the neonatal rat cardiac fibroblast [59]. In this pull down assay, only the α_3 integrin chain was detectable in the recovered material (Figure 2). From these experiments it is clear that $\alpha_3\beta_1$ integrin and MMP-2 are present in a complex that runs at 210-220 kDa.

FIGURE 2

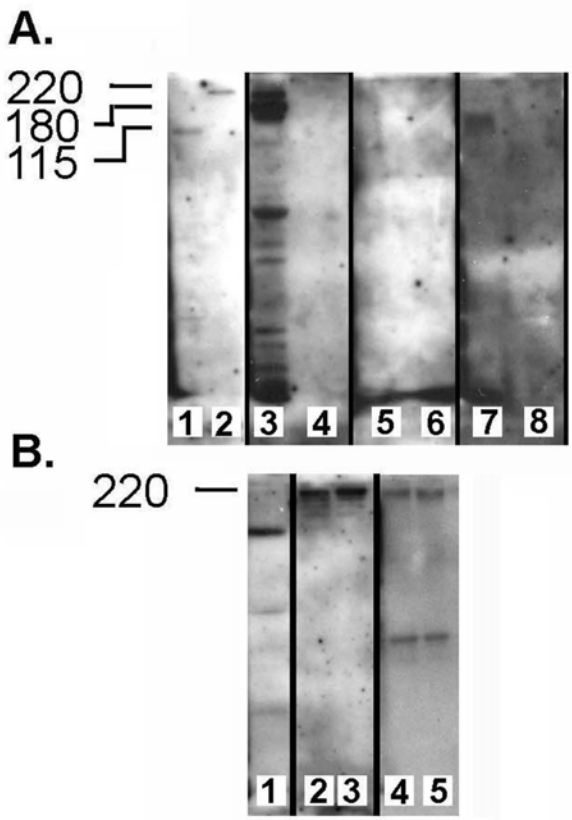

Figure 2

Figure 2. *Alpha integrin subunit analysis, composite image* (all data from non-reduced gels). MMP-2 was recovered by IP from 2 X 10^6 cells; this material was then subjected to Western blot analysis for specific integrin subtypes. Panel (A): Lanes 1 and 2 Western blot of β_1, Lanes 3 and 4=α_1, Lanes 5 and 6=α_2, Lanes 7 and 8=α_5 integrin. In this series of experiments we were able to detect the β_1, α_1, and α_5 integrin in the whole cell lysate (lanes 1, 3, 5, and 7). The β_1 chain was the only integrin subunit present in the fractions recovered by IP to MMP-2 (Lane 2). Panel (B) represents a detailed analysis of the α_3 subunit. Lane 1= Western blot against α_3 in a whole cell lysate. Lanes 2 and 3 represent the detection of the α_3 subunit in enriched material recovered by IP to MMP-2, Lanes 4 and 5 represent the detection of the MMP-2 molecule in a pull down assay against the α_3 integrin.

In vivo, MMP-2 and MMP-9 present in the ECM are bound to a TIMP molecule; these small inhibitory peptides play a role in regulating the activation state of these enzymes [199,143]. To determine if TIMP-1 or TIMP-2 are component elements of the integrin:MMP-2 complex an IP against β_1 or α_3 integrin was recovered from a suspension of cells. This material was then run under non-reducing or reducing conditions and probed for TIMP-1 and TIMP-2. Immunoreactive TIMP-1 was not detected in this assay (See Appendix 5, for representative Western blot of TIMP-1 analysis). Immunoreactive TIMP-2 was present in the recovered material. In an IP against β_1 integrin that was separated for Western blot analysis under non-reducing conditions, 2 bands of TIMP-2 positive staining were present, one prominent band at 220 kDa and a minor band at 56 kDa (Figure 3, A). When these same samples were run under reducing conditions the 220 kDa band was lost and bands running at 65, 50, 45 and 41 kDa were observed (Figure 3B). TIMP-2 has a molecular weight of 24kDa; we assume that these higher molecular weight bands detected under reducing conditions might represent complexes or multimers. In the analysis of an IP to α_3 integrin no reactivity was detected against TIMP-2 in the non-reduced format (Figure 3, C). However, when these samples were run under reducing conditions, TIMP-2 was detected in the IP from α_3 (Figure 3, D). Non-reduced samples of IPs directed against α_3 (Figure 3, E) and β_1 integrin (Figure 3, F) from these experiments were blotted against MMP-2 to confirm the existence of the putative complex. MMP-2 immunoreactivity was present in both samples at a MW of 220 kDa.

Using a starting IP against the α_3 integrin and then probing for TIMP molecules produced similar, albeit not identical results when an IP against β_1 integrin was used as the

starting material. Under non-reducing conditions no TIMP-2 was detectable in the recovered material. However, when this same sample was separated under reducing conditions, protein bands running at 86, 55 and 50 kDa were detected. These data would suggest that the antigenic site for the TIMP-2 peptide is sequestered when the complex is isolated by an IP against α_3 integrin and separated under non-reducing conditions. This sequestration may occur because this aspect of the peptide represents the linkage site to the α_3 integrin [200].

FIGURE 3

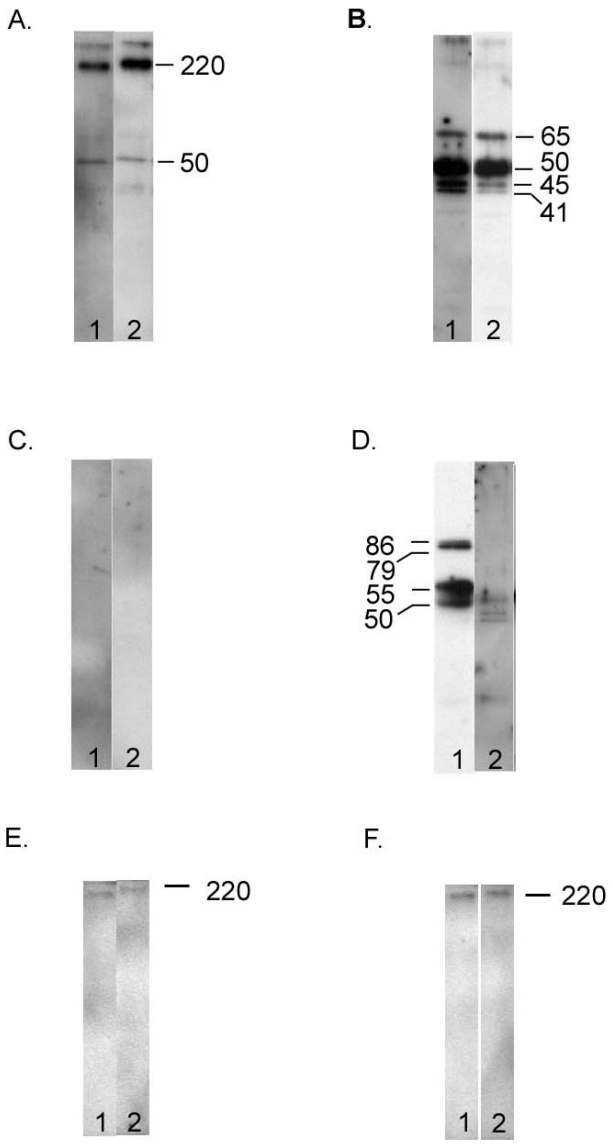

Figure 3

Figure 3. *Identification of TIMP-2 as a component of the $\alpha_3\beta_1$ integrin / MMP-2 complex.* Cells (2 X 10^6) were suspended and then incubated in the presence or absence of 10 μM SB-3CT or Vehicle for 30 minutes, immunoprecipitated and separated under non-reducing or reducing conditions. Panel (A) represents the detection of TIMP-2 from a β_1 directed IP under non-reducing conditions: lane 1 with SB-3CT, lane 2 without SB-3CT. Panel (B) represents the detection of TIMP-2 from a β_1 directed IP under reducing conditions: lane 1 with SB-3CT, lane 2 without SB-3CT. Panel (C) represents the detection of TIMP-2 from an α_3 directed IP under non-reducing conditions: lane 1 with SB-3CT, lane 2 without SB-3CT. Note the absence of staining. Panel (D) represents the detection of TIMP-2 from an α_3 directed IP under reducing conditions: lane 1 with SB-3CT, lane 2 without SB-3CT. Panel (E) and Panel (F) represent blotting against MMP-2 as non-reduced samples from IP to α_3 or to β_1, respectively; lane 1 with SB-3CT, lane 2 without SB-3CT.

To address the possibility that MMP-2 might become secondarily associated with the $\alpha_3\beta_1$ integrin complex when the cell lysates are prepared for IP pull down analysis, live cardiac fibroblasts were treated with the cross-linking agent DTSSP (Pierce). In these experiments the cross-linking reagent links peptides that are within 12 Angstrom of one another. Live, surface cross-linked cells were then processed for Western blot analysis. In these experiments MMP-2 was present in association with a 200-210 kDa complex. These results indirectly suggest that MMP-2 is bound to the $\alpha_3\beta_1$ integrin prior to the IP process and is not secondarily associated with this receptor as a consequence of the extraction procedures (for documentation of these results see Appendix 6).

Summary. These experiments indicate that MMP-2 and TIMP-2 exist in a complex with the $\alpha_3\beta_1$ integrin of the neonatal cardiac fibroblast. This complex is stable enough to withstand the processes used to recover IP isolated material for Western blot analysis under non-reducing conditions. One aspect of these results that is difficult to fully reconcile concerns the total MW of the isolated complex.

If the β_1 represents the ***predominate*** binding site for MMP-2, it would be expected that the α_3 subunit would run at a substantially lower MW (120-130 kDa *vs.* 210-220 kDa). The converse argument also holds true. If the α_3 subunit was the exclusive binding partner for MMP-2, the β_1 subunit should run at approximately (110-120 kDa *vs.* 210-220 kDa). However, regardless of the starting material used to recover MMP-2 in these pull down assays, immunoreactive β_1 and α_3 are present in association with MMP-2 in a complex that

has an estimated MW of 200-2120 kDa. There are several possibilities to explain these results. For example, it is possible that under non-reducing conditions that the complex runs at an aberrant MW due to its overall topography. However, it is also possible that the MMP-2 molecule is linked to both integrin subunits.

When the MMP-2:TIMP-2:$\alpha_3\beta_1$ complex is separated by SDS gel electrophoresis the 2 integrin chains may separate from one another but the linkages that the anchor MMP-2 to β_1 and MMP-2 to α_3 may be more stable, resulting in the appearance of the "common" 210-220 kDa complex that is observed. One may be composed of MMP-2, β_1 and TIMP-2 and one may be composed of MMP-2, α_3 and TIMP-2. In one case, the MMP-2 may be bound to the β_1 through the hemopexin domain [201] or the collagen binding domain [187] and to the α_3 through TIMP-2 [200]. Additional molecular experimentation will be necessary to define the exact nature of the complex.

CHAPTER VIII

Functional Implications of MMP-mediated Protease Activity In Cell Adhesion Processes in the Cultured Neonatal Cardiac Fibroblast.

INTRODUCTION

The association of MMP-2 with the $\alpha_3\beta_1$ integrin suggests this protease plays a role in the process of cell adhesion and/or migration. To explore this putative aspect of MMPs function in the neonatal cardiac fibroblast conventional 30 minute adhesion assays were conducted with plates coated with various amounts of collagen, laminin, or fibronectin. From these experiments, the optimized density of each ECM substrate that was necessary to support maximal cell adhesion was determined. Centrifugal adhesion assays were then used to characterize the relative strength of adhesion to each surface. These experiments were all conducted in the presence and absence of protease inhibitors designed to block MMP associated enzymatic activity. To limit the potential of untoward of serum elements these assays were conducted in ITS supplemented media. These experiments suggest a role for MMP in the maturation of adhesion in the Cardiac Fibroblast.

RESULTS

Conventional Adhesion Assays. In 30 min conventional adhesion assays maximal cell adhesion occurred at surface coating densities of 0.07 μg collagen/mm^2, 0.035 μg laminin/mm^2 and 0.07 μg fibronectin /mm^2 (Figure 4A). On plates coated with 0.07 μg ECM/mm^2, the minimal amount of each protein necessary to support maximal cell adhesion for each type of surface, collagen, laminin and fibronectin all supported more adhesion than tissue culture plastic or BSA ($P<0.001$). Further, at this same coating density, collagen and laminin supported more adhesion than fibronectin ($P<0.001$). When the plating interval was extended to 60 minutes under these same coating conditions, collagen, laminin and fibronectin supported similar rates of adhesion (Figure 4B). Based on these results all other experiments were conducted at an optimized surface coating density of 0.07 μg ECM protein /mm^2.

FIGURE 4

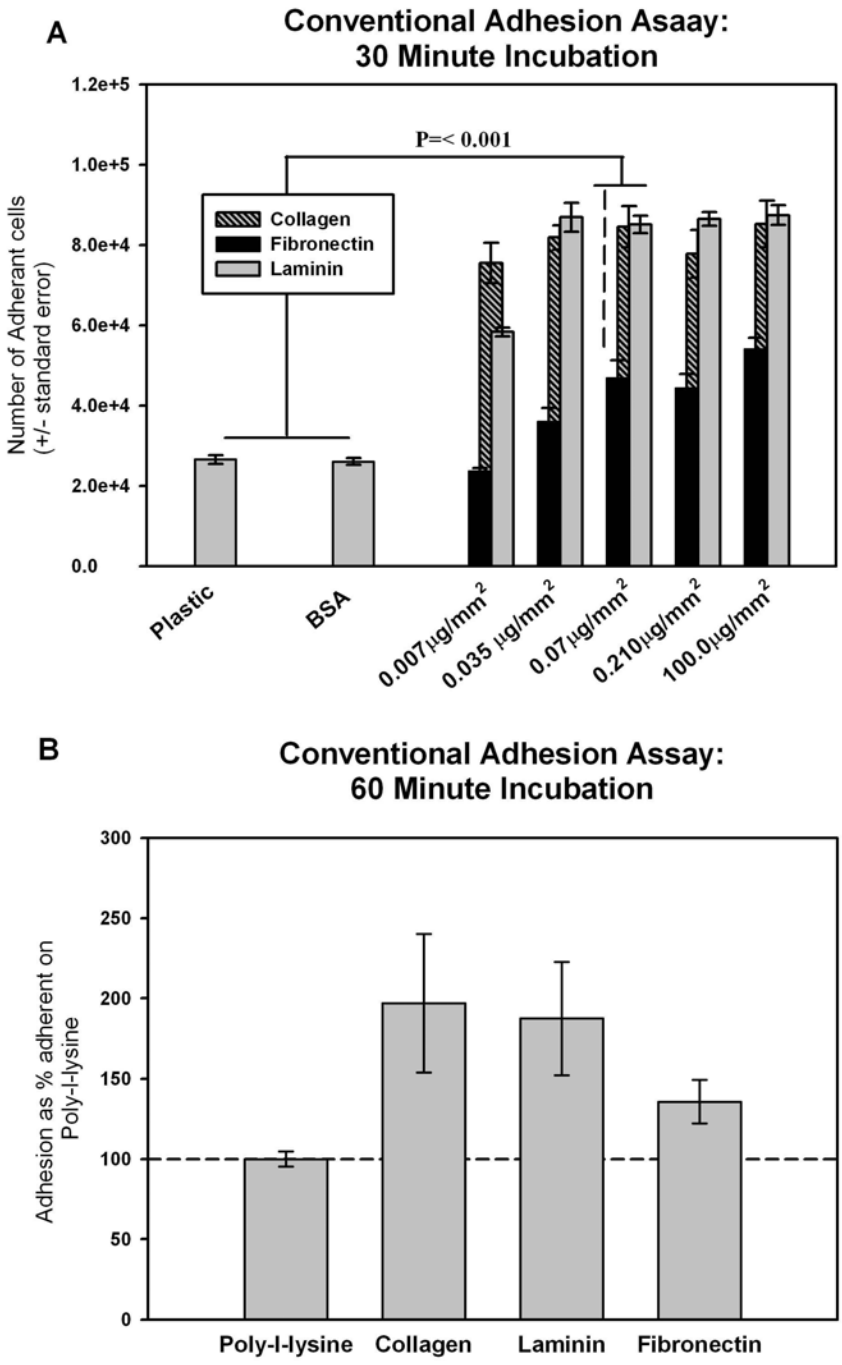

Figure 4

Figure 4. *Optimization of conventional adhesion assays:* Panel (A) 30 minute incubation and Panel (B) 60 minute incubation. The adhesion of cardiac fibroblasts to different ECM substrates increases as a function of the coating density used to prepare the plates (A). When equal numbers of cells were applied to collagen, laminin or fibronectin for 30 min maximal adhesion occurred when the plating surfaces were coated with at least 0.07 $\mu g/mm^2$ ECM protein ($P<0.001$). Each of these ECM substrates supported similar rates of adhesion at this threshold value of coating density when the plating interval was extended to 60 min (B). Each data point +/- S.E. N=3 of 3 replicates.

Pharmacological inhibition of MMP function with the inhibitor SB-3CT did not alter cell adhesion in conventional adhesion assays conducted over a 60 min incubation interval (see Appendix 3 for characterization of SB-3CT effects on MMP function). SB-3CT is a potent and highly specific inhibitor of gelatinases[198] Rates of adhesion to collagen, laminin, fibronectin, and poly-l-lysine were similar in the presence and absence of this inhibitor (Figure 5). Experiments conducted with the more general and broader spectrum, and less potent[197] MMP proteinase inhibitor, GM6001, yielded similar results (Figure 6).

FIGURE 5

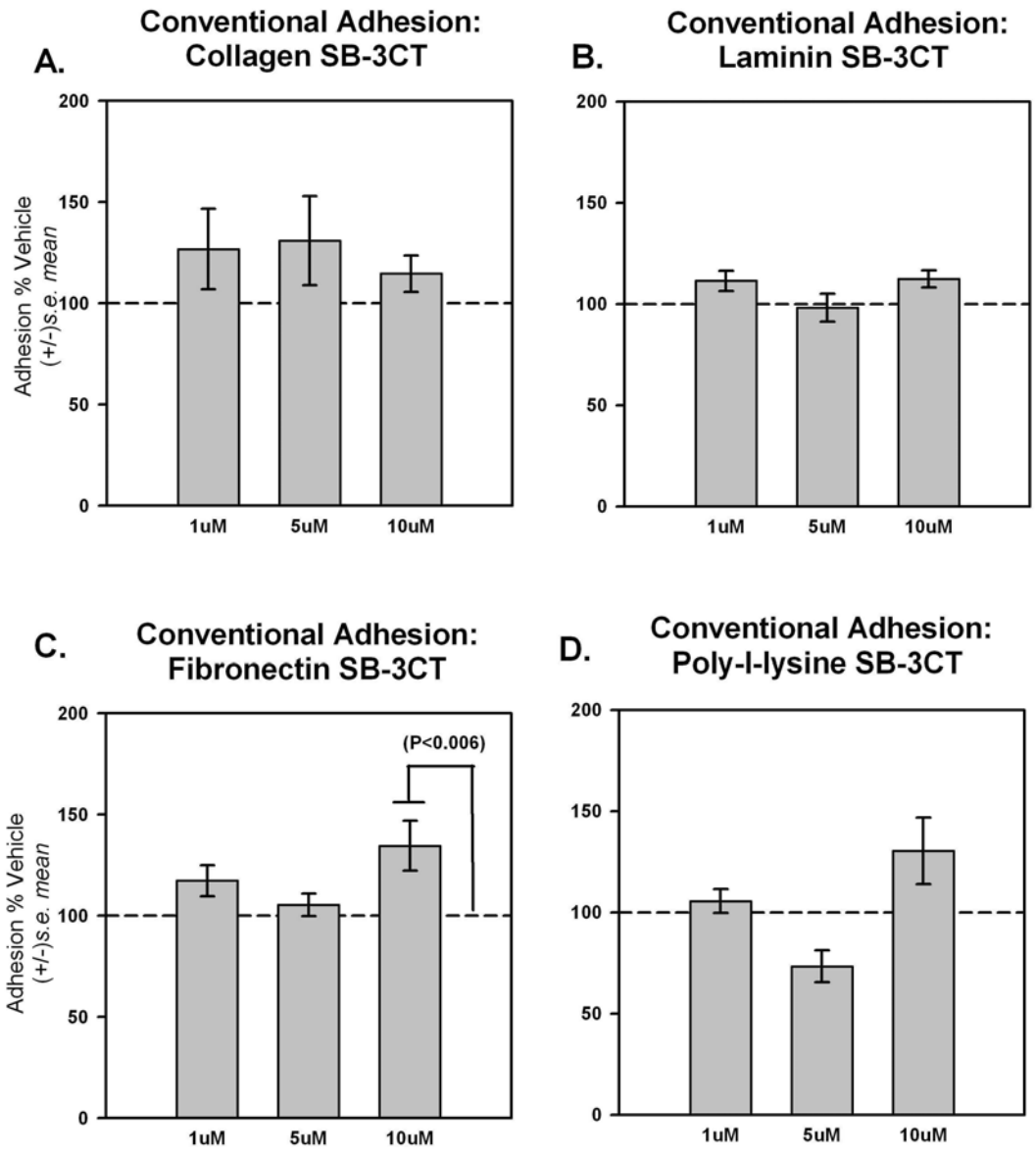

Figure 5

Figure 5. *SB-3CT does not alter initial adhesion*. Cells were plated for 60 min onto collagen, laminin or fibronectin (plates coated at 0.07 μg ECM protein/mm^2) in presence or absence of SB-3CT or vehicle. MMP inhibition with this reagent had little effect in this assay. Cultures plated onto fibronectin in the presence of this inhibitor exhibited a modest increase in adhesion with respect to vehicle treated cultures ($P<0.006$), but not to the naïve controls. Each data point +/- S.E. N=3 of 3 replicates.

FIGURE 6

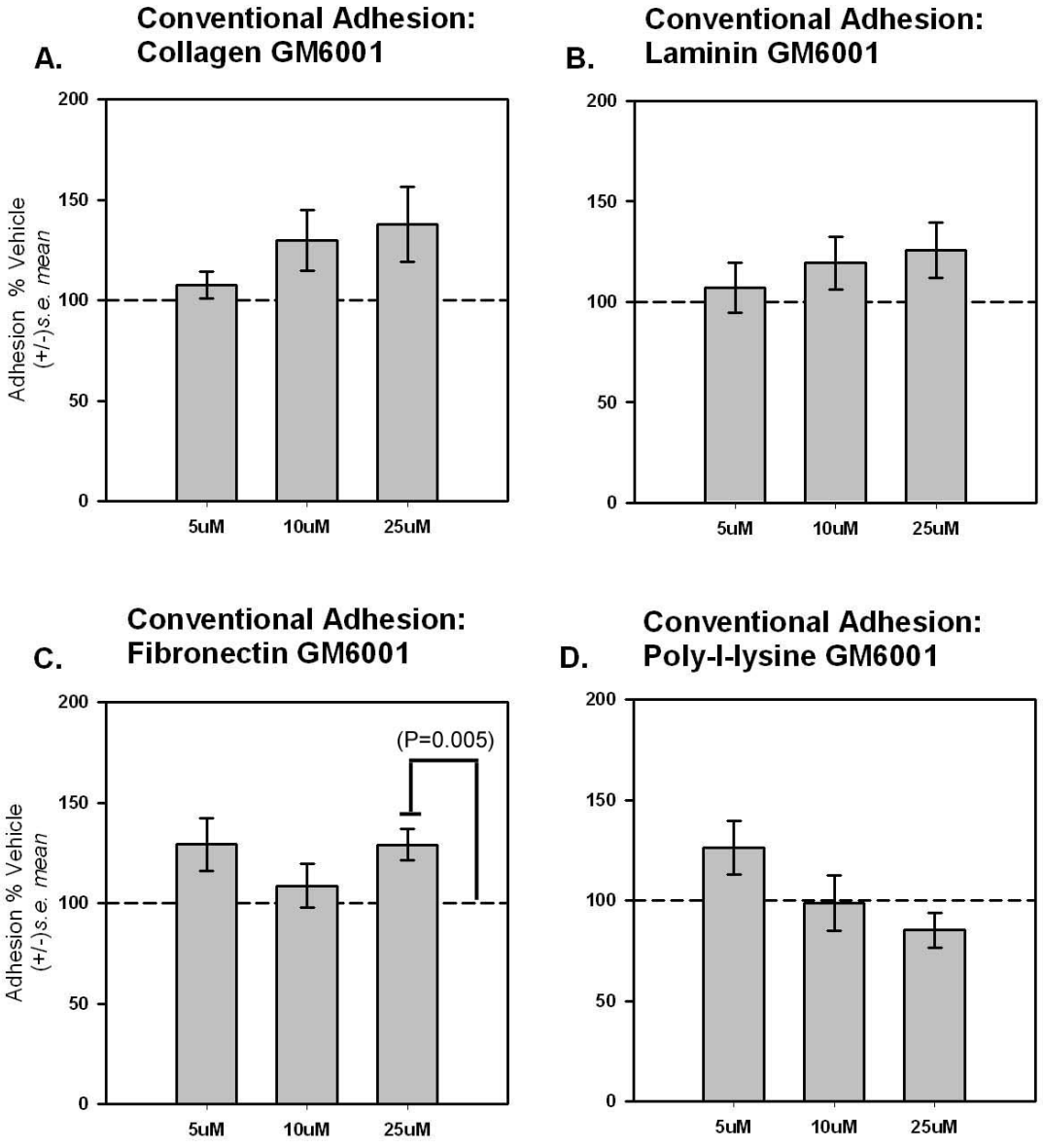

Figure 6

Figure 6. *GM6001 does not alter initial adhesion*. Cells were plated for 60 min onto collagen, laminin or fibronectin (plates coated at 0.07 μg ECM protein/mm^2) in presence or absence of GM6001 or vehicle. MMP inhibition with this reagent had little effect in this assay. An increase in the number of adherent cells was detected in cultures plated onto fibronectin in the presence of 25μm GM6001 as compared to vehicle treated cultures(P=0.005) but not to the naïve controls. Each data point +/- S.E. N=3 of 3 replicates.

Centrifugal Adhesion Assays. To characterize the strength of adhesion that was achieved over a 1 hour plating interval centrifugal adhesion assays were conducted. For these experiments, culture plates were coated with collagen, laminin or fibronectin using the optimized conditions established in the conventional adhesion assays. After the initial 1 hour plating interval the plates were inverted and decanted as if they were to be processed for a conventional adhesion assay. The plates were rinsed and a determination of the total cell number that was present was made, the plates were then centrifuged upside down to subject the cells to a calibrated force. In the centrifugal assays neonatal cardiac fibroblasts plated onto collagen and fibronectin were more strongly adherent (*i.e.* resistant to detachment by centrifugation) than cells plated on laminin or poly-l-lysine ($P<0.001$, Figure 7).

Incubating cultures with SB-3CT selectively ***reduced*** adhesion strength in cultures plated onto collagen and fibronectin with respect to non-treated controls and vehicle controls ($P<0.003$, Figure 8). This inhibitor had no effect on adhesion in cultures plated onto laminin or poly-l-lysine. Treatment with GM6001 did not impact adhesion strength in this assay (Figure 9).

FIGURE 7

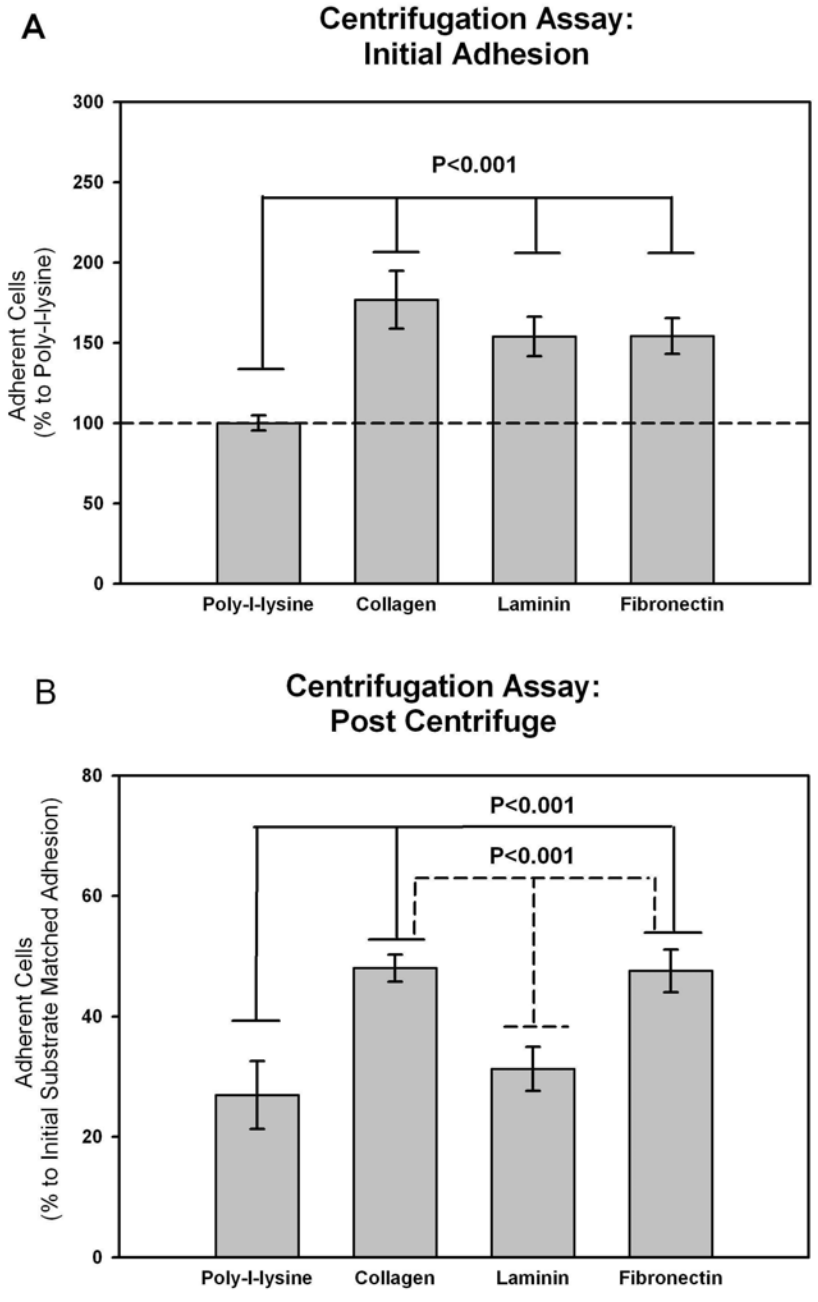

Figure 7

Figure 7. *Baseline Centrifugal adhesion assays*. Panel (A) illustrates the relative number of cells adherent to culture dishes coated with 0.07 μg/mm^2 ECM protein after a 60 min plating interval. Rates of adhesion to collagen, laminin and fibronectin were similar and all 3 supported more adhesion than poly-l-lysine ($P<0.001$). These cultures were then turned upside down and centrifuged at a calibrated force. Adhesion data in this panel is expressed as a percent cells adherent to poly-l-lysine. Panel (B) illustrates the relative number of cells adherent at the conclusion of centrifugation. Data is expressed as the per cent cells remaining adherent with respect to the number of cells present at the onset of centrifugation. Each data point +/- S.E. N=3 of 3 replicates.

FIGURE 8

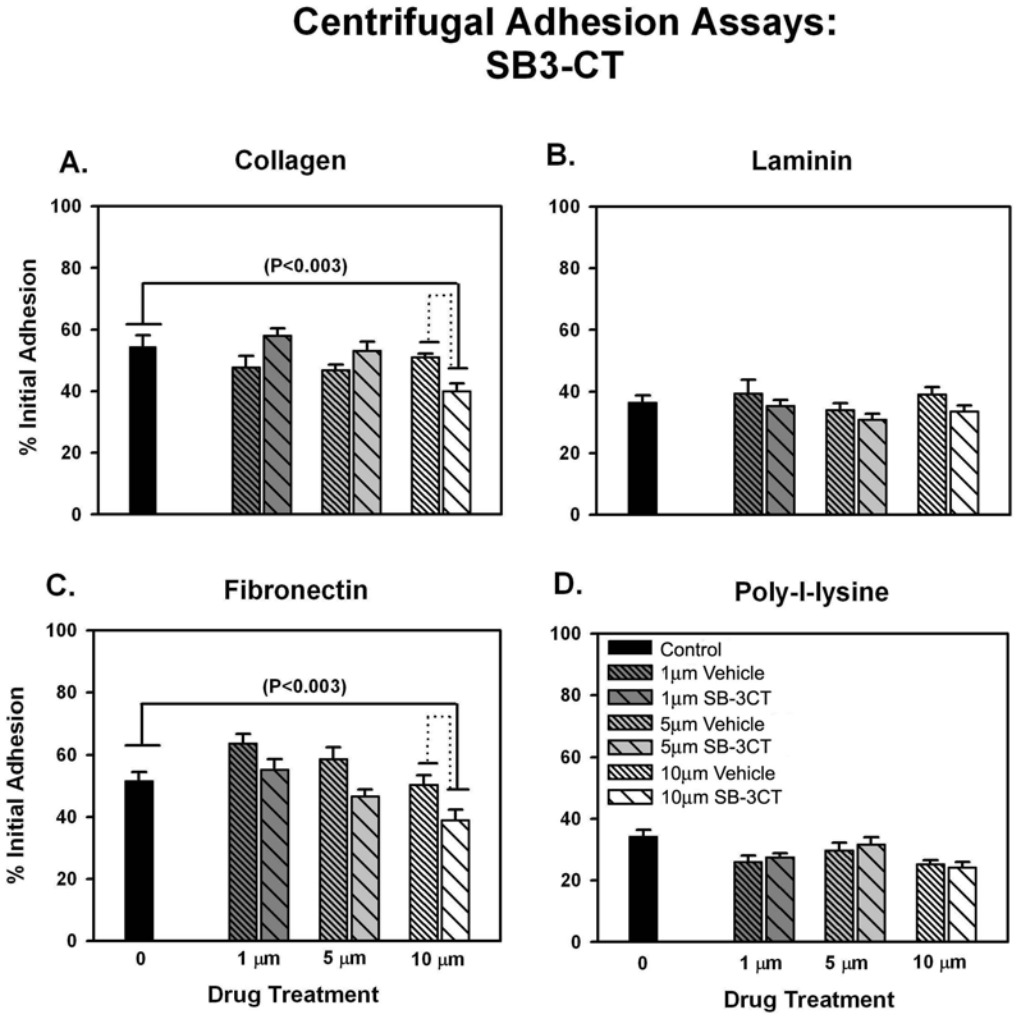

Figure 8

Figure 8. *SB-3CT impacts the strength of cell adhesion.* Cells were plated for 60 min onto collagen, laminin or fibronectin (plates coated at 0.07 μg ECM protein/mm^2) in presence or absence of SB-3CT or vehicle and subjected to a calibrated centrifugal force. Cells plated onto collagen and fibronectin ($P<0.003$) were preferentially displaced from these ECM substrates when treated with SB-3CT (A,C). Adhesion to laminin and poly-l-lysine was un-effected by this drug treatment. Each data point +/- S.E. N=3 of 3 replicates.

FIGURE 9

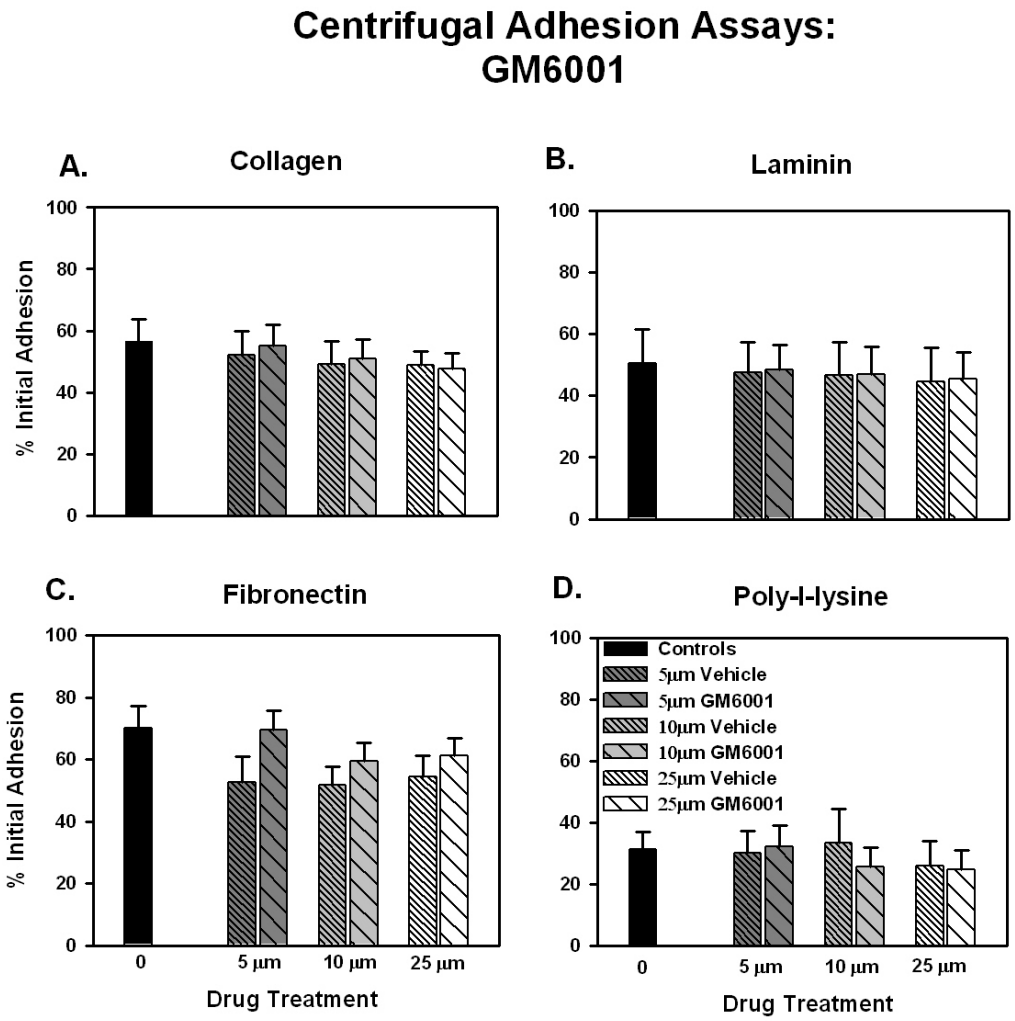

Figure 9

Figure 9. *GM6001 does not impact the strength of cell adhesion*. Cells were plated Cells were plated for 60 min onto collagen, laminin or fibronectin (plates coated at 0.07 μg ECM protein/mm^2) in presence or absence of GM6001 or vehicle and subjected to a calibrated centrifugal force. No significant change in the adhesion of CF was attributable to the application of this inhibitor. The reason for the differences in the effects of SB-3CT and GM6001 in the adhesion of CF may be a reflection of the differences in specificity of these inhibitors. N=3 of 3 replicates.

Cell Viability in the face of protease inhibition. There is a technical limitation to the adhesion based viability assays used in this study. These assays assume that any intervention that reduces the number of cells present at the conclusion of the assay will be reported as a reduction in cell adhesion. Unfortunately, any intervention that reduces cell viability also will be reported by these assays as a reduction in cell number. A 10% loss of cells due to cell death will be reported as a 10% loss of cells from the assay. A further complication arises when a particular intervention is used to study the process of cell adhesion, a variety of cell types will undergo apoptosis when adhesion is blocked or lost [202].

To verify that protease inhibition reduces cell number in the adhesion assays used in this study occurs as a consequence of impacting the adhesion process, cell viability assays were conducted under a variety of conditions (See also Appendix 7). These experiments indicate that SB-3CT has nominal effects on cell viability over the time intervals used in the assays described in this chapter (Figure 10). As per the discussion in the preceding paragraph, conducting an assay for cell viability in which the agents to be tested have an effect on cell adhesion implies inherent limitations in the design of these assays (interventions that kill cells reduce cells in the adhesion assay, interventions that reduce adhesion reduce cells in the viability assays). To address the major concern that cells will not attach if plated in the presence of inhibitors, viability was first assessed on cells that had been plated for 24 hours. In these assays there was no detectable change in metabolic activity in cultures treated with 1μM, 5μM SB3-CT or vehicle with 2, 4, and 6

hours of treatment. However, within 2 hours of treatment at the 10μM dose of SB3-CT the cultures plated on collagen and laminin exhibited approximately a 20% decrease in metabolic activity as compared to naïve and vehicle controls (P=<0.001). Under these same conditions CF plated on fibronectin were similar to naïve and vehicle controls.

FIGURE 10

A.

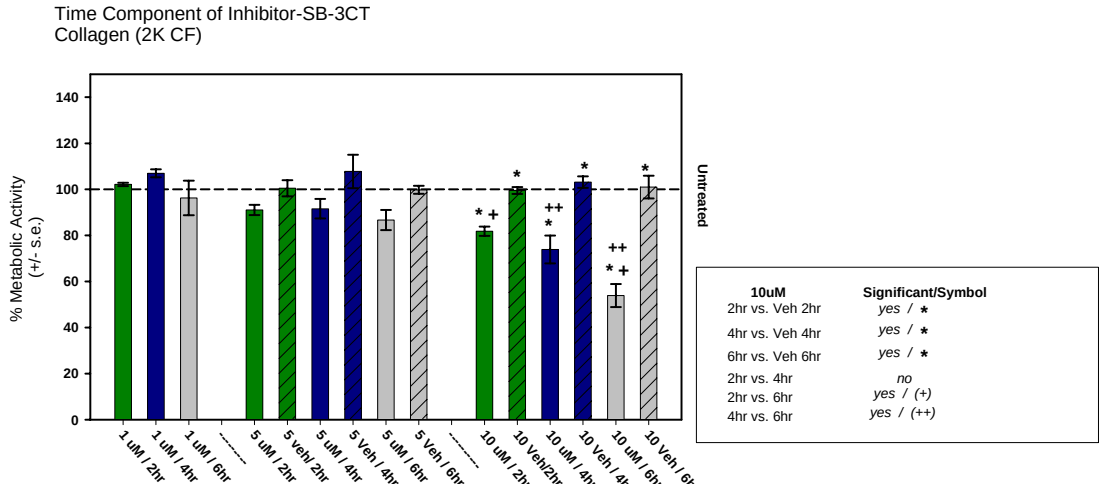

B.

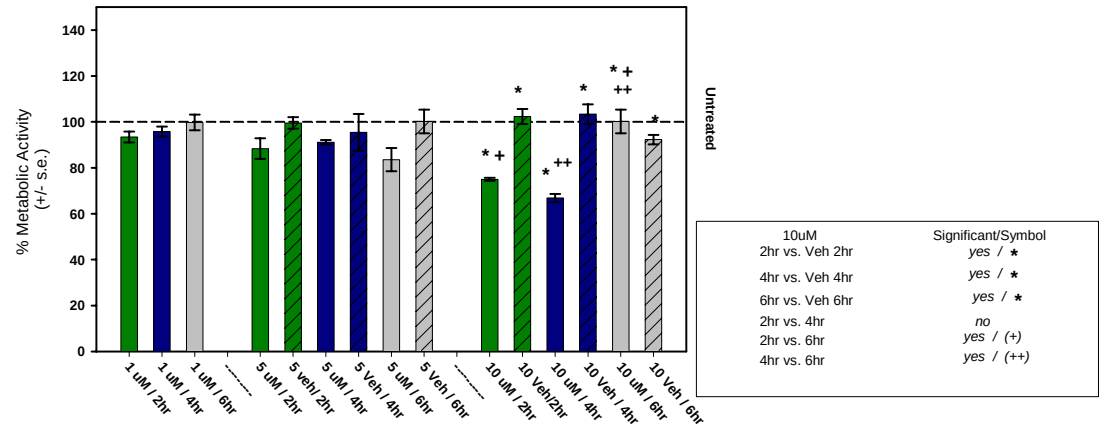

C.

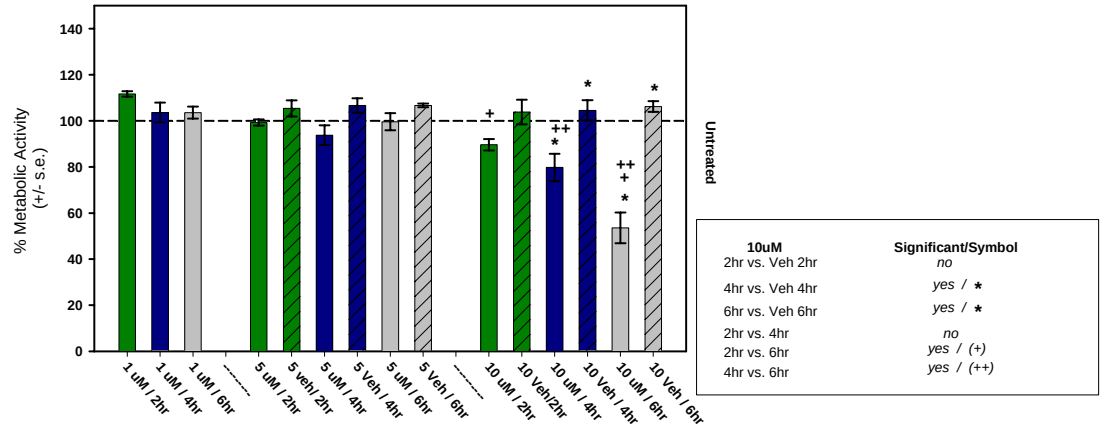

Figure 10. *Time component of cell viability.* Cultures were plated out onto collagen (A), laminin (B), and fibronectin (C) for a total of 30hours. At time points 2, 4, and 6 hours prior to assessing metabolic activity, media was aspirated and replaced with media supplemented with 1, 5, and 10um or vehicle control. No change in metabolic activity was detected at the 1 and 5uM doses in CF plated on these surfaces. At 10uM the inhibitor appeared to impact the metabolic activity of CF in a time dependant manner. In cultures plated on collagen (A) and laminin(B) there was a decrease in metabolic activity following 2hours of exposure to 10uM SB-3CT as compared to vehicle and untreated, naïve controls (P=<0.001)(with overall significance level of 0.05 for multiple comparisons). We note that initial cell adhesion was similar when CF were plated in the presence of inhibitors as compared to vehicle and naïve controls in 1hr adhesion assays. N=3

Summary. Overall the results of the conventional adhesion assays and the centrifugal adhesion assays demonstrate that cardiac fibroblasts adhere relatively slowly to fibronectin (this surface supported the least adhesion in conventional adhesion assays conducted over a 30 minute interval). However, the cells that do attach to this ECM protein are more strongly anchored than cells plated onto laminin or poly-l-lysine (more cells are retained on this surface in the centrifugal adhesion assays). The strength of adhesion of cells to collagen and fibronectin was similar in the centrifugal assays.

Treatment with SB-3CT selectively reduced cell adhesion when cells were plated onto collagen and fibronectin. GM6001 did not impact cell adhesion in these assays. Together, the cell adhesion assays and cell viability assays suggest that SB3-CT alters the total number of cells present in the adhesion assays by perturbing the processes that lead to the maturation of adhesion sites. Perhaps the most compelling series of experiments that support this conclusion are the results of the centrifugal adhesion assays. First, at the initial 1 hour time point SB3-CT does not alter the total number of cells present in the assay on any of the surfaces examined. Second, in the centrifugal portion of this same assay (which is conducted and concluded within 10 minutes of taking the initial cell number reading) SB3-CT selectively reduced cell number on collagen and fibronectin but not laminin or poly-l-lysine.

CHAPTER IX

In Situ Structural Relationships between MMP-2, Specific Integrin Subunits and MT-1 MMP in the Cultured Neonatal Cardiac Fibroblast.

INTRODUCTION

Pull down assays have detected a complex composed of the $\alpha_3\beta_1$ Integrin, MMP-2 and TIMP-2. Adhesion assays have implicated MMP mediated activity in the regulation of cell adhesion to collagen and fibronectin, but not laminin or poly-l-lysine. In this series of experiments the spatial relationships of specific integrin sub-units with respect to MMP-2 is examined using high resolution scanning confocal microscopy. The spatial relationship of MMP-2 and MT1-MMP is also evaluated with this approach. Observations made in this study were constrained to the ventral surfaces of the cells as defined by Interference Reflection Microscopy.

RESULTS

Qualitative Scanning Confocal Microscopy. To investigate the spatial relationships that exist *in situ* between β_1 integrin, specific integrin α chains, and MMP-2 qualitative and quantitative, scanning confocal microscopy was used to examine cultures of fibroblasts plated onto collagen, laminin, fibronectin or poly-l-lysine for 1 hour. These experiments suggest that the distribution and relative overlap of the integrins and MMP-2 with respect to one another is subject to regulation by the identity of the surrounding ECM. At the light microscopic level a gross examination of the cultures revealed that fibroblasts plated for 1 hour onto each of these surfaces exhibited, ***on average***, a rounded-cell shape. Cell processes extended from the central rounded domain of the cells out over the coated surfaces in a concentric pattern. Other cells within the cultures appeared less symmetrical in shape; however, the general staining pattern described for the rounded cells was still present in cells that displayed this phenotype.

A qualitative survey of cells plated onto collagen revealed that staining for β_1 integrin was scattered over the basal surface of the cells in a punctate pattern (Figure 11A). Staining for MMP-2 was present in a prominent band that was localized along the distal boarders of the spreading fibroblasts (Figure 11Ab). β_1 integrin and MMP-2 were co-incident with one another at low density and in small clusters along these distal domains (Figure 11Ae). The central regions of the rounded cells exhibited punctate staining for β_1 integrin but were largely devoid of MMP-2.

On laminin, staining for β_1 integrin appeared in two distinct patterns (Figure 11B). First, this receptor subunit was present in the punctate pattern along the basal surfaces that was reminiscent of cells plated onto collagen (Figure 11Bb). Second, staining for β_1 integrin was concentrated in a prominent, concentric band along the edges of the forming cell processes. MMP-2 was concentrated in these distal domains and was co-incident with the larger aggregates of β_1 (Figure 11Be). On fibronectin, staining for both β_1 integrin and MMP-2 appeared in a population of small scattered spots (Figure 11C). These antigens were co-incident with one another in restricted domains, many cells exhibited a poorly defined band of β_1 integrin and MMP-2 staining that appeared just proximal to the distal boarders of the cells (Figure 11Ce). Finally, on poly-l-lysine β_1 integrin and MMP-2 were scattered over the basal surfaces of the cells, as with cells plated onto fibronectin there was a degree of overlap in specific sub-domains (Figure 11D).

FIGURE 11- Qualitative imaging of MMP-2 and β_1

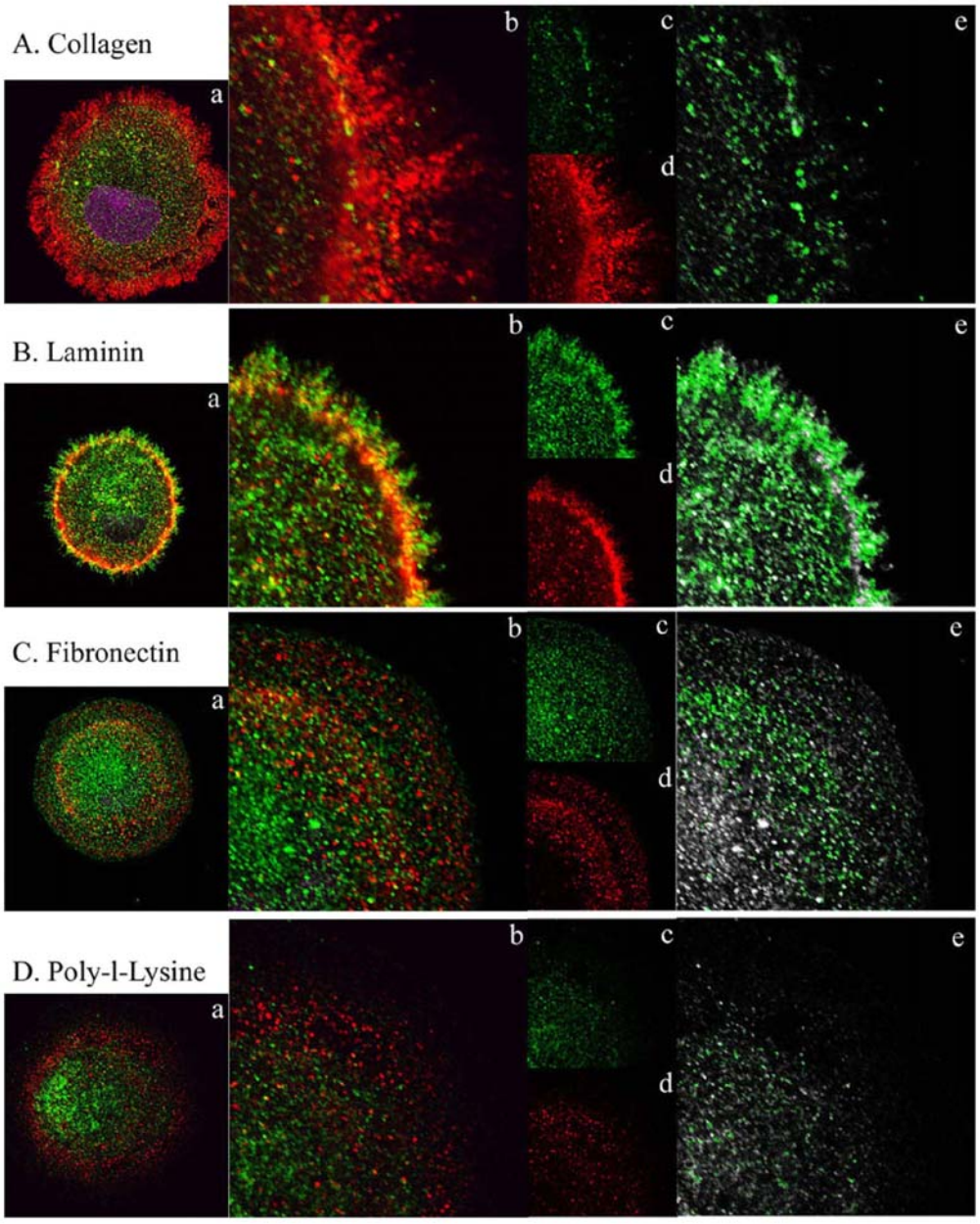

Figure 11

Figure 11. *Scanning confocal images of cells plated for 1 hour on various ECM substrates*. Panel (a) in each set of images represents a typical survey image taken at low magnification (63X) of cells plated onto collagen, laminin, fibronectin or poly-l-lysine stained for β_1 integrin (green) and MMP-2 (red). Panel (b) for each image represents data sets captured in zoomed section of the cell periphery. Note in Ab (collagen) the MMP-2 associated signal nearly overwhelms any β_1 integrin staining. Panel (c) (green: β_1 integrin) and (d) (red: MMP-2) for each data set represent projection of the individual channels. Panel (c) in each image set represents a subtraction analysis; the green projection depicts the sites of β_1 integrin and MMP-2 that are co-localized. The grey pixels in this image represent the population of β_1 integrin that exists independent of MMP-2 staining.

Quantitative Scanning Confocal Microscopy. Next, the distribution of α_1, α_2, α_3, α_5, and β_1 with respect to MMP-2 and the overlap of MMP-2 with respect to MT1-MMP were evaluated by quantitative methods. For these experiments data was captured at the interface of the ventral surfaces of the cultured cells and the substratum as defined by interference reflection microscopy. This approach makes it possible to concentrate on domains within the cell that are actively undergoing remodeling during cell spreading (example, domains similar to those depicted in Figure 11 panel e). As with the adhesion assays the cells were plated for 1 hour onto each of the different substrates and then processed for microscopic analysis. Representative images depicting the interference reflection, the distribution of each antigen that was assayed, an overlay of the IRM with the antigens, and an overlap image of the antigens are provided in Figures 12-16.

The overlap image (panel 5) in this type of analysis represents the distribution of the relevant integrin chain (in grey) with regions of overlap with MMP-2 (in green). In Figures 12-15, MMP-2 is represented in red and the integrin chains are represented in green. In Figure 16, staining for MMP-2 was captured in the red channel (panel 2), staining for MT1-MMP was captured in green channel (panel 3). In the overlap image (panel 5) the green represents domains where staining for MMP-2 is co-incident with MT1-MMP (in grey). For quantitative analysis the following parameters were maintained during image collection; 1) Channels were scanned sequentially with a line average setting of 4, 2) Images (1024 X 1024) were collected at the same voxel dimension of 69 nm x 69 nm to obtain Nyquist limits, 3) PMT settings were set and maintained at levels that reflect the

dynamic range, 4) PMT settings were adjusted for image capture to insure no bleed through from one channel to the other could occur. A similar treatment of images was used during post imaging analysis with JaCoP (Just another Colocalization Plugin) within Image J. Overlap images presented within figures 11-17 were generated with Colocalization Finder within Image J.

Representative Image Panels Used in Overlap Analysis: Integrin α chains/MMP-2

The following series of confocal images depict the distribution of integrin chains of the cardiac fibroblast with MMP-2. Figure legends are not provided as this information is integrated within the results section preceding these images. In each image series, Panel 1 represents the Interference Reflection, Panel 2 represents MMP-2 (red), Panel 3 represents the specific integrin alpha chain, Panel 4 is the overlay of these images, and Panel 5 is an overlap image with the integrin chain distribution shown in grey and the areas coincident with MMP-2 in green.

Figure 12: ***Distribution of α_1 integrin subunit with respect to MMP-2.*** Interference reflection images of cells plated onto collagen reveals a series of contact sites along the distal boarders of the spreading membrane processes that are arranged into a series of concentric rings (Figure 12A, Collagen Panel 1). MMP-2 (Collagen Panel 2) is scattered over this domain and appears as a broad band of staining that is distributed into a concentric pattern that appears like a hollow ring encircling the middle of the cell. A subset of this staining appears to lie within domains in contact with the underlying substratum as defined by interference reflection microscopy (see Collagen Panel 4). Staining for the α_1 subunit on these ventral cell surfaces is generally distributed as punctate spots. Examining the images depicted in Collagen figure 12, panels 2 and 3 reveals that staining for MMP-2 occurs more prominently along the outer edges of the cells while staining for α_1 is mainly concentrated in the more central domains of the rounded cells. This central concentration of α_1 staining is approximately encircled by the concentric rings of focal adhesions as defined by interference reflection microscopy. It is along the edges of this central area that the most overlap between MMP-2 appears to occur (green, Collagen Panel 5). A similar staining and overlap pattern was observed in cells plated onto laminin (Figure 12B, Laminin).

No attempt has been made to conduct overlap analysis for the relative distribution of α_1 (or other integrin subunits or MMP-2) with respect to the focal adhesions as defined by interference reflection. While technically possible, processing samples for immuno-fluorescence microscopy will cause the cells to collapse to an uncertain degree. This does not obviate the usefulness of this technique for defining the focal plane at which the cell is

in contact with the substratum. However, this can increase the total surface contact area to some degree, thereby reducing the accuracy of the technique with respect to defining individual contact sites.

Cells plated onto fibronectin did not display the pronounced concentric distribution of contact sites defined by interference reflection microscopy that cells plated onto collagen and laminin exhibited (Figure 12C, Fibronectin Panel 1). Instead, these cells developed a series of small triangular adhesion sites along the distal boarders of the spreading membranes (Fibronectin Panels 1 and 3). The concentric ring-like staining pattern for MMP-2 that was observed in cells plated onto collagen and laminin was some what less pronounced in cells that were plated onto fibronectin (Fibronectin Panel 2). This pattern was present, just not as clearly delineated. The α_1 chain was distributed as fine punctate dots over the entire basal surface, but there was evidence that this integrin subunit was present in somewhat higher abundance in the central domains (Fibronectin Panel 3). Overlap analysis indicates that most of the co-localization appears to be of low level across the surface of the cells (Fibronectin Panel 5).

Cells plated onto poly-l-lysine were not in full contact with the substratum. Focal contacts were scattered over the basal surfaces that were in contact with the underlying surface. Staining for MMP-2 and α_1 integrin appeared to be scattered over the ventral surfaces, the concentric (MMP-2) and circular patterns (α_1) observed in the other cells were largely absent in these cultures (Figure 12, Poly-l-Lysine).

FIGURE 12- Distribution of a1 integrin with MMP-2

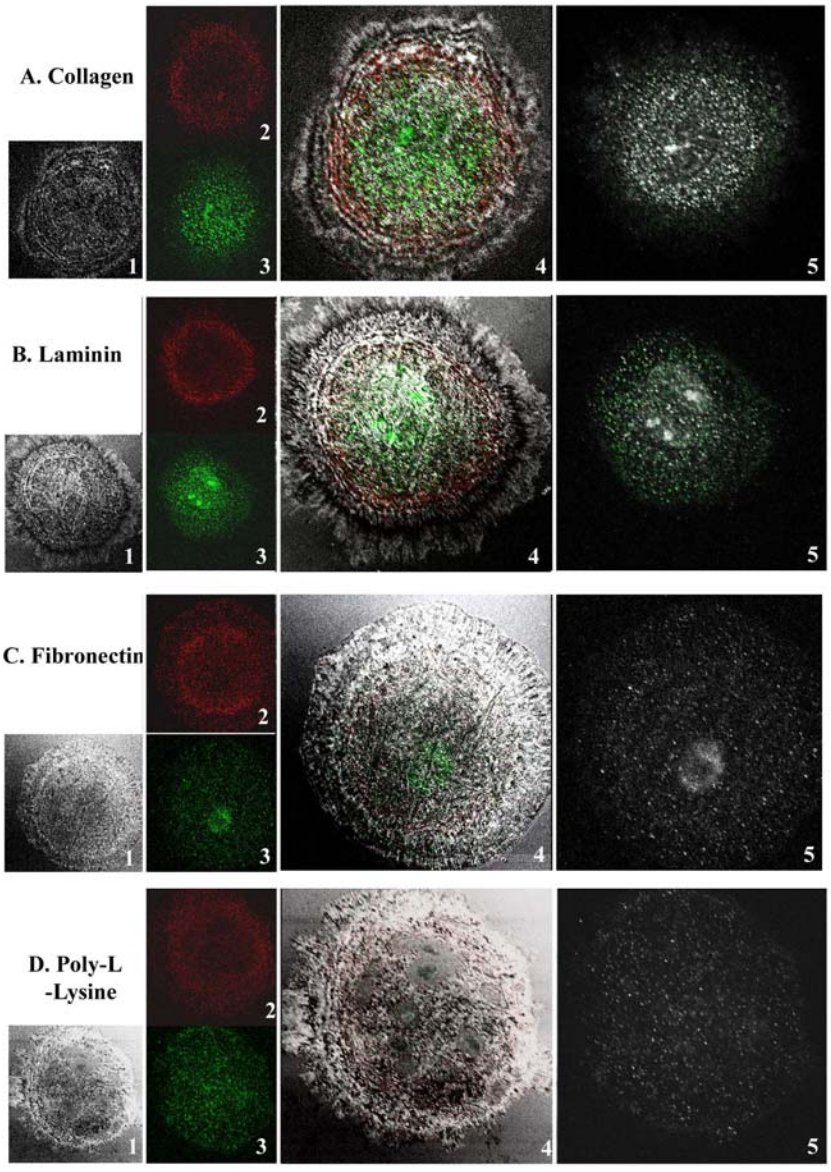

Figure 12

Figure 13: ***Distribution of α_2 integrin subunit with respect to MMP-2.*** Not surprisingly, and as expected, the distribution of MMP-2 is clearly similar in the experiments and data sets collected to evaluate the distribution of this protease with respect to the α_2 integrin. Of some note, as before, staining for MMP-2 appeared in concentric pattern in cells plated onto collagen and laminin, and somewhat less so on fibronectin (Figure 13). This result was very consistent and characteristic throughout these experiments. From the distribution of MMP-2 and the morphology of plated cells at 1 hour localize the protease within a region of transition. At this time point in the adhesion of cells the central region of the cell is rounded with the edges spreading out giving "fried-egg" morphology to the cell. The typical concentric distribution and concentration of MMP-2 within the region of transition between the central and peripheral regions of the cell suggests that this protease may be functioning in the process of adhesion. Once again, MMP-2 was more widely and uniformly distributed over the basal surfaces of cells plated onto poly-l-lysine (Figure 13D, Panel 2).

While the staining for the α_2 integrin subunit was also similar to the pattern observed for the α_1 subunit there were some minor differences. The bulk (*e.g.* not all) of staining for this integrin was roughly encircled by the outer concentric focal adhesions as defined by interference reflection microscopy. On collagen, this integrin subunit was more evenly distributed across the basal surfaces of the cells (Figure 13A, Collagen Panel 3) than the α_1 subunit. The localization overlap image for α_2 and MMP-2 indicates these antigens were co-incident within the central domains of the cells (Figure 13 Collagen Panel

5). There was not extensive staining (*e.g.* low "copy number") but there appeared to be very little MMP-2 staining that was co-incident with this integrin chain.

On laminin the α_2 subunit appeared to be mainly concentrated in the central domains of the spreading cells (Figure 13B, Laminin Panel 3). This integrin was largely excluded from areas of close contact as judged by interference reflection microscopy (Figure 13B Panel 4). The overlap analysis indicated that there was a moderate association between the α_2 integrin and MMP-2 protease (Figure 13B, Laminin Panel 5). The data image clearly indicates considerable MMP-2 staining that is co-incident with the α_2 integrin.

On fibronectin, the staining patterns for MMP-2 and the α_2 integrin were very similar to that observed for MMP-2 and the α_1 integrin on this ECM substrate. One minor difference, the α_2 integrin appeared to be somewhat more widely distributed and not so nearly confined to the central domains of the spreading cells (Figure 13C, Fibronectin Panel 3). Overlap analysis indicated a very low frequency of co-localization (Figure 13C Panel 5).

On poly-l-lysine the α_2 integrin was sparsely distributed and appeared to be aggregated into small clumps within the central domains of the cultured cells (Figure 13, Poly-l-lysine Panel 3). These structures appeared to be independent of close contacts as defined by interference reflection microscopy (Figure 13D, Panels 3 and 4). Overlap analysis indicated very little co-localization between MMP-2 and the α_2 integrin occurs on this non-specific surface (Figure 13D, Panel 5).

FIGURE 13- ***Distribution of α_2 integrin subunit with respect to MMP-2.***

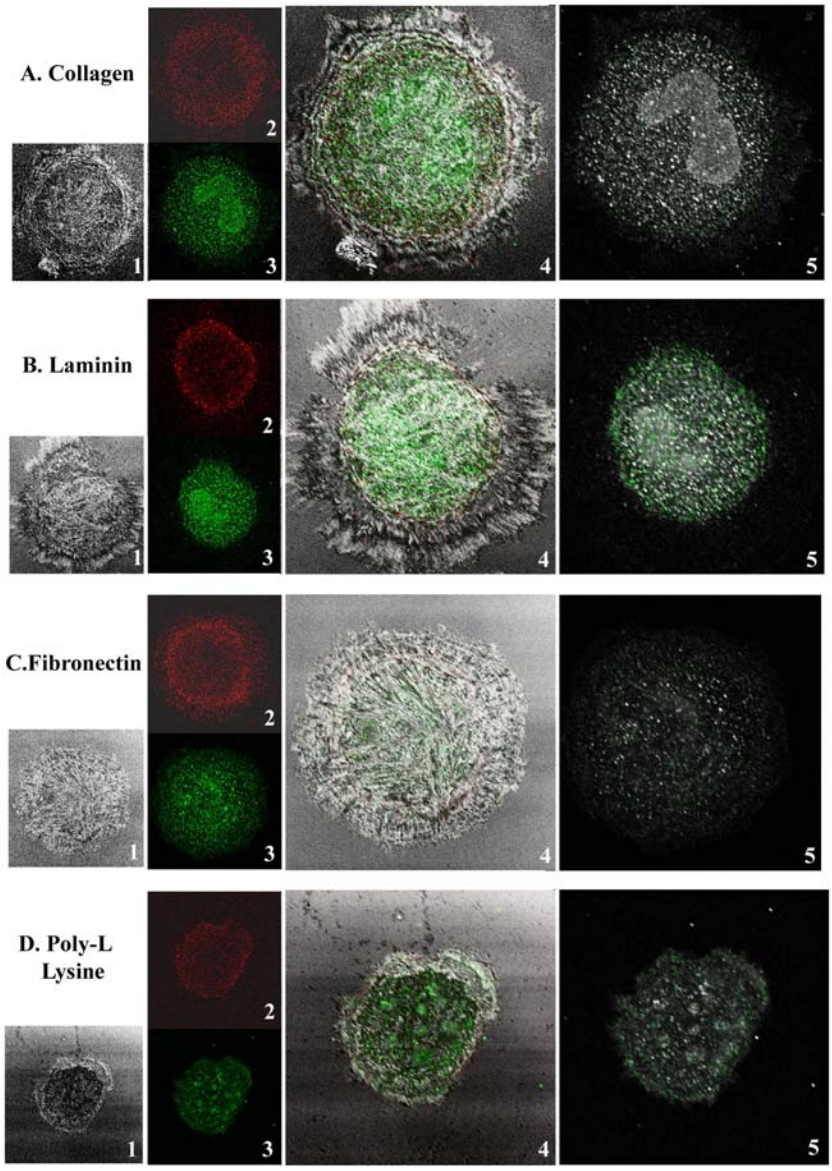

Figure 13

Figure 14: ***Distribution of α_3 integrin subunit with MMP-2.*** Staining for MMP-2 on collagen, laminin, fibronectin and poly-l-lysine was again consistent with the other experiments conducted to define the distribution of this protease with the α_1 and α_2 integrins (Figures 12 and 13). Cells in this particular data set are representative of the cells that exhibit a less-well defined rounded cell shape (see Figure 14B and 14C).

The α_3 integrin was widely distributed across the basal surfaces of the cells on all of the surfaces assayed. The overall staining intensity for this integrin subunit was much higher than either the α_1 or α_2 integrin (This increased signal intensity can result from a difference in antibody affinities or from absolute differences in the amount of integrin. The IP experiments would suggest that there is more α_3 integrin). On collagen the α_3 integrin was nearly evenly distributed over the entire basal surfaces of the cells (Figure 15 Collagen, Panel 3). However, staining for the cell surface receptor did appear to be excluded from the very distal boarders of the cells. The overlap image indicates that co-localization between MMP-2 and the α_3 subunit occurs predominately in the peripheral domains of the spreading cells (Figure 14A, Panel 5).

On laminin the α_3 subunit appeared in a distribution that was essentially identical to that observed on collagen (Figure 14B, Laminin Panel 3 and 4). The overlap analysis images were also very similar to that observed in cell cultured on collagen. Co-localization was predominately along the edges of the central domains of the cells (Figure 14B, Panel 5).

Cells cultured on fibronectin exhibited distribution of the α_3 subunit on the basal cell surfaces that was very similar to that observed on collagen and laminin (Figure 14C, Fibronectin Panel 3 and 4). The overlap images indicated that co-localization also occurred in the central cell domains (Figure 14C, Panel 5). Qualitatively the overlap images suggested that there was more MMP-2 that was co-incident with the α_3 subunit on this ECM surface (Figure 14C, Panel 5) than on collagen or laminin.

On poly-l-lysine, MMP-2 and the α_3 subunit were scattered over the basal surfaces of the cells (Figure 14D, Poly-l-lysine Panels 2-4). Overlap between these 2 antigens occurred mainly along the periphery, there appeared to be far less MMP-2 on the surface of these cells (Figure 14D, Panel 5).

FIGURE 14- ***Distribution of α_3 integrin subunit with MMP-2***

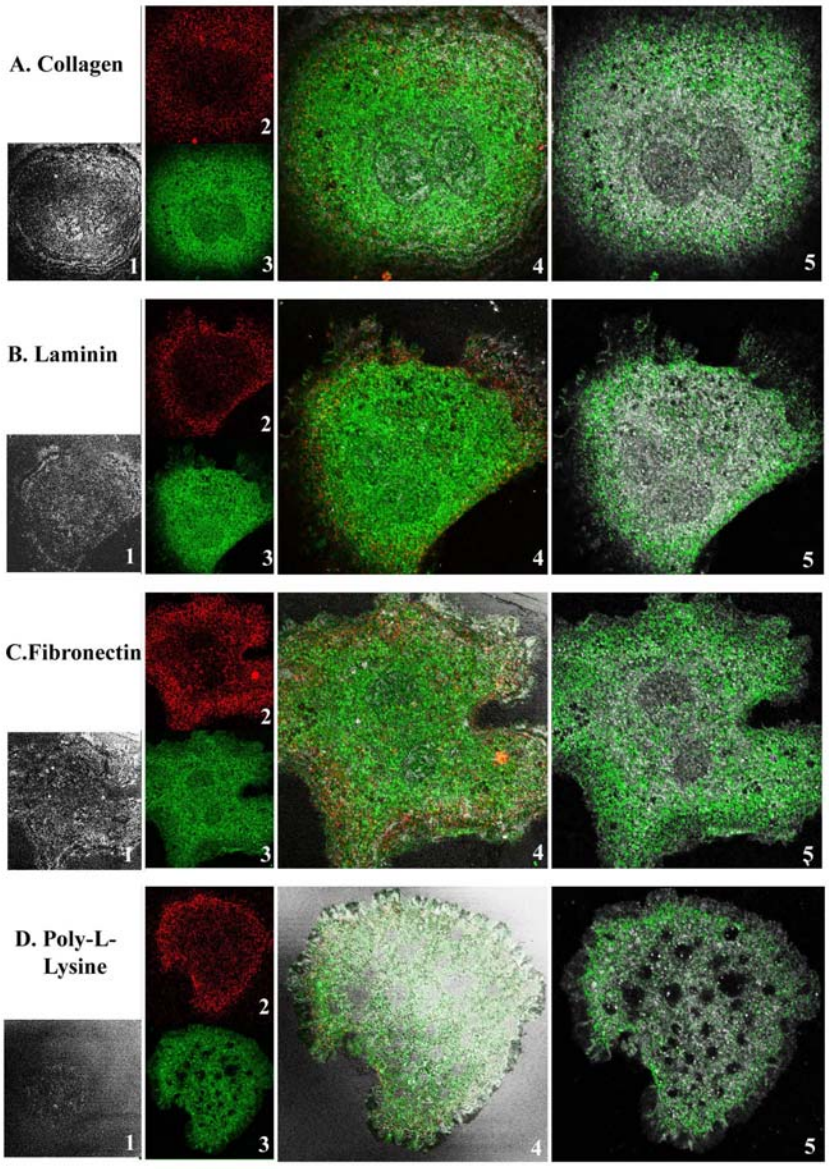

Figure 14

Figure 15: ***Distribution of α_5 integrin subunit with MMP-2.*** On collagen and laminin the α_5 integrin was distributed as punctate spots that were mainly concentrated in the central domains of the spreading cells. Again, the bulk of this staining appeared to be encircled by the focal contact structures (Figure 15A and B, Panels 3 and 4). Overlap analysis indicated the was co-localization of MMP-2 and α_5 integrin in the more central domains of the spreading cells; however, there was considerable integrin chain that was independent of MMP-2 (Figure 15A and B, Panel 5).

On fibronectin staining for MMP-2 was, as before, present in a less well defined concentric pattern (as compared to collagen and laminin) on the ventral surfaces (Figure 15C Fibronectin Panel 2). The α_5 integrin was concentrated in triangular focal contacts that were scattered over the surfaces of the cells. Interference reflection microscopy confirmed that these structures corresponded to focal contact sites (Figure 15, Panel 4). In overlap images MMP-2 and α_5 integrin were concentrated and co-localized in these domains (Figure 15C, Panel 5).

On poly-l-lysine MMP-2 appeared in a poorly defined concentric pattern that encircled the central domains of the spreading cells (Figure 15D, Poly-l-lysine Panel 2). Staining for the α_5 integrin appeared within the central "doughnut" pattern of the MMP-2 labeling (Figure 15D, Panel 3). Qualitatively, there was less overall α_5 integrin positive staining in these cells. Overlap analysis indicated that co-localization was predominately present around the outer portions of the α_5 positive spots and on the inner ring of the concentric staining pattern that characterized MMP-2 staining (Figure 15D, Panel 5).

FIGURE 15 ***Distribution of α_5 integrin subunit with MMP-2.***

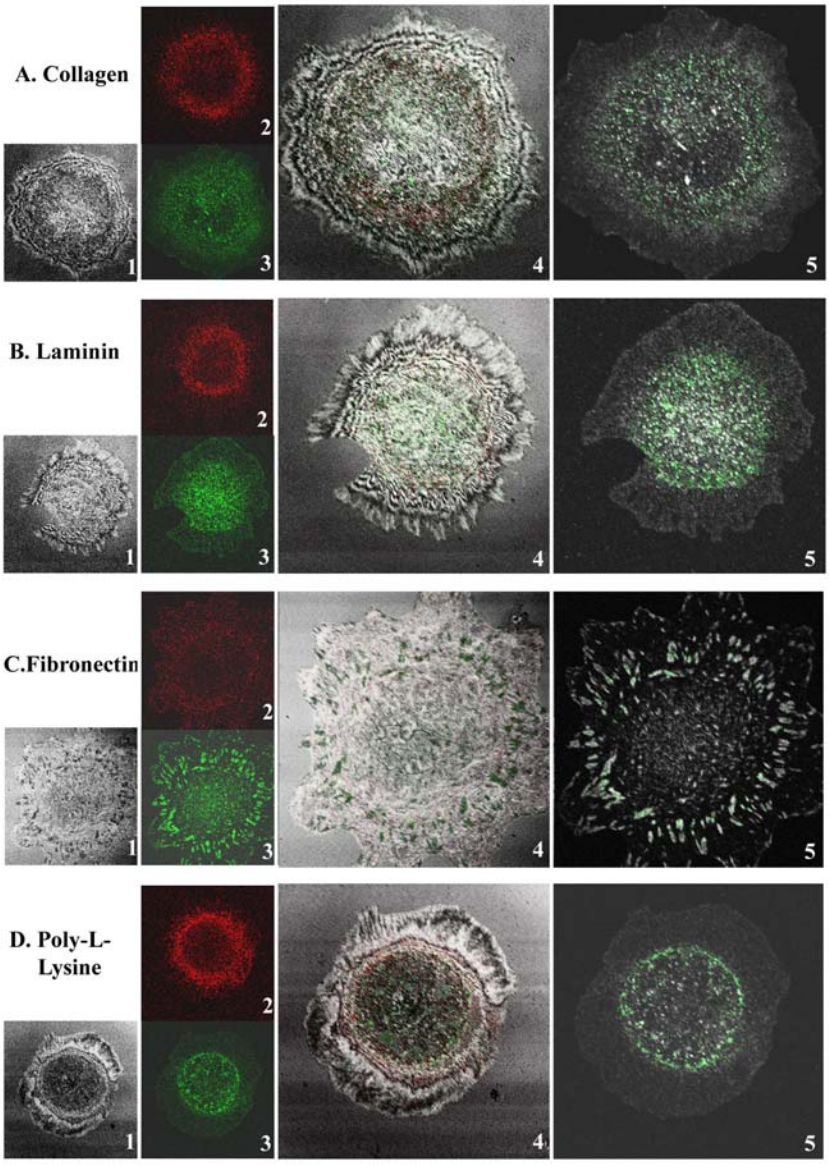

Figure 15

Representative Image Panels Used in Overlap Analysis: Integrin β_1 chain/MMP-2

The following series of confocal images depicts the distribution of integrin chains of the cardiac fibroblast with MMP-2. A Figure legend is not provided as this information is integrated within the results section preceding these images. Panel 1 represents the Interference Reflection, Panel 2 represents MMP-2 (red), Panel 3 represents β_1 chain (green), Panel 4 is the overlay of these images, and Panel 5 is an overlap image with the β_1 integrin chain distribution shown in grey and the areas coincident with MMP-2 in green.

Figure 16. ***Distribution of β_1 integrin with MMP-2.*** In many ways the distribution of the β_1 integrin can be expected to exhibit an average/aggregate distribution that resembles the distribution of individual α chains (because it is the binding partner to each of the α chains described in this study). On collagen (Figure 16A Collagen, Panel 3) and laminin (Figure 16B, Laminin Panel 3) β_1 integrin appears in small aggregates of staining in the central domains of the spreading cells. On fibronectin, β_1 appeared in a less well defined circular pattern on many cells (e.g. see Figure 16C, Fibronectin Panel 3). In the illustrated sample a roughly circular pattern of staining is evident. Within this domain there appears to be a broader, more continuous region of staining that corresponds with contact sites (Figure 16C, Panels 3 and 4). The clearly defined triangular focal adhesions that were delineated by α_5 staining were not obviously present (see Figure 15C, Panel 5). Undoubtedly, these structures are present but not visible because the β_1 partners with all of the other α chains (*e.g.* not able to see the trees {focal adhesions} because of the forest {extensive β_1 staining in association with other α chains}). Moreover, similar shaped focal adhesions were detected in cells plated on fibronectin as depicted by interference reflection microscopy.

In the overlap analysis for MMP-2 and β_1 integrin the co-localization of these antigens occurred primarily within the central domains of the cultured cells. The extent of co-localization varied across the different substrates. For example on collagen, the overlap analysis suggested that there was far less co-localization and there was considerable MMP-2 staining that appeared to be separate and distinct from the β_1 integrin (Figure 16A,

Collagen Panel 5). On laminin, this analysis indicated that there was extensive co-localization between MMP-2 and β_1 integrin within the central domains of the cells (Figure 16B Laminin, Panel 5). Very little β_1 integrin staining appeared to be independent of MMP-2 on this particular surface. Qualitatively, cells plated onto fibronectin (Figure 16C, Fibronectin Panel 5) exhibited overlap images that were similar to cells plated onto laminin. There were clear examples of overlap, and clear examples of β_1 chain that was independent of MMP-2. On poly-l-lysine (Figure 16 Poly-l-lysine, Panel 5) the overlap images were intermediate to the staining patterns observed on laminin and fibronectin.

FIGURE 16- ***Distribution of β_1 integrin with MMP-2***

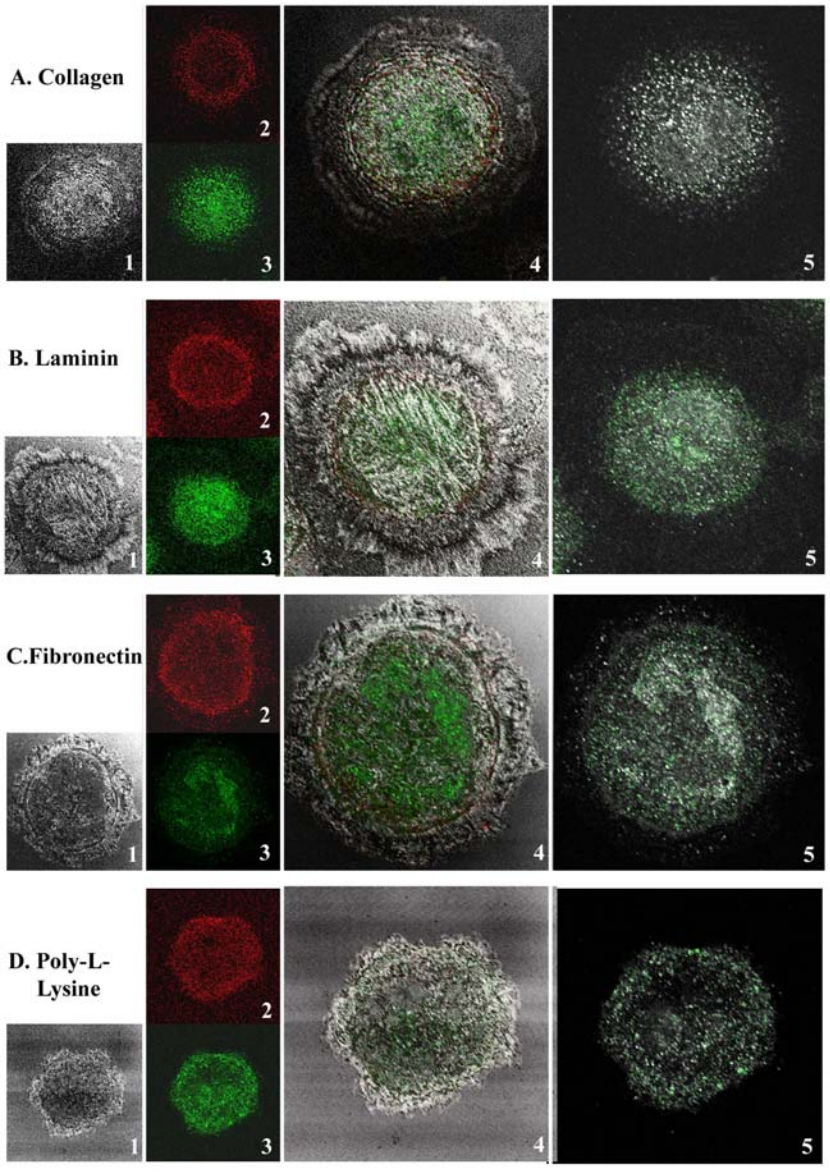

Figure 16

Representative Image Panels Used in Overlap Analysis: MT-1 MMP and MMP-2

The following series of confocal images depict the distribution of MT1-MMP and MMP-2 on the cardiac fibroblast. A Figure legend is not provided as this information is integrated within the results section ***preceding*** these images. Panel 1 represents the Interference Reflection, Panel 2 represents MMP-2 (red), Panel 3 represents MT1-MMP (green), Panel 4 is the overlay of these images, and Panel 5 is an overlap image with the distribution of MT1-MMP shown in grey and the areas coincident with MMP-2 in green.

Figure 17: ***Distribution of MT1-MMP and MMP-2.*** These experiments were conducted to characterize the distribution of MMP-2 with respect to a known binding partner. The activation of proMMP-2 to the active isoform is mediated at the cell surface by MT1-MMP. As with all of the other conditions assayed in this study, staining for MMP-2 appeared in a concentric circular pattern around the "central core" of the cells. This pattern was evident regardless of cell shape in cells cultured for 1 hour. Staining for MT1-MMP was scattered over the ventral surfaces of the cells in a nearly uniform pattern (Figure 17A-D Panel 3). There did not appear to be any preferential localization of this protease in any particular subcellular domain. This pattern was evident in cells plated onto collagen, laminin, and fibronectin.

In the overlap analysis areas depicted in green (Panel 5) represent colocalization of MMP-2 on MT1-MMP whereas areas depicted in grey represent MT1-MMP independent of MMP-2. On collagen (Figure 17, Collagen Panel 5) and laminin (Figure 17, Laminin Panel 5) the overlap analysis indicated that perhaps half of the MT1-MMP and MMP-2 are associated with one another. Cells on these surfaces exhibited distinct spots of MT1-MMP that were co-incident with MMP-2, but nearly an equal number of MT1-MMP positive sites were independent of staining for this antigen. On fibronectin (Figure 17 Fibronectin Panel 5) and poly-l-lysine (Figure 17 Poly-l-lysine Panel 5) the relative amount of sites that were positive (co-incident) for both MT1-MMP and MMP-2 was visibly increased with respect to cells plated onto collagen and laminin. While MMP-2 appeared in the characteristic concentric staining pattern, the overlap analysis on collagen, laminin and fibronectin did not recapitulate this pattern. Co-localization analysis suggested that MT1-

MMP and MMP-2 appeared to be present in association with one another in a nearly uniform pattern on the cultured cells (*i.e.* scattered over the basal surfaces). This is in contrast to cells plated onto poly-l-lysine. On this non-specific surface there was an obvious zone of co-localization between MT1-MMP and MMP-2. The overlap images reveal a concentric staining pattern similar to that observed to MMP-2 (Figure 17 Poly-l-lysine Panel 5).

FIGURE 17- ***Distribution of MT1-MMP and MMP-2.***

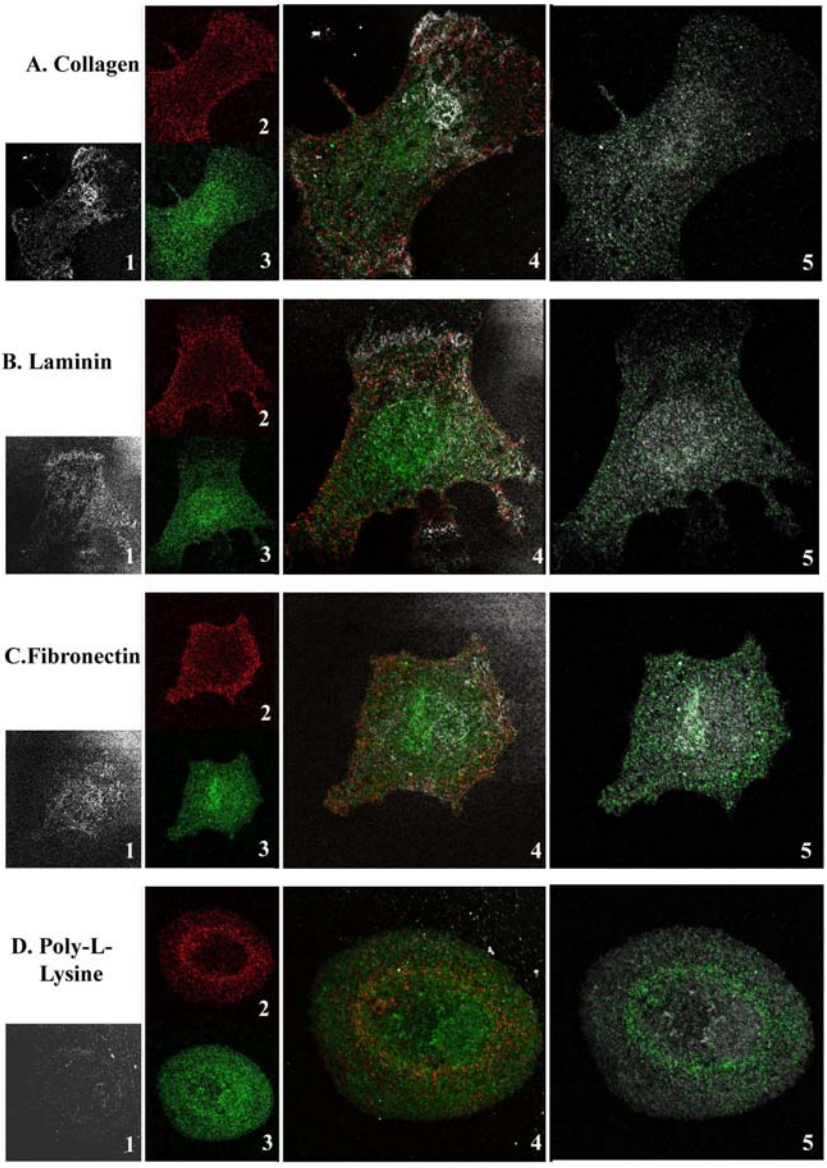

Figure 17

Overlap analysis:

Scanning confocal microscopy indicates that MMP-2 is co-incident to varying degrees with specific integrin α chains; co-localization appears to vary as a function of the plating substrate. The visual analysis of these images is highly subjective, even if the methods used to collect the data are quantitative in nature. Overlap analysis generates a numerical representation of the raw overlap between signals present in different channels in a microscopic data image. This process essentially distills the visual image into a far less subjective form. The term "raw" overlap is a qualifier that denotes that this analysis occurred without each channel being divided by the average intensity value of the representative channel. This type of manipulation essentially represents a smoothing of the data and sets a threshold at which signals from different channels will be accepted as data. No such filtering is used in raw overlap analysis. The resulting graphical representation of the overlap images represents an approximation of the coincidence of the two antigens without regard to differences in signal intensity that can exist between the two channels. This approach was used in this analysis to detect the relative differences in the overlap of MMP-2 with specific integrin chains, or with MT1-MMP and the degree to which this relationship is affected by ECM composition.

Figure 18: ***Overlap analysis.*** The overlap coefficient for each of the specific integrin subunits with respect to MMP-2 varied as a function of ECM composition. For example, for cells plated onto collagen and laminin (Figure 18), on a scale of 0 (no overlap) to + 1.0 (complete overlap), the coefficient of overlap for α_1 integrin and MMP-2

was approximately 0.27-0.29, on fibronectin the overlap value was 0.15 for this integrin subunit. On poly-l-lysine the overlap coefficient was approximately 0.31. Values for the α_2 integrin ranged from about 0.18 on collagen to approximately 0.35 on laminin and fibronectin. ***The α_3 integrin and MMP-2 exhibited the highest coefficient of overlap on all of the surfaces evaluated***. The overlap coefficient for these two antigens was also greater than the coefficient of overlap for MT1-MMP and MMP-2 on all surfaces. On collagen the overlap coefficient between α_3 and MMP-2 was 0.4, and on laminin, fibronectin and poly-l-lysine it was approximately 0.5. Analysis of the α_5 integrin and MMP-2 generated overlap coefficients of 0.26 on collagen, 0.35 on laminin, 0.3 on fibronectin and 0.37 on poly-l-lysine. For the β_1 integrin and MMP-2 the overlap coefficient was 0.3 on collagen, approximately 0.42 on laminin, and 0.3 on fibronectin and poly-l-lysine.

As a comparison, the association of MMP-2 with MT1-MMP generated values of 0.26 on collagen, 0.29 on laminin and approximately 0.38 on fibronectin and poly-l-lysine. (Horizontal dashed line Figure 18 represents overlap of MMP-2 and MT1-MMP).

FIGURE 18

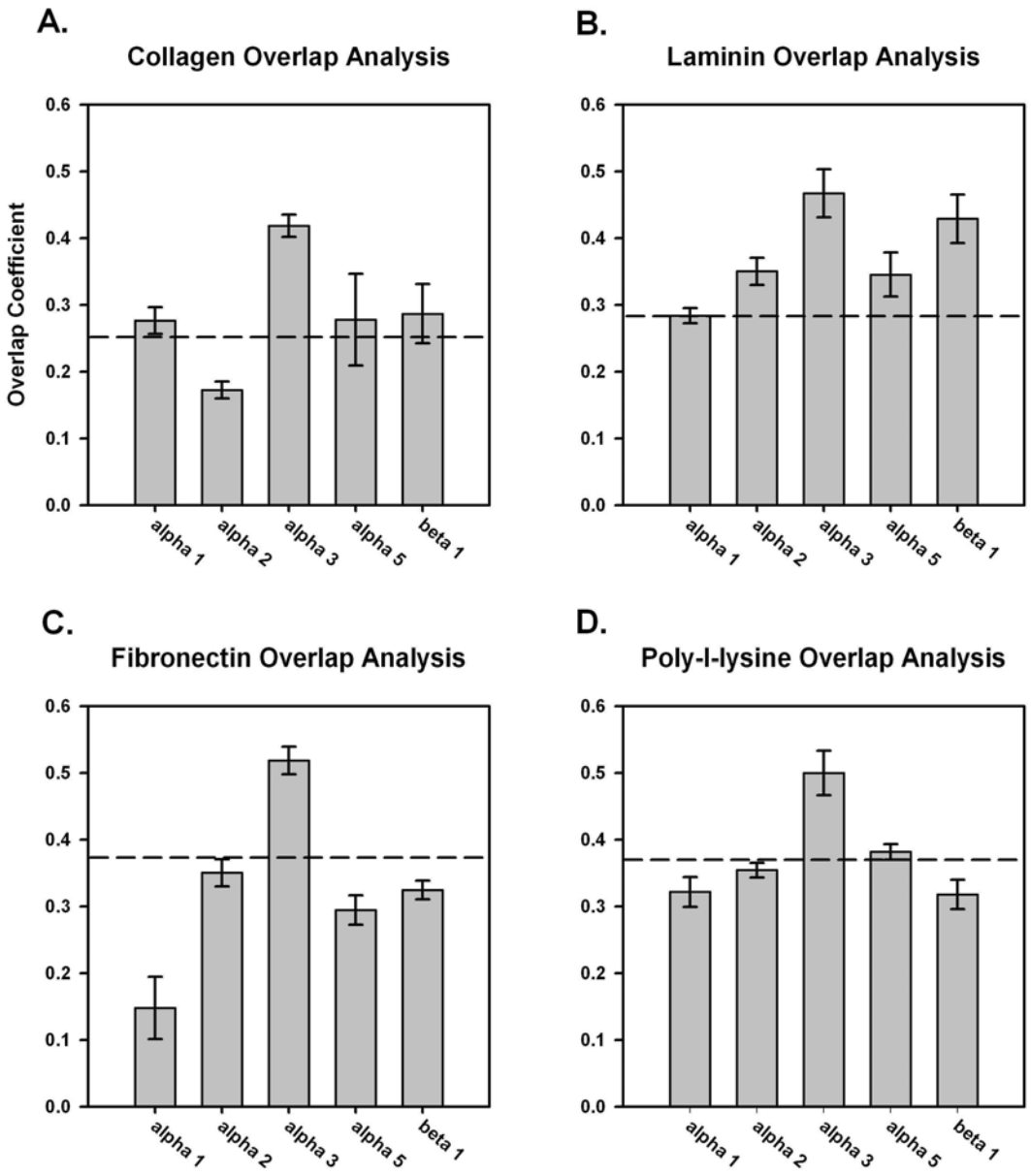

Figure 18

Figure 18. *Overlap analysis of specific integrin subunits and MMP-2.* The extent of overlap varied as a function of the ECM substrate used to plate the cells. The overlap coefficient was highest between α_3 and MMP-2; this relationship existed on each of the substrates examined. The dashed line in each panel represents the average overlap value generated from an analysis of MT1-MMP and MMP-2 for each ECM substrate.

Mander's Coefficient

Mander's analysis takes overlap analysis one step further and determines the percentage of an antigen that is involved in the overlap with a second antigen. The output of this analysis determines the fractional population of one antigen that is co-localized with a second antigen. The analysis then reverses this process and determines the percentage of the second antigen that is co-localized with the first antigen. Values are expressed on a scale of 0 (no overlap) to +1.0 (total overlap). Data considered for Mander's analysis was thresholded automatically within the JACoPlugin within Image J. This manipulation eliminates from the analysis data points that are on the low end of the intensity scale (grey pixel intensity from 0- 256) (potential noise). Data from the upper end of the intensity scale are not clipped in this filter. This thresholding tightens the data by eliminating low intensity signal present in each channel that potentially could dilute the relationships of these antigens.

Figure 19: ***Mander's Coefficient.*** Once again the relative fraction of each antigen that was associated with the putative companion molecule varied as a function of the plating conditions. For all surfaces assayed, Mander's coefficient was highest for the association of MMP-2 with the α_3 subunit (Figure 19). In the converse analysis of this relationship the relative fraction of α_3 integrin that was localized in association with MMP-2 was substantially less. For example, on collagen, Mander's coefficient for the association of MMP-2 with the α_3 integrin was about 0.35. However, for the converse circumstance the association of the α_3 integrin with MMP-2 generated a value of 0.14. This data

indicates that a considerable amount of the MMP-2 molecule is present in association with the α_3 integrin. The low value generated for the association of α_3 integrin with MMP-2 indicates that there is a much higher copy number of this integrin subunit on the cell surface than MMP-2. (More α_3 integrin is without MMP-2 than α_3 integrin that is with MMP-2) Mander's coefficient for MMP-2 with β_1 integrin was similar on all surfaces and ranged from 0.2 to 0.3. Finally, Mander's coefficient for MT1-MMP and MMP-2 ranged from about 0.1 on collagen to 0.2 on fibronectin, values that are substantially less (by nearly 2 fold) than that reported for the association of MMP-2 and the α_3 integrin.

FIGURE 19

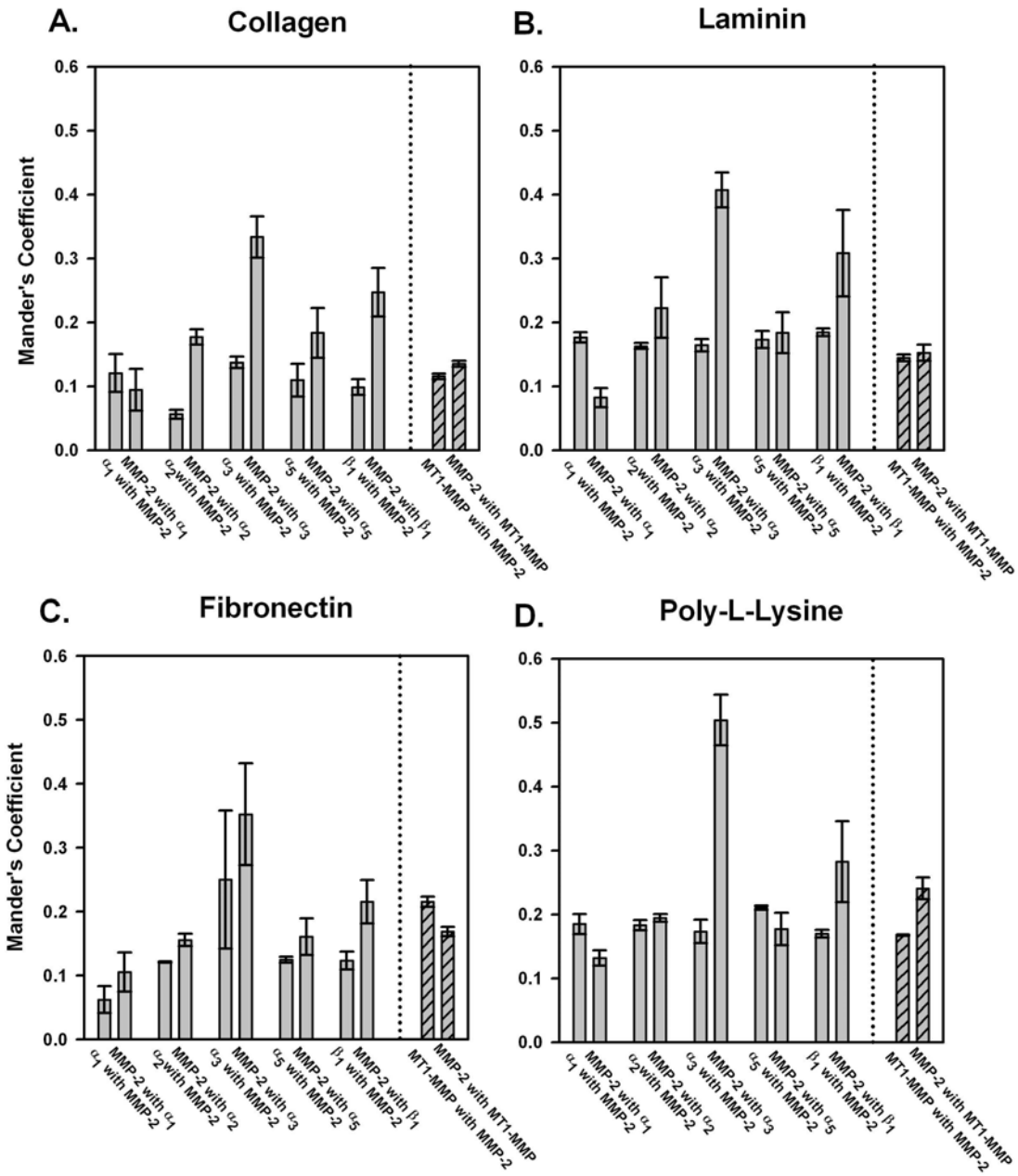

Figure 19

Figure 19. *Mander's coefficient of co-localization analysis for specific integrin subunits and MMP-2.* For all substrates, Mander's coefficient was highest for the association of MMP-2 with α_3 integrin. However, this analysis indicates that the bulk of the α_3 subunit exists independent of the MMP-2 molecule. The fractional co-localization for the other integrin subunits, including β_1 integrin, and MMP-2 were more similar on all substrates. The converse analysis yielded similar results. Mander's coefficients for the association of MMP-2 and MT1-MMP-2 were consistently less than the coefficients calculated for the association of MMP-2 with the α_3 integrin subunit.

Summary

Data presented in this document demonstrates the association of MMP-2 with the β_1 integrin in an interaction that specifically involves the integrin alpha chain α_3. Pharmacologically blocking MMP protease activity with SB-3CT decreases the strength of cells adherent on collagen and fibronectin. Both qualitative and quantitative confocal microscopy was implemented to define the *in situ* relationship of MMP-2 with the primary integrins of the neonatal cardiac fibroblast plated on to specific ECM components for 1 hour. Similar analysis was conducted with MMP-2 and MT1-MMP, a known cell surface binding partner and activator of MMP-2

Overlap analysis demonstrates the highest association of MMP-2 occurs with the α_3 integrin chain. This result is in agreement with biochemical data of the reciprocal interaction of this integrin alpha chain with MMP-2. Pull down assays did not demonstrate this relationship with the other alpha integrin chains addressed in these assays, namely the α_1, α_2, α_5 integrin chains. These alpha chains, however, demonstrate some degree of overlap with MMP-2. It is unclear as to why these alpha integrin chains demonstrate a level (albeit low) of overlap with MMP-2 with microscopy, but did not demonstrate a physical connection with this protease in our pull down assays. One possibility is related to the α_3 integrin being promiscuous in both substrate specificity[203] and in participating with heterogeneous integrins in forming adhesions [73]. Perhaps the overlap of MMP-2 with α_1, α_2, α_5 that is detected is actually MMP-2 bound to α_3 integrin intermingled in close proximity with these integrin chains.

Overlap of MMP-2 with the β_1 integrin chain reflects a lower level of association than was detected with the α_3 chain. This result is expected as the β_1 chain partners with a number of integrin alpha chains. The overlap present between the α_1, α_2, α_5 integrin chain with MMP-2 was low in comparison to the overlap present between α_3 and MMP-2 on all substrates. As a consequence of β_1 integrin having multiple alpha chain binding partners the degree of overlap that is present between MMP-2 and β_1 integrin reflects the average of the association of MMP-2 with all of the alpha chains that are present with β_1 integrin. This averaging provides indirect evidence to the specificity of the interaction of MMP-2 with the $\alpha_3\beta_1$ integrin.

Evident from the images of cells plated for 1 hour was a typical distribution pattern of MMP-2 as a clearly discernable ring shape at the region of transition between the central rounded region and the flattened edges that are spreading outward. This is of note as this location places this protease at the base of spreading adhesion structures. More elaborate techniques may delineate how this implication relates to the changes in adhesion maturation that occur with protease inhibition in cells plated on collagen and fibronectin. The substrate specific response likely represents a combination of factors both intrinsic and extrinsic to the cell; the integrin profile, the identity of the substrate, and the role of this protease.

In adhesion experiments, blocking MMP associated protease activity alters the strength of adhesion fibronectin and collagen. It is tempting to connect the separate results of adhesion and the distribution of MMP-2 with integrins on specific surfaces; however,

these connections would be largely speculative. One clear interpretation is the overlap of MMP-2 with the $\alpha_3\beta_1$ integrin is present on cells following 1 hour of adhesion and this overlap is predominate and of a greater degree that the association of MMP-2 and MT1-MMP. Moreover, this interaction was defined to the cell surface interface by interference refection microscopy. This evidence supports our isolation of a complex of MMP-2: $\alpha_3\beta_1$ from the surface of cardiac fibroblast.

Chapter X.

Discussion

Biochemistry of the MMP-2 integrin complex. This study has demonstrated 2 distinct results. First, MMP-2 is present in a complex that contains the $\alpha_3\beta_1$ integrin and TIMP-2. Second, pharmacological inhibition of MMP activity disrupts the maturation of cell attachment sites in an ECM specific manner. Circumstantial evidence links these two observations and suggests that MMP-2 bound at the cell surface modulates the maturation of adhesion sites in the cultured cardiac neonatal fibroblast. Biochemical assays (IP, Western blot assays, cell culture experiments, and pharmacological inhibition assays) and scanning confocal microscopic examination (distribution of MMP-2 with respect to integrin receptors) of cultured cells indicates that MMP-2 present at the cell surface mediates this process.

IP pull down experiments conducted on cell-suspensions reveal that MMP-2 is physically, and preferentially, associated with the $\alpha_3\beta_1$ integrin complex. Conducting a pull down assay directed against either the α_3 or β_1 integrin chains recovered immunoreactive MMP-2 (as judged by Western blot analysis and zymographic analysis of material recovered by IP). Conversely, IP experiments conducted against MMP-2 recovered α_3 and

β_1 integrin. The complex recovered in these conventional IP pull down assays is stable enough to withstand the elution buffers used to recover the complex and subsequent SDS treatments during rinses, although running these samples on SDS gels under reducing conditions will break down the MMP-2:integrin complex. On one hand these data suggest the complex is very stable. However, an alternative explanation, and clearly one potential criticism of these experiments, comes from the standpoint that the extraction procedures used to put the antigens of interest into solution during the initial stages of the IP could lead to the secondary association of the MMP-2 with the $\alpha_3\beta_1$ integrin. During extraction the association of MMP-2 with the different integrin subunits could occur through non-physiological means as a consequence of the assay conditions. Under these circumstances the non-specific association of the MMP with the integrin complex could appear to be very stable-if the proteins of interest are literally entangled and denatured with one another. Several lines of evidence argue against this explanation.

First, in selected experiments cells were processed with the cross-linker DTSSP in the living state prior to Western blot analysis. This particular cross-linker functions at the cell surface and will chemically cross-link proteins together that are within 12 Å (See Appendix 6). An analysis of cells that have been processed in this manner for the detection of MMP-2 reveals an immunoreactive protein running at a MW of 200-210 kDa (See Appendix 6). This experiment provides compelling evidence that MMP-2 is in, at least, close proximity to the integrin complex in the living cell. Similar experiments conducted to assay for the presence of MMP-9 failed to detect this closely related (both structurally and functionally) protease. These results, in conjunction with pull down assays directed against

MMP-2 that failed to detect interactions between MMP-2 and any other α chains, provides additional (albeit indirect) evidence that the MMP-2: $\alpha_3\beta_1$ integrin interaction exhibits a considerable degree of specificity.

Second, scanning confocal microscopic observations of cultured cells were conducted under circumstances that make it possible to assess the extent to which different antigens are co-localized with one another within a spatial resolution of 0.1394μm in the x-y dimension, 0.2358μm in the x-z with the 63x objective. These experiments demonstrated that the association of MMP-2 with the α_3 integrin was the highest under all circumstances that were assayed. In fact, Mander's coefficient of co-localization for MMP-2 and the α_3 chain was higher than Mander's coefficient of co-localization for MMP-2 and the MT1-MMP protease (a well known and well characterized binding partner for MMP-2).

The results of these different types of experiments are consistent with a complex composed of MMP-2: $\alpha_3\beta_1$ integrin. However, there is at least one discrepancy in the analysis of the present results that remains to be fully resolved. The MW of the complex detected in this study can not easily be reconciled with existing literature. Given the caveat that it can be dangerous to estimate the MW of a protein complex that has been separated on a SDS gel run under non-reducing conditions (the tertiary structure of a multi-molecular complex that has been run in a non-reduced state can result in the calculation of a highly anomalous MW), the 210 kDa complex is still exhibits a very unusual mass. Using a median estimate of mass and adding the reported MWs of β_1 (115-130 kDa, non-reduced) [204, 59, 61], α_3 integrin (120-130 kDa non-reduced)[204], MMP-2 (72 kDa for the pro-isoform and 64 kDa for the active isoform) TIMP-2 (20 kDa non-reduced) generates a complex that

would have a nominal total MW of approximately 340 kDa (β_1 @ 123 + α_3 @ 125 + MMP-2 @ 70 kDa + TIMP-2 @ 20 kDa = 338 kDa). While changes in the Stokes radius can greatly alter the movement of proteins within the electric field of the gels this mass is considerably higher than the mass observed for the complex defined in this study.

The MW of the various integrin subunits have been defined in different cell types (isolated from various stages of rat development) and rat hepatocytes by chemically labeling their surfaces by iodination. This approach places a radioactive marker on, just, the surface associated molecules [61, 113]. The labeled material was then extracted and subjected to an IP against different integrin subunits. The incorporated radioactivity was used to detect the recovered antigens. IPs against the β_1 chain have been conducted against rat cardiac fibroblasts [59, 205], cardiac myocytes [113] and hepatocytes [61] using this cell surface labeling technique. When the recovered material was separated by SDS under ***non-reducing conditions*** the β_1 integrin generated an estimated MW of approximately 115-130 kDa, substantially lower than the mass of the complex described in this study [59, 61, 113].

In addition, when cell surface radio-labeled β_1 chain is recovered under non-reducing conditions all of the α chains that are associated with that β_1 chain on the cell surface are also labeled. When a pull down directed against β_1 is used to recover the α_3 chain it exhibits an apparent MW of approximately 120-130 kDa, again much smaller in mass than was detected in this study. The published gels and the written discussion in these studies do not disclose any evidence of a high MW band that could correspond to the complex detected by this study. In addition to these observations, there is yet one more complicating factor. In Western blot analysis conducted in this study of whole cell extracts

the estimated MWs of α_3 and β_1 more closely approximated the expected MWs of these antigens (see Figure 2). Together, these observations generate two questions: Why are the α and β chains that are recovered by IP in this study remaining as a very high MW complex? Second: Why does this complex exhibit a low MW compared to the reported MWs of the individual proteins detected in the complex. Unfortunately, there is no clear answer to these questions.

If the samples processed in this study by IP responded as has been described in the literature it may have been possible to make more definitive conclusions about how the recovered complex might be structurally organized. For example, if this precondition had been met and the β_1 represented ***the predominate*** binding site for MMP-2 in the complex; it would be expected that the α_3 subunit would run at a substantially lower MW the SDS gels (closer to 120-130 kDa vs. 210-220 kDa). Recovering the complex with an IP against β_1 or MMP-2 would bring down the α chain(s) that were present in the putative complex. Once the sample was run on the gels the α and β chains should dissociate and separate. Assuming the MMP was linked to the β chain, these two proteins would run together while the α chain would separate and run at its expected, and substantially, lower MW. The converse argument also holds true. If the α_3 integrin represented the exclusive binding partner for MMP-2, the β_1 integrin should have been dissociated from the "complex" and run at approximately (110-120 kDa vs. the observed 210-220 kDa).

Still recognizing that it is an inexact science to predict an exact molecular weight of a protein complex that has been separated under non-reducing conditions, the existing literature and the present data can be used to argue that MMP-2 is linked to both integrin

subunits. Western blot analysis of the complex recovered in this study has indicated that TIMP-2 is present in association MMP-2 and the $\alpha_3\beta_1$ integrin in the neonatal cardiac fibroblast. In these experiments, a pull down assay was conducted against β_1 integrin and the recovered material was probed by Western blot for TIMP-1 and TIMP-2. This approach was used because an IP against MMP-2 ***would ordinarily be expected*** to bring down one or both of the TIMP peptides (the normal binding partners for MMP-2). An IP against the β_1 should represent a fairly stringent approach in determining if the TIMP molecule(s) represent component elements of the complex. The TIMP-1 molecule was present in the whole cell lysates but was not clearly associated with the 210-220 kDa MMP-2:$\alpha_3\beta_1$ complex. TIMP-2 was clearly present in the complex and a Western blot analysis of this type of an IP confirms that both α_3 and MMP-2 are present in the recovered material and running at the 210-220 kDa mass (Figure 2 and Figure 3).

There is at least one scenario that can be used to defend model that MMP-2 actually interacts with both the α_3 and the β_1 chains of the integrin complex. It is possible that when the recovered complex is separated by SDS gel electrophoresis that the 2 integrin chains separate from one another but the linkages that the anchor MMP-2 to β_1 and MMP-2 to α_3 may be more stable, resulting in the appearance of the "common" 210-220 kDa complex that we have observed. One maybe composed of β_1 MMP-2 and TIMP-2 (β_1 @ 115-130 kDa + MMP-2 @ 68-72 kDa = 183 kDa to **202 kDa**). One other complex could be composed of α_3, MMP-2, and TIMP-2 (α_3 @ 120-130 kDa + MMP-2 @ 68-72 kDa + TIMP-2 @ 20 kDa = **208 kDa to 222 kDa**). Under these conditions a Western blot analysis would detect a complex composed of $\alpha_3\beta_1$ integrin, MMP-2 and TIMP-2 running

at a "common" MW of 210-220 kDa. This result would occur because IP against α_3 or β_1 integrin or MMP-2 will bring down the entire complex; the complex then partially breaks down in the gel run into the composite structures described. Analysis by Western blot of the individual components would then detect all of component elements running at a MW of 210-220 kDa.

In order to unambiguously define the exact nature of the interactions that mediate the interaction between MMP-2 and the $\alpha_3\beta_1$ integrin it will be necessary to specifically design and conduct experiments to explore the structural properties of this complex. Various proteases of the MMP family exhibit interactions with different integrins. Somewhat surprisingly the nature of the MMP integrin interaction varies considerably across cell type. For example, in human gingival fibroblasts MMP-2 is indirectly linked to β_1 integrin through a collagen peptide fragment [187]. In this system one domain of the collagen peptide appears to be bound to the active site in the integrin, while the MMP, which recognizes and binds to native collagen [132], is bound by the collagen fragment. The association of MMP-1 (collagenase) with the $\alpha_2\beta_1$ integrin is primarily defined by structural motifs that are present in the α_2 chain [184,185]. The binding events that anchor the C-terminal hemopexin domain of the MMP-2 molecule to the $\alpha_v\beta_3$ integrin remain ill defined [186]. However, this interaction is specific to this integrin. In the gel shift assays described in this latter study mixing MMP-2 with the $\alpha_v\beta_3$ integrin results in an increase in MW. Conducting this same experiment with the $\alpha_5\beta_1$ integrin and MMP-2 resulted in no apparent shift in MW in the samples in the gel analysis. Given these observations the MMP-2 in cardiac myocytes may be could be bound to the β_1 through the hemopexin

domain [201] or the collagen binding domain [187] and to the α_3 through TIMP-2 mediated events [200]. A specific binding site for TIMP-2 on α_3 has been detected [200].

Experiments conducted to examine the association of TIMP-2 with the integrin complex provide some insights into how this interaction might be mediated. In this series of IPs were conducted against the α_3 and β_1 integrin. Material from these isolations were then run under non-reducing and reducing conditions and blotted for TIMP-2. (Figure 3). Interestingly material that was pulled down with α_3 and run under non-reducing conditions did not show reactivity to TIMP-2. This is not an artifact of the antibody used to detect TIMP-2 as this antibody recognized this antigen in non-reducing conditions in isolates of a β_1 integrin pull down. Under reducing conditions, however, TIMP-2 is detected in the α_3 pull down. Blotting for MMP-2 in the isolates from the α_3 pulldown confirm that the differences in the detection of TIMP-2 in the non-reduced and reduced conditions were not resultant from an ineffective pull down of the complex of MMP-2: $\alpha_3\beta_1$:TIMP-2. One likely explanation for the differences in detection of TIMP-2 in α_3 isolates is that in the non-reduced condition the binding of TIMP-2 to the α_3 integrin chain conceals the epitope recognized by the antibody used in this study. The immunogen or target for this antibody directs this antibody to the N-terminal, loop-1 domain of TIMP-2. The structure of TIMP is maintained as a series of 5-6 loops by disulfide bonds. Presumably, in the non-reduced condition this epitope is concealed in the binding to the α_3 integrin chain. With reduction TIMP-2 was detected. Defining the exact site of interaction is beyond the scope of these studies; however, the interaction of TIMP-2 with α_3 likely mediated by the N-terminal domains of TIMP-2. Additionally TIMP-2 was detected from IP to the β_1 chain under non-

reducing and reducing conditions implying that the interaction sites of TIMP-2 with α_3 and β_1 are different[200].

In summary, experimental evidence suggests that MMP-2, $\alpha_3\beta_1$ and TIMP-2 exist as a complex on the surface of the cardiac fibroblast. It remains unclear how this complex is organized and selecting one model over another to explain the present results is difficult at best. Alternative models to explain the composition of the 210-220 kDa complex that was identified in this study include:

- A much higher mass complex that runs at an "anomalously low" MW of 210-220 kDa as a consequence of the running conditions used to separate the proteins for analysis. In this model the tertiary structure of the intact complex causes it to run at a low MW in the SDS gels under non-reducing conditions.
- A high MW complex in which the MMP-2 is linked to both the α and β chains. The 210-220 kDa complex is generated when the intact complex is broken down into 2 separate complexes composed of β_1 @ 115-130 kDa + MMP-2 @ 68-72 kDa and then α_3 @ 120-130 kDa + MMP-2 @ 68-72 kDa + TIMP-2 @ 20 kDa.

Of the two alternatives presented the first may be the most tenable for two reasons. First, the buffers used to isolate and recover the IP material for analysis appear to be relatively gentle, allowing the integrin chains to remain intact with one another. When conventional IPs were processed by boiling in SDS to recover the antigens the chains would occasional remain intact other times they would breakdown. This result appeared to be very variable and dependent upon the length of time (or temperature?) the samples were processed (very

small changes resulted in very inconsistent results which is one reason the Seize IP kits were used). Second, the test tube and gel shift assays conducted with MMP-2 and $\alpha_v\beta_3$ and $\alpha_5\beta_1$ would appear to indicate that MMP-2 alone will not bind to the $\alpha_5\beta_1$ (this circumstance may be changed if the TIMP-2 molecule alters the structure of the MMP-2 molecule in such a way that MMP-2 would now bind the $\alpha_5\beta_1$ integrin).

Functional implications of the MMP-2 integrin complex. The association of MMP-2 with the $\alpha_3\beta_1$ integrin is particularly interesting when one considers the promiscuous nature of the substrate specificity of this integrin. Collagen, laminin and fibronectin are all surfaces engaged by the $\alpha_3\beta_1$ integrin. The MMP-2 protease exhibits activity against each of these surfaces [18,130,131]

Adhesion assays conducted in this study provide evidence that the MMP-2:TIMP-2:α3β1 complex plays a role in the maturation of cell adhesion sites in an ECM specific fashion. Pharmacological inhibition of MMP function with SB-3CT did not alter cell adhesion in conventional cell adhesion experiments (30 or 60 minute incubation intervals). This is perhaps not surprising; these early events of adhesion are relatively non-specific in nature and are largely driven by electrostatic interactions [106]. When these same cultures were plated for 60 min and then challenged with a calibrated centrifugal force treatment with SB-3CT selectively reduced the adhesion of the neonatal cardiac fibroblast to collagen and fibronectin, but not laminin or poly-l-lysine. It seems unlikely that this substrate specific effect on adhesion represents a reflection of the intrinsic proteolytic properties of MMP-2. This protease can degrade a broad spectrum of ECM proteins,

including laminin [18]. The proteolytic processing of collagen and fibronectin can uncover RGD binding sites that are not ordinarily accessible in these ECM proteins by the integrins of the cardiac fibroblast [206,207]. Proteolytic processing of laminin exposes this very same type of binding site; however, the cardiac fibroblast typically exhibits low expression of the integrin that mediates adhesion to these (now uncovered) cryptic sites[208,209].

It is not possible to entirely discount the role that the MT1-MMP:MMP-2 complex might play in the adhesion studies [136]. Our co-localization experiments clearly demonstrate this complex is present, and presumably active, in cells that have been plated for 1 hour. However, at this time point the coefficient of colocalization for MMP-2 with the α3 integrin is far larger than the coefficient of colocalization of this enzyme with β1 or its more classic binding partner, MT1-MMP. The low values generated by the co-localization analysis for the MT1-MMP and MMP-2 suggest that very little MMP-2 is associated with this binding partner during this early stage of culture. Nor can we detect active MMP-2 (or MMP-9) in the supernatant of the cultures at this time interval (Figure 2, Appendix 3). Given these results it seems likely that our inhibition experiments are impacting MMP-2 activity on a very local scale [210]. We have been unable to "rescue" cell adhesion in cultures treated with inhibitors by first pre-treating the ECM coated culture dishes with exogenous proteases. This result also suggests the impact of SB-3CT is a very local event specific to the cell surface. By implication and the shear volume (number) of MMP-2 molecules associated with the α3 integrin this seems like the most likely site at which protease inhibition effects the cells.

In confocal localization experiments MMP-2 exhibited a low background of association with the other integrin α chains. If there this association is "real" it occurs at a very low level, if an IP is conducted from a known number of cells only the α_3 and β_1 chains are detectable in the final isolate. The low "background" of association of MMP-2 with the other α chains could be reflection of the relatively promiscuous nature of the $\alpha_3\beta_1$ integrin. This particular integrin complex can bind to a variety of ECM substrates and co-operates with other integrins in the maturation and formation of adhesion sites [73]. During adhesion the $\alpha_3\beta_1$ integrin does not necessarily participate in the very earliest stages of cell attachment, rather it appears to play a more distal role in the process. The $\alpha_3\beta_1$ integrin accumulates in developing adhesions and is an integral component of the formation of heterogeneous adhesion sites (sites composed of multiple integrin subtypes).

The constraints placed on the co-localization analysis by the inherent limits of optical resolution of confocal microscopy (63X objective, x-y resolution 0.1394μm; x-z resolution 0.2358μm) makes it impossible to determine if the overlap represents an association of the $\alpha_3\beta_1$: MMP-2 complex with other integrins, the association MMP-2 with a common β_1 chain, or the true association of the MMP-2 molecule with other α subunits. Together the data suggests that MMP-2 is selectively associated with the $\alpha_3\beta_1$ integrin, the integrin most closely associated with the maturation of adhesion sites.

Whenever a study involves the application of pharmacologic agents a common concern is that these agents will adversely impact cell viability. Any loss of cells from the adhesion assays as a result of death would be reported as a reduction in cell adhesion. Conversely, any loss of cells from a viability assay due to changes in cell adhesion will be

reported by the viability assay as a reduction in cell viability. These characteristics represent a major limitation in conducting and interpreting the data presented in this study.

In attempts to mitigate and circumvent these technical limitations necessitates conducting the viability assays on full attached cells. This assumes that once the cells are attached that protease inhibition over a short interval of time will not greatly impact adhesion. Several observations form the basis for the argument that cell viability was not adversely affected over the 1 hour plating interval used during the adhesion assays in this study. Evidence supporting this conclusion is first provided by the conventional adhesion assays in which indicated equal initial adhesion in cells treated with inhibitors. The preliminary stages of the centrifugal adhesion assays support this result. A vital dye is added to the cultures immediately prior to centrifugation (essentially a conventional adhesion assay at this point). In these experiments all cultures exhibited similar numbers of cells. Perhaps the most convincing evidence that viability was not adversely affected by protease inhibition (or the vehicle carrier) during the 1 hour culture interval used in the adhesion assays is that the adhesion strength was selectively reduced on collagen and fibronectin, and not on laminin or poly-l-lysine. While this line of reasoning is not a "direct" line of evidence, it may be more accurate than the metabolite based assay in assessing viability. The reality is that metabolic assays are inherently limited in determining cell number. It is possible for these types of assays to represent similarly a low number of cells with high activity with a high number of cells with low activity.

One result in the viability assays of note concerns the observation that changes in metabolic activity in response to SB-3CT were dependant on the density at which cells

were initially plated. Cells plated at high density for 24 hours have elevated rates of metabolism compared to cells plated for the same interval at low density (see Figure 3 and Figure 4 Appendix 7). In cultures plated at low density (2k) for 24 hours and then supplemented with inhibitor a depression in metabolic rates was evident within 2 hours of treatment.(Figure 10) A broad interpretation of these results would suggest that they are consistent in some ways with the presented model that MMP-2 mediated activity is necessary for focal adhesion maturation. In cells that have reached adhesion equilibrium the inhibition of protease activity can be expected to impair the ability of the cells to routinely turn over existing adhesions and express nascent sites. At low density cells are much more mobile and in contact with the underlying substrate. In this type of culture the turnover and expression of nascent focal adhesions would be relatively robust. Interventions that effect adhesion may cause the displacement and loss of cells from this type of culture. In contrast at high density cells are more stationary and contact with one another. Under these conditions focal adhesion turnover and contact with the substratum may be relatively unimportant. Muscle cells express very prominent focal adhesions when maintained at low cell density and extremely rudimentary focal adhesions when cultured at very high density [211].

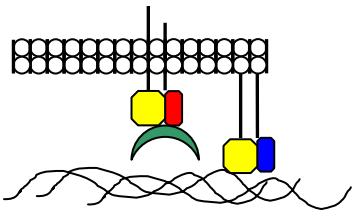

Figure 20 Schematic of Adhesion Maturation
MMP-2 bound to of $\alpha_3\beta_1$.

A During initial adhesion, the native ECM component fibronectin has available a number of sites for adhesion. For example, the binding site for the α5β1 is present in the on the surface of this glycoprotein.

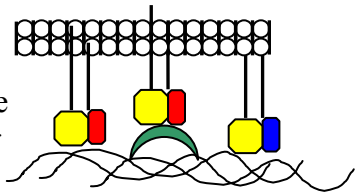

B MMP-2 bound to $\alpha_3\beta_1$ integrin is positioned to cleave ECM constituents. Proteolysis of fibronectin exposes additional RGD binding sites that are unavailable in the native peptide. Additional binding sites increase the number of potential sites for integrin binding. Moreover, these sites can be bound by integrin such as $\alpha_3\beta_1$ in addition to the $\alpha_5\beta_1$ thereby increasing not only the number of binding sites but also the complement of integrin that bind to a unique ECM protein. Conventional adhesion assays at 30 minutes and 1hour support the maturation of adhesion during this time interval Proteolytic events may contribute to this maturation process.

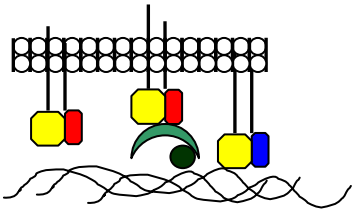

C. Treating cells with a specific protease inhibitor against MMP-2, blocks this proteolysis and as a consequence there is a decrease in the strength, ***maturation*** of adhesion. Theoretically, the increase in the number of binding sites would not occur. Under these circumstances the absolute or potential number of binding sites in the ECM is reduced and as a consequence there are fewer sites for attachment. Secondarily, the complement and number of receptors participating in adhesion are reduced. However, there are adequate binding sites on the native fibronectin substrate that support equal levels of initial adhesion and spreading as compared cells plated Taken together these considerations suggest MMP-2 and potentially the complex of MMP-2 and $\alpha_3\beta_1$ are involved in the ***maturation*** of adhesion in cells plated on fibronectin (and collagen but not on laminin or poly-l-lysine).

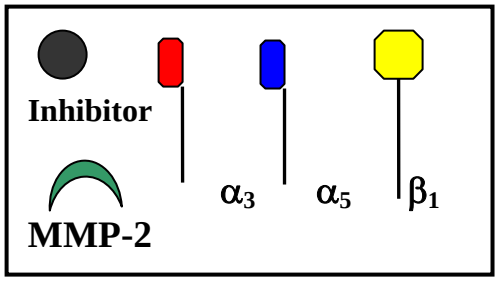

Physiological implications. The integrin MMP-2 complex identified in this study brings together both the receptors that mediate adhesion to the ECM, integrins, with the main class of enzymes responsible for the proteolysis of ECM components, the MMPs. Relevant to this discussion is the role of the cardiac fibroblast in development and disease. This cell type represents the major nexus responsible for the deposition, turnover, maintenance, and remodeling of the cardiac ECM. In the postnatal period rapid changes in hemodynamic load are associated with the turnover of existing matrix constituents and the elaboration of a robust cardiac ECM. A complex composed of MMP-2 and the $\alpha_3\beta_1$ integrin may represent a self-contained mechano-sensitive site that can detect changes in load while mediating aspects of the proteolytic processing of the local microenvironment to facilitate cell migration and the shedding of integrins [212]

Early in the progression of cardiac hypertrophy the myocardium adapts and increases performance to meet peripheral demand. However, the onset of changes in the composition (myocardial compliance) of the ECM parallels the transition to decompensation and failure of the myocardium[174, 175]. As in cardiac development, the deposition of nascent matrix components requires the remodeling or degradation of the preexisting ECM. Similarly, changes in the hemodynamic load initiate the elaboration and accumulation of these components. MMP-2 is expressed in concert, temporally and spatially during the developmental period[171, 172]. Likewise, in the adult changes in hemodynamic stress trigger a similar sequence of events and are a prelude to remodeling of the ventricular wall[127]. The developmental mechanisms and relationships between mechanical stretch, the expression of proteases, and elaboration of ECM components are

carried over and relevant to the adult. In the adult heart changes in the compliance (composition) of the ventricular wall and systolic dysfunction can be induced by the over-expression of MMP-2 [177]; whereas, deleterious remodeling can be attenuated by pharmacologically interventions that decrease the levels of this protease[178, 179].

Treatment paradigms for hypertension, a complex disease entity of multiple etiologies, are focused on reducing the mechanical load on the heart. This treatment strategy delays the progression toward and the transition of compensated heart disease to decompensated heart disease. If this complex represents a mechanosensitive site for the detection of mechanical load on the cardiac interstitium and at the same time is a site for effecting both changes in fibroblast cell adhesion and matrix turnover, interventions targeting this complex could augment current treatment paradigms. These strategies may decrease the migration of cardiac fibroblast and attenuate maladaptive changes in the cardiac interstitium. However, the extent that these *in vitro* observations carry over into the *in vivo* situation is unclear. The complex of MMP-2 and $\alpha_3\beta_1$ integrin represents a site on the surface of the cultured cardiac fibroblast that combines mechano-sensitive and proteolytic elements that may mediate substrate specific maturation of adhesion.

References

References

1. Dard N, Breuer M, Maro B, Louvet-Vallée S. Morphogenesis of the mammalian blastocyst. Mol Cell Endocrinol. 2008 Jan 30;282(1-2):70-7.

2. Steinberg MS. Differential adhesion in morphogenesis: a modern view. Curr Opin Genet Dev. 2007 Aug;17(4):281-6.

3. Edelman GM. Cell adhesion molecules in the regulation of animal form and tissue pattern. Annu Rev Cell Biol. 1986;2:81-116.

4. Lu P, Werb Z.Patterning mechanisms of branched organs. Science. 2008 Dec 5;322(5907):1506-9.

5. De Arcangelis A, Mark M, Kreidberg J, Sorokin L, Georges-Labouesse E Synergistic activities of alpha3 and alpha6 integrins are required during apical ectodermal ridge formation and organogenesis in the mouse. Development. 1999 Sep;126(17):3957-68.

6. Legouis R, Hardelin JP, Levilliers J, Claverie JM, Compain S, Wunderle V, Millasseau P, Le Paslier D, Cohen D, Caterina D, et al. The candidate gene for the X-linked Kallmann syndrome encodes a protein related to adhesion molecules. Cell. 1991 Oct 18;67(2):423-35.

7. Yang JT, Rayburn H, Hynes RO. Cell adhesion events mediated by α_4 integrins are essential in placental and cardiac development. Development. 1995 (121): 549-560.

8. Baudino TA, McFadden A, Fix C, Hastings J, Price R, Borg TK. Cell patterning: interaction of cardiac myocytes and fibroblasts in three-dimensional culture. Microsc Microanal. 2008 Apr;14(2):117-25.

9. Meng L, Bian Z, Torensma R, Von den Hoff JW. Biological mechanisms in palatogenesis and cleft palate. J Dent Res. 2009 Jan;88(1):22-33.

10. Shimizu T, Yabe T, Muraoka O, Yonemura S, Aramaki S, Hatta K, Bae YK, Nojima H, Hibi M. E-cadherin is required for gastrulation cell movements in zebrafish. Mech Dev. 2005 Jun;122(6):747-63.

11. Hodivala-Dilke KM, McHugh KP, Tsakiris DA, Rayburn H, Crowley D, Ullman-Culleré M, Ross FP, Coller BS, Teitelbaum S, Hynes RO. Beta3-integrin-deficient mice are a model for Glanzmann thrombasthenia showing placental defects and reduced survival. J Clin Invest. 1999 Jan;103(2):229-38.

12. Springer, TA. Adhesion receptors of the immune system. Nature. 1990 Aug 2; 346: 425-434.

13. Czyz J, Wiese C, Rolletschek A, Blyszczuk P, Cross M, Wobus AM. Potential of embryonic and adult stem cells in vitro. Biol Chem. 2003 Oct-Nov;384(10-11):1391-409.

14. Grzesiak JJ, Bouvet M. Activation of the alpha2beta1 integrin-mediated malignant phenotype on type I collagen in pancreatic cancer cells by shifts in the concentrations of extracellular Mg2+ and Ca2+.Int J Cancer. 2008 May 15;122(10):2199-209.

15. Watanabe K, Takahashi H, Habu Y, Kamiya-Kubushiro N, Kamiya S, Nakamura H, Yajima H, Ishii T, Katayama T, Miyazaki K, Fukai F.Interaction with heparin and matrix metalloproteinase 2 cleavage expose a cryptic anti-adhesive site of fibronectin. Biochemistry. 2000 Jun 20;39(24):7138-44.

16. Harburger DS, Calderwood DA. Integrin signalling at a glance. J Cell Sci. 2009 Jan 15;122(Pt 2):159-63.

17. Telemeco, Todd A.(2004) Regulation of Gelatinases in neonatal cardiac fibroblast: the interaction between substrate and strain specific signals. Doctoral Thesis, Virginia Commonwealth University. Richmond, VA

18. Telemeco T, Ellis R, Bowman JR, Bowlin GL and DG Simpson. "Matrix Metalloproteinases in Bioengineering Interventions". In Wnek GE, and Bowlin GL, editors. Encyclopedia of Biomaterials and Biomedical Engineering. New York: Marcel Dekker. 2004.

19. Shirayoshi Y, Hatta K, Hosoda M, Tsunasawa S, Sakiyama F, Takeichi M. Cadherin cell adhesion molecules with distinct binding specificities share a common structure. EMBO J. 1986 Oct;5(10):2485-8.

20. Vaughn DE, Bjorkman PJ.The (Greek) key to structures of neural adhesion molecules. Neuron. 1996 Feb;16(2):261-73.

21. Lasky LA. Selectins: interpreters of cell-specific carbohydrate information during inflammation. Science. 6 November 1992: Vol. 258. no. 5084, pp. 964 – 969.

22. Rubin K, Gullberg D, Borg TK, Obrink B. Hepatocyte adhesion to collagen. Isolation of membrane glycoproteins involved in adhesion to collagen. Exp Cell Res. 1986 May;164(1):127-38.

23. Takeichi, M. The cadherins: cell-cell adhesion molecules controlling animal morphogenesis. Development. 1988(102) 639-655.

24. Yagi T, Takeichi M. Cadherin superfamily genes: functions, genomic organization, and neurologic diversity. Genes Dev. 2000 May 15;14(10):1169-80.

25. Hamaguchi M, Matsuyoshi N, Ohnishi Y, Gotoh B, Takeichi M, Nagai Y.p60v-src causes tyrosine phosphorylation and inactivation of the N-cadherin-catenin cell adhesion system.EMBO J. 1993 Jan;12(1):307-14.

26. McCrea PD, Brieher WM, Gumbiner BM. Induction of a secondary body axis in Xenopus by antibodies to beta-catenin.J Cell Biol. 1993 Oct;123(2):477-84.

27. Nakagawa S, Takeichi M. Neural crest cell-cell adhesion controlled by sequential and subpopulation-specific expression of novel cadherins.Development. 1995 May;121(5):1321-32.

28. Yokoyama H, Tamura K, Ide H. Anteroposterior axis formation in Xenopus limb bud recombinants: a model of pattern formation during limb regeneration. Developmental Dynamics. 2002(255) 277-288.

29. Yajima H, Yonei-Tamura S, Watanabe N, Tamura K, Ide H. Role of N-Cadherin in the sorting-out of mesenchymal cells and in the positional identity along the proximodistal axis of the chick limb bud. Developmental Dynamics. 1999(216) 274-284

30. Knudsen KA, Myers L, McElwee SA.A role for the Ca2(+)-dependent adhesion molecule, N-cadherin, in myoblast interaction during myogenesis. Exp Cell Res. 1990 Jun;188(2):175-84.

31. Letourneau PC, Roche FK, Shattuck TA, Lemmon V, Takeichi M. Interactions of Schwann cells with neurites and with other Schwann cells involve the calcium-dependent adhesion molecule, N-cadherin. J Neurobiol. 1991 Oct;22(7):707-20.

32. Müller EJ, Williamson L, Kolly C, Suter MM. Outside-in signaling through integrins and cadherins: a central mechanism to control epidermal growth and differentiation? J Invest Dermatol. 2008 Mar;128(3):501-16.

33. Cunningham BA, Hemperly JJ, Murray BA, Prediger EA, Brackenbury R, Edelman GM.Neural cell adhesion molecule: structure, immunoglobulin-like domains, cell surface modulation, and alternative RNA splicing. Science. 1987 May 15;236(4803):799-806.

34. Schmid RS, Maness PF.L1 and NCAM adhesion molecules as signaling coreceptors in neuronal migration and process outgrowth. Curr Opin Neurobiol. 2008 Jun;18(3):245-50.

35. Alon R, Kassner PD, Carr MW, Finger EB, Hemler ME and Springer TA. The integrin VLA-4 supports tethering and rolling in flow on VCAM-1. J Cell Biology. 1995. March, 1. Vol 128, 1243-1253.

36. Takai Y, Ikeda W, Ogita H, Rikitake Y. The immunoglobulin-like cell adhesion molecule nectin and its associated protein afadin. Annu.Rev.Cell Dev Bio. 2008. (24): 309-342.

37. Bevilacqua MP, Stengelin S, Gimbrone MA Jr, Seed B.Endothelial leukocyte adhesion molecule 1: an inducible receptor for neutrophils related to complement regulatory proteins and lectins. Science. 1989 Mar 3;243(4895):1160-5.

38. Springer TA, Lasky LA.Cell adhesion. Sticky sugars for selectins. Nature. 1991 Jan 17;349(6306):196-7.

39. Lawrence MB, Springer TA. Leukocytes roll on a selectin at physiologic flow rates: distinction from and prerequisite for adhesion through integrins. Cell. 1991 May 31;65(5):859-73.

40. Alon R, Ley K.Cells on the run: shear-regulated integrin activation in leukocyte rolling and arrest on endothelial cells. Curr Opin Cell Biol. 2008 Oct;20(5):525-32.

41. Carver W, Price RL, Raso DS, Terracio L, Borg TK. Distribution of β-1 Integrin in the developing rat heart. J Histochem Cytochem 1994 42:167-175.

42. Akiyama SK, Yamada SS, Chen WT, Yamada KM. Analysis of fibronectin receptor function with monoclonal antibodies: roles in cell adhesion, migration, matrix assembly, and cytoskeletal organization. J Cell Biol. 1989 Aug;109(2):863-75.

43. Montgomery AM, Reisfeld RA, Cheresh DA. Integrin alpha v beta 3 rescues melanoma cells from apoptosis in three-dimensional dermal collagen. Proc Natl Acad Sci U S A. 1994 Sep 13;91(19):8856-60.

44. Simpson, DG. Integrins. In Wnek GE, and Bowlin GL, editors. Encyclopedia of Biomaterials and Biomedical Engineering. New York: Marcel Dekker. (2005).

45. Tadokoro S, Shattil SJ, Eto K, Tai V, Liddington RC, de Pereda JM, Ginsberg MH, Calderwood DA. Talin binding to integrin beta tails: a final common step in integrin activation. Science. 2003 Oct 3;302(5642):103-6.

46. Moser M, Nieswant B, Ussar S, Pozgajova M, Fassler R. Kindlin-3 is essential for integrin activation and platelet aggregation. Nature Medicine. 2008 Mar; 14(3):325-330.

47. Mulrooney J, Foley K, Vineberg S, Barreuther M, Grabel L. Phosphorylation of the beta1 integrin cytoplasmic domain: toward an understanding of function and mechanism. Exp Cell Res. 2000 Aug 1;258(2):332-41.

48. Briesewitz R, Kern A, Marcantonio EE.Assembly and function of integrin receptors is dependent on opposing alpha and beta cytoplasmic domains. Mol Biol Cell. 1995 Aug;6(8):997-1010.

49. Litvinov RI, Vilaire G, Li W, DeGrado WF, Weisel JW, Bennett JS Activation of individual alphaIIbbeta3 integrin molecules by disruption of transmembrane domain interactions in the absence of clustering. Biochemistry. 2006 Apr 18;45(15):4957-64.

50. Humphies MJ. Integrin structure. Biochemical Society Transactions. 2000 (28:4) 311-339.

51. Xiong JP, Stehle T, Zhang R, Joachimiak A, Frech M, Goodman SL, Arnaout MA. Extracellular segment of integrin $\alpha v\beta_3$ in complex with an arg-gly-asp ligand. Science. 2002 Apr 5 (296); 151-155.

52. Takagi J, Petre BM, Walz T, Springer TA.Global conformational rearrangements in integrin extracellular domains in outside-in and inside-out signaling. Cell. 2002 Sep 6;110(5):599-11.

53. Luo BH, Carman CV, Springer TA. Structural basis of integrin regulation and signaling. Annu Rev Immunol. 2007;25:619-47.

54. Olsen IM, Ffrench-Constant C.Dynamic regulation of integrin activation by intracellular and extracellular signals controls oligodendrocyte morphology. BMC Biol. 2005 Nov 12;3:25.

55. Goksoy E, Ma YQ, Wang X, Kong X, Perera D, Plow EF, Qin J Structural basis for the autoinhibition of talin in regulating integrin activation. Mol Cell. 2008 Jul 11;31(1):124-33.

56. Lee HS, Lim CJ, Puzon-McLaughlin W, Shattil SJ, Ginsberg MH. RIAM activates integrins by linking talin to ras GTPase membrane-targeting sequences. J Biol Chem. 2009 Feb 20;284(8):5119-27.

57. Critchley DR. Smurf1 zaps the talin head. Nat Cell Biol. 2009 May;11(5):538-40.

58. del Rio A, Perez-Jimenez R, Liu R, Roca-Cusachs P, Fernandez JM, Sheetz MP. Stretching Single Talin Rod Molecules Activates Vinculin Binding. Science. 30 January 2009: 638-641.

59. Kanekar S, Hirozanne T, Terracio L, Borg TK. Cardiac fibroblast: form and function. Cardiovascular Pathology. 6 May 1998; 7(3): 127-133.

60. Burgess ML, Terracio L, Hirozane T, Borg TK. Differential integrin expression by cardiac fibroblasts from hypertensive and exercise-trained rat hearts. Cardiovasc Pathol. 2002 Mar-Apr;11(2):78-87.

61. Gullberg D, Terracio L, Borg TK, Rubin K.Identification of integrin-like matrix receptors with affinity for interstitial collagens. J Biol Chem. 1989 Jul 25;264(21):12686-94.

62. Tomaselli KJ, Damsky CH, Reichardt LF.Purification and characterization of mammalian integrins expressed by a rat neuronal cell line (PC12): evidence that they function as alpha/beta heterodimeric receptors for laminin and type IV collagen.J Cell Biol. 1988 Sep;107(3):1241-52.

63. Languino LR, Gehlsen KR, Wayner E, Carter WG, Engvall E, Ruoslahti E. Endothelial cells use alpha 2 beta 1 integrin as a laminin receptor. J Cell Biol. 1989 Nov;109(5):2455-62.

64. Gullberg D, Gehlsen KR, Turner DC, Ahlén K, Zijenah LS, Barnes MJ, Rubin K.Analysis of alpha 1 beta 1, alpha 2 beta 1 and alpha 3 beta 1 integrins in cell--collagen interactions: identification of conformation dependent alpha 1 beta 1 binding sites in collagen type I.EMBO J. 1992 Nov;11(11):3865-73.

65. Calderwood DA, Tuckwell DS, Eble J, Kühn K, Humphries MJ.The integrin alpha1 A-domain is a ligand binding site for collagens and laminin.J Biol Chem. 1997 May 9;272(19):12311-7.

66. Reyes CD, Garcia AJ. Engineering integrin specific surfaces with a triple-helical collagen mimetic peptide. Journal of biomedical materials research. 2003, May 13 (65:4) 511-523.

67. Herr AB, Farndale RW.Structural insights into the interactions between platelet receptors and fibrillar collagen. J Biol Chem. 2009 Apr 28.

68. Knight CG, Morton LF, Onley DJ, Peachey AR, Messent AJ, Smethurst PA, Tuckwell DS, Farndale RW, Barnes MJ.Identification in collagen type I of an integrin alpha2 beta1-binding site containing an essential GER sequence.J Biol Chem. 1998 Dec 11;273(50):33287-94.

69. Forsberg E, Paulsson M, Timpl R, Johansson S. Characterization of a laminin receptor on rat hepatocytes. J Biol Chem. 1990 Apr 15;265(11):6376-81.

70. Tulla M, Lahti M, Puranen JS, Brandt AM, Käpylä J, Domogatskaya A, Salminen TA, Tryggvason K, Johnson MS, Heino J. Effects of conformational activation of Integrin alpha 1I and alpha 2I domains on selective recognition of laminin and collagen subtypes. Exp Cell Res. 2008 May 1;314(8):1734-43.

71. Elices MJ, Urry LA, Hemler ME. Receptor functions for the integrin VLA-3: fibronectin, collagen, and laminin binding are differentially influenced by Arg-Gly-Asp peptide and by divalent cations. J Cell Biol. 1991 Jan;112(1):169-81.

72. Wu C, Chung AE, McDonald JA. A novel role for alpha 3 beta 1 integrins in extracellular matrix assembly J Cell Sci. 1995 Jun;108 (Pt 6):2511-23.

73. Di Persio CM, Shah S, Hynes RO. Alpha 3A beta 1 integrin localizes to focal contacts in response to diverse extracellular matrix proteins. J Cell Sci.1995 108 (Pt 6):2321-36.

74. Conforti G, Zanetti A, Colella S, Abbadini M, Marchisio PC, Pytela R, Giancotti F, Tarone G, Languino LR, Dejana E.Interaction of fibronectin with cultured human endothelial cells: characterization of the specific receptor Blood. 1989 May 1;73(6):1576-85.

75. Wu C, Bauer JS, Juliano RL and McDonald JA The alpha 5 beta 1 integrin fibronectin receptor, but not the alpha 5 cytoplasmic domain, functions in an early and essential step in fibronectin matrix assembly J. Biol. Chem., Vol. 268, Issue 29, 21883-21888, Oct, 1993

76. Zhong C, Chrzanowska-Wodnicka M, Brown J, Shaub A, Belkin AM, Burridge K. Rho-mediated contractility exposes a cryptic site in fibronectin and induces fibronectin matrix assembly.J Cell Biol. 1998 Apr 20;141(2):539-51.

77. Sekiguchi K, Hakomori S. Functional domain structure of fibronectin. Proc Natl Acad Sci U S A. 1980 May;77(5):2661-5.

78. Smith ML, Gourdon D, Little WC, Kubow KE, Eguiluz RA, Luna-Morris S, Vogel V. Force-induced unfolding of fibronectin in the extracellular matrix of living cells. PLoS Biol. 2007 Oct 2;5(10):e268.

79. Fukai F, Ohtaki M, Fujii N, Yajima H, Ishii T, Nishizawa Y, Miyazaki K, Katayama T. Release of biological activities from quiescent fibronectin by a conformational change and limited proteolysis by matrix metalloproteinases. Biochemistry. 1995 Sep 12;34(36):11453-9.

80. Nobes CD, Hall A. Rho, rac, and cdc42 GTPases regulate the assembly of multimolecular focal complexes associated with actin stress fibers, lamellipodia, and filopodia. Cell. 7;81(1):53-62. (1995).

81. Lotz MM, Burdsal CA, Erickson HP, McClay DR. Cell adhesion to fibronectin and tenascin: quantitative measurements of initial binding and subsequent strengthening response. J Cell Biol. 109(4 Pt 1):1795-805 (1989).

82. Dejana E, Colella S, Conforti G, Abbadini M, Gaboli M, Marchisio PC. Fibronectin and vitronectin regulate the organization of their respective Arg-Gly-Asp adhesion receptors in cultured human endothelial cells. J Cell Biol. 1988 Sep;107(3):1215-23.

83. Cairo CW, Mirchev R, Golan DE. Cytoskeletal regulation couples LFA-1 conformational changes to receptor lateral mobility and clustering. Immunity. 2006 Aug;25(2):297-308

84. Machesky LM, Hall A. LiRole of actin polymerization and adhesion to extracellular matrix in Rac- and Rho-induced cytoskeletal reorganization. J Cell Biol. 1997 Aug 25;138(4):913-26.

85. Riveline D, Zamir E, Balaban NQ, Schwarz US, Ishizaki T, Narumiya S, Kam Z, Geiger B, Bershadsky AD. Focal contacts as mechanosensors: externally applied local mechanical force induces growth of focal contacts by an mDia1-dependent and ROCK-independent mechanism. J Cell Biol. 153(6):1175-86. (2001).

86. Balaban NQ, Schwarz US, Riveline D, Goichberg P, Tzur G, Sabanay I, Mahalu D, Safran S, Bershadsky A, Addadi L, Geiger B. Force and focal adhesion assembly: a close relationship studied using elastic micropatterned substrates. Nat Cell Biol. 2001 May;3(5):466-72.

87. Kawakami K, Tatsumi H, Sokabe M. Dynamics of integrin clustering at focal contacts of endothelial cells studied by multimode imaging microscopy.J Cell Sci. 2001 Sep;114(Pt 17):3125-35.

88. Geiger B. The association of rhodamine - labelled alpha-actinin with actin bundles in demembranated cells.Cell Biol Int Rep. 1981 Jun;5(6):627-34.

89. Hilenski LL, Terracio L, Borg TK.Myofibrillar and cytoskeletal assembly in neonatal rat cardiac myocytes cultured on laminin and collagen. Cell Tissue Res. 1991 Jun;264(3):577-87.

90. Li F, Zhang Y, Wu C. Integrin-linked kinase is localized to cell-matrix focal adhesions but not cell-cell adhesion sites and the focal adhesion localization of integrin-linked kinase is regulated by the PINCH-binding ANK repeats. J Cell Sci. 1999 Dec;112 (Pt 24):4589-99.

91. Shen Y, Schaller MD. Focal adhesion targeting: the critical determinant of FAK regulation and substrate phosphorylation. Mol Biol Cell. 1999 Aug;10(8):2507-18.

92. Sun Z, Martinez-Lemus LA, Trache A, Trzeciakowski JP, Davis GE, Pohl U, Meininger GA.Mechanical properties of the interaction between fibronectin and alpha5beta1-integrin on vascular smooth muscle cells studied using atomic force microscopy. Am J Physiol Heart Circ Physiol. 2005 Dec;289(6):H2526-35.

93. Nobes CD, Hall A.Rho GTPases control polarity, protrusion, and adhesion during cell movement. J Cell Biol. 1999 Mar 22;144(6):1235-44.

94. Chrzanowska-Wodnicka M, Burridge K.Rho-stimulated contractility drives the formation of stress fibers and focal adhesions. J Cell Biol. 1996 Jun;133(6):1403-15.

95. Leung T, Chen XQ, Manser E and Lim L. The p160 RhoA-binding kinase ROK alpha is a member of a kinase family and is involved in the reorganization of the cytoskeleton Mol. Cell. Biol., Oct 1996, 5313-5327, Vol 16, No. 10

96. Chen W.-T., Mechanism of retraction of the trailing edge during fibroblast movement. J. Cell Biol. 90 (1981), pp. 187–200.

97. Ezratty EJ, Partridge MA, Gundersen GG.Microtubule-induced focal adhesion disassembly is mediated by dynamin and focal adhesion kinase. Nat Cell Biol. 2005 Jun;7(6):581-90.

98. Bretscher MS. Endocytosis and recycling of the fibronectin receptor in CHO cells. EMBO J. 1989 May;8(5):1341-8.

99. Geiger B, Bershadsky A.Assembly and mechanosensory function of focal contacts.Curr Opin Cell Biol. 2001 Oct;13(5):584-92.

100. Chao WT, Kunz J. Focal adhesion disassembly requires clathrin-dependent endocytosis of integrins. FEBS Lett. 2009 Apr 17;583(8):1337-43.

101. Burridge K, Chrzanowska-Wodnicka M. Focal adhesions, contractility, and signaling. Annu Rev Cell Dev Biol. 1996;12:463-518.

102. Fox MA, Colello RJ, Macklin WB, Fuss B.Phosphodiesterase-Ialpha/autotaxin: a counteradhesive protein expressed by oligodendrocytes during onset of myelination.Mol Cell Neurosci. 2003 Jul;23(3):507-19.

103. Ylänne J, Chen Y, O'Toole TE, Loftus JC, Takada Y, Ginsberg MH. Distinct functions of integrin alpha and beta subunit cytoplasmic domains in cell spreading and formation of focal adhesions. J Cell Biol. 1993 Jul;122(1):223-33.

104. Noiri E, Gailit J, Sheth D, Magazine H, Gurrath M, Muller G, Kessler H, Goligorsky MS. Cyclic RGD peptides ameliorate ischemic acute renal failure in rats.Kidney Int. 1994 Oct;46(4):1050-8.

105. MacKenna DA, Dolfi F, Vuori K, Ruoslahti E. Extracellular signal-regulated kinase and c-Jun NH2-terminal kinase activation by mechanical stretch is integrin-dependent and matrix-specific in rat cardiac fibroblasts. J Clin Invest. 1998 Jan 15;101(2):301-10.

106. Wegener J, Kesse CR, Giaever I. Electric Cell–Substrate Impedance Sensing (ECIS) as a Noninvasive Means to Monitor the Kinetics of Cell Spreading to Artificial Surfaces. Experimental Cell Research. Volume 259, Issue 1, 25 August 2000, Pages 158-166

107. Sharma KV, Koenigsberger C, Brimijoin S, Bigbee JW.Direct evidence for an adhesive function in the noncholinergic role of acetylcholinesterase in neurite outgrowth.J Neurosci Res. 2001 Jan 15;63(2):165-75.

108. Lehenkari PP, Horton MA. Single integrin molecule adhesion forces in intact cells measured by atomic force microscopy.Biochem Biophys Res Commun. 1999 Jun 16;259(3):645-50.

109. Wang N, Butler JP, Ingber DE. Mechanotransduction across the cell surface and through the cytoskeleton. Science. 1993 May 21;260(5111):1124-7.

110. Hilenski LL, Ma XH, Vinson N, Terracio L, Borg TK. The role of beta 1 integrin in spreading and myofibrillogenesis in neonatal rat cardiomyocytes in vitro. Cell Motil Cytoskeleton. 1992;21(2):87-100.

111. Bell PB Jr, Lindroth M, Fredriksson BA.Use of sputter coating to prepare whole mounts of cytoskeletons for transmission and high-resolution scanning and scanning transmission electron microscopy. J Electron Microsc Tech. 1987 Nov;7(3):149- 59.

112. Hilenski LL, Terracio L, Sawyer R, Borg TK.Effects of extracellular matrix on cytoskeletal and myofibrillar organization in vitro. Scanning Microsc. 1989 Jun;3(2):535-48.

113. Sharp WW, Simpson DG, Borg TK, Samarel AM, Terracio L. Mechanical forces regulate focal adhesion and costamere assembly in cardiac myocytes. Am J Physiol. 1997 Aug;273(2 Pt 2):H546-56.

114. Mallavarapu A, Mitchison T. Regulated actin cytoskeleton assembly at filopodium tips controls their extension and retraction. J Cell Biol. 1999 Sep 6;146(5):1097-106.

115. Vikstrom KL, Lim SS, Goldman RD, Borisy GG.Steady state dynamics of intermediate filament networks. J Cell Biol. 1992 Jul;118(1):121-9.

116. Booz GW, Baker KMMolecular signalling mechanisms controlling growth and function of cardiac fibroblasts.Cardiovasc Res. 1995 Oct;30(4):537-43.

117. Husse B, Briest W, Homagk L, Isenberg G, Gekle M Cyclical mechanical stretch modulates expression of collagen I and collagen III by PKC and tyrosine kinase in cardiac fibroblasts.Am J Physiol Regul Integr Comp Physiol. 2007 Nov;293(5):R1898-907.

118. Sadoshima J, Izumo S.The cellular and molecular response of cardiac myocytes to mechanical stress.Annu Rev Physiol. 1997;59:551-71.

119. Xu J, Rodriguez D, Petitclerc E, Kim JJ, Hangai M, Moon YS, Davis GE, Brooks PC. Proteolytic exposure of a cryptic site within collagen type IV is required for angiogenesis and tumor growth in vivo. J Cell Biol. 2001 Sep 3;154(5):1069-79.

120. Cook H, Davies KJ, Harding KG, Thomas DW. Defective extracellular matrix reorganization by chronic wound fibroblasts is associated with alterations in TIMP-1, TIMP-2, and MMP-2 activity. J Invest Dermatol. 2000 Aug;115(2):225-33.

121. Davis GE. Affinity of integrins for damaged extracellular matrix: alpha v beta 3 binds to denatured collagen type I through RGD sites. Biochem Biophys Res Commun. 1992 Feb 14;182(3):1025-31.

122. Pilcher BK, Dumin JA, Sudbeck BD, Krane SM, Welgus HG, Parks WC.The activity of collagenase-1 is required for keratinocyte migration on a type I collagen matrix. J Cell Biol. 1997 Jun 16;137(6):1445-57.

123. Sakakura Y, Hosokawa Y, Tsuruga E, Irie K, Yajima T. In situ localization of gelatinolytic activity during development and resorption of Meckel's cartilage in mice. Eur J Oral Sci. 2007 Jun;115(3):212-23.

124. VanSaun MN, Matrisian LM. Matrix metalloproteinases and cellular motility in development and disease. Birth Defects Res C Embryo Today. 2006 Mar;78(1):69-79.

125. Van Wart H E and Birkedal-Hansen H. The cysteine switch: a principle of regulation of metalloproteinase activity with potential applicability to the entire matrix metalloproteinase gene family. Proc Natl Acad Sci U S A. 1990 July; 87(14): 5578–5582.

126. Ratajska A, Cleutjens JP. Embryogenesis of the rat heart: the expression of collagenases. Basic Res Cardiol. 2002 May;97(3):189-97.

127. Spinale FG, Coker ML, Thomas CV, Walker JD, Mukherjee R, Hebbar L.Time-dependent changes in matrix metalloproteinase activity and expression during the progression of congestive heart failure: relation to ventricular and myocyte function. Circ Res. 1998 Mar 9;82(4):482-95.

128. Nakagawa M, Terracio L, Carver W, Birkedal-Hansen H, Borg TK. Expression of collagenase and IL-1 alpha in developing rat hearts. Dev Dyn. 1992 Oct;195(2):87-99

129. Allan JA, Docherty AJ, Barker PJ, Huskisson NS, Reynolds JJ, Murphy G. Binding of gelatinases A and B to type-I collagen and other matrix components. Biochem J. 1995 Jul 1;309 (Pt 1):299-306.

130. Aimes R.T., Quigley J.P. Matrix metalloproteinase-2 is an interstitial collagenase. Inhibitor-free enzyme catalyzes the cleavage of collagen fibrils and soluble native type I collagen generating the specific 3/4- and 1/4-length fragments. J Biol Chem (1995) 270:5872–5876

131. Patterson M.L., Atkinson S.J., Knäuper V., Murphy G. Specific collagenolysis by gelatinase A, MMP-2, is determined by the hemopexin domain and not the fibronectin-like domain. FEBS Lett (2001) 503:158–162.

132. Xu X, Chen Z, Wang Y, Yamada Y, Steffensen B. Functional basis for the overlap in ligand interactions and substrate specificities of matrix metalloproteinases-9 and -2. Biochem J. 2005 Nov 15;392(Pt 1):127-34.

133. Wysocki AB, Staiano-Coico L, Grinnell F. Wound fluid from chronic leg ulcers contains elevated levels of metalloproteinases MMP-2 and MMP-9. J Invest Dermatol. 1993 Jul;101(1):64-8.

134. Xu X, Wang Y, Chen Z, Sternlicht MD, Hidalgo M, Steffensen B.Matrix metalloproteinase-2 contributes to cancer cell migration on collagen. Cancer Res. 2005 Jan 1;65(1):130-6.

135. Feng Y, Sun B, Li X, Zhang L, Niu Y, Xiao C, Ning L, Fang Z, Wang Y, Zhang L, Cheng J, Zhang W, Hao X. Differentially expressed genes between primary cancer and paired lymph node metastases predict clinical outcome of node-positive breast cancer patients.Breast Cancer Res Treat. 2007 Jul;103(3):319-29.

136. Strongin AY, Collier I, Bannikov G, Marmer BL, Grant GA, Goldberg GI.Mechanism of cell surface activation of 72-kDa type IV collagenase. Isolation of the activated form of the membrane metalloprotease. J Biol Chem. 1995 Mar 10;270(10):5331-8.

137. Stanton H, Gavrilovic J, Atkinson SJ, d'Ortho MP, Yamada KM, Zardi L, Murphy G. The activation of ProMMP-2 (gelatinase A) by HT1080 fibrosarcoma cells is promoted by culture on a fibronectin substrate and is concomitant with an increase in processing of MT1-MMP (MMP-14) to a 45 kDa form. J Cell Sci. 1998 Sep;111 (Pt 18):2789-98.

138. Okada Y, Morodomi T, Enghild JJ, Suzuki K, Yasui A, Nakanishi I, Salvesen G, Nagase H.Matrix metalloproteinase 2 from human rheumatoid synovial fibroblasts.

Purification and activation of the precursor and enzymic properties. Eur J Biochem. 1990 Dec 27;194(3):721-30.

139. Crabbe T, Ioannou C, Docherty AJ. Human progelatinase A can be activated by autolysis at a rate that is concentration-dependent and enhanced by heparin bound to the C-terminal domain.Eur J Biochem. 1993 Dec 1;218(2):431-8.

140. Ramos-DeSimone N, Hahn-Dantona E, Sipley J, Nagase H, French DL, Quigley JP. Activation of matrix metalloproteinase-9 (MMP-9) via a converging plasmin/stromelysin-1 cascade enhances tumor cell invasion.J Biol Chem. 1999 May 7;274(19):13066-76.

141. Parks WC and Mecham, eds. Matrix Metalloprotienases. NewYork: Academic Press, 1998.

142. Balachandran K, Sucosky P, Jo H, Yoganathan AP.Elevated cyclic stretch alters matrix remodeling in aortic valve cusps: implications for degenerative aortic valve disease. Am J Physiol Heart Circ Physiol. 2009 Mar;296(3):H756-64.

143. Olson MW, Gervasi DC, Mobashery S, Fridman R. Kinetic analysis of the binding of human matrix metalloproteinase-2 and -9 to tissue inhibitor of metalloproteinase (TIMP)-1 and TIMP-2. J Biol Chem. 1997 Nov 21;272(47):29975-83.

144. Howard EW, Bullen EC, Banda MJ. Preferential inhibition of 72- and 92-kDa gelatinases by tissue inhibitor of metalloproteinases-2. J Biol Chem. 1991 Jul 15;266(20):13070-5.

145. Ogata Y, Itoh Y, Nagase H. Steps involved in activation of the pro-matrix metalloproteinase 9 (progelatinase B)-tissue inhibitor of metalloproteinases-1 complex by 4-aminophenylmercuric acetate and proteinases. J Biol Chem. 1995 Aug 4;270(31):18506-11.

146. Baramova EN, Bajou K, Remacle A, L'Hoir C, Krell HW, Weidle UH, Noel A, Foidart JM. Involvement of PA/plasmin system in the processing of pro-MMP-9 and in the second step of pro-MMP-2 activation.FEBS Lett. 1997 Mar 24;405(2):157-62.

147. Ogata Y, Enghild JJ, Nagase H.Matrix metalloproteinase 3 (stromelysin) activates the precursor for the human matrix metalloproteinase 9.J Biol Chem. 1992 Feb 25;267(6):3581-4.

148. Hahn-Dantona E, Ramos-DeSimone N, Sipley J, Nagase H, French DL, Quigley JP. Activation of proMMP-9 by a plasmin/MMP-3 cascade in a tumor cell model.

Regulation by tissue inhibitors of metalloproteinases. Ann N Y Acad Sci. 1999 Jun 30;878:372-87.

149. Hsieh YS, Yang SF, Lue KH, Chu SC, Lu KH. Effects of different molecular weight hyaluronan products on the expression of urokinase plasminogen activator and inhibitor and gelatinases during the early stage of osteoarthritis. J Orthop Res. 2008 Apr;26(4):475-84.

150. Yoshihara Y, Nakamura H, Obata K, Yamada H, Hayakawa T, Fujikawa K, Okada Y. Matrix metalloproteinases and tissue inhibitors of metalloproteinases in synovial fluids from patients with rheumatoid arthritis or osteoarthritis. Ann Rheum Dis. 2000 Jun;59(6):455-61.

151. Buisson-Legendre N, Smith S, March L, Jackson C. Elevation of activated protein C in synovial joints in rheumatoid arthritis and its correlation with matrix metalloproteinase 2. Arthritis Rheum. 2004 Jul;50(7):2151-6.

152. Jackson MT, Smith MM, Smith SM, Jackson CJ, Xue M, Little CB. Activation of cartilage matrix metalloproteinases by activated protein C. Arthritis Rheum. 2009 Mar;60(3):780-91.

153. Miller MC, Manning HB, Jain A, Troeberg L, Dudhia J, Essex D, Sandison A, Seiki M, Nanchahal J, Nagase H, Itoh Y.Membrane type 1 matrix metalloproteinase is a crucial promoter of synovial invasion in human rheumatoid arthritis. Arthritis Rheum. 2009 Mar;60(3):686-97.

154. Zeng ZS, Cohen AM, Guillem JG.Loss of basement membrane type IV collagen is associated with increased expression of metalloproteinases 2 and 9 (MMP-2 and MMP-9) during human colorectal tumorigenesis.Carcinogenesis. 1999 May;20(5):749-55.

155. Kenny HA, Kaur S, Coussens LM, Lengyel E.The initial steps of ovarian cancer cell metastasis are mediated by MMP-2 cleavage of vitronectin and fibronectin. J Clin Invest. 2008 Apr;118(4):1367-79.

156. Sholley MM, Gimbrone MA Jr, Cotran RS.Cellular migration and replication in endothelial regeneration: a study using irradiated endothelial cultures.Lab Invest. 1977 Jan;36(1):18-25.

157. Belotti D, Paganoni P, Manenti L, Garofalo A, Marchini S, Taraboletti G, Giavazzi R. Matrix metalloproteinases (MMP9 and MMP2) induce the release of vascular endothelial growth factor (VEGF) by ovarian carcinoma cells: implications for ascites formation. Cancer Res. 2003 Sep 1;63(17):5224-9.

158. Kamat AA, Fletcher M, Gruman LM, Mueller P, Lopez A, Landen CN Jr, Han L, Gershenson DM, Sood AK.The clinical relevance of stromal matrix metalloproteinase expression in ovarian cancer. Clin Cancer Res. 2006 Mar 15;12(6):1707-14.

159. Morgia G, Falsaperla M, Malaponte G, Madonia M, Indelicato M, Travali S, Mazzarino MC. Matrix metalloproteinases as diagnostic (MMP-13) and prognostic (MMP-2, MMP-9) markers of prostate cancer. Urol Res. 2005 Feb;33(1):44-50.

160. Kunishio K, Okada M, Matsumoto Y, Nagao S.Matrix metalloproteinase-2 and -9 expression in astrocytic tumors. Brain Tumor Pathol. 2003;20(2):39-45.

161. Zhang K, Li C, Liu Y, Li L, Ma X, Meng X, Feng D.Evaluation of invasiveness of astrocytoma using 1H-magnetic resonance spectroscopy: correlation with expression of matrix metalloproteinase-2. Neuroradiology. 2007 Nov;49(11):913-919.

162. Lossos IS, Morgensztern D. Prognostic biomarkers in diffuse large B-cell lymphoma. J Clin Oncol. 2006 Feb 20;24(6):995-1007.

163. Redondo-Muñoz J, Escobar-Díaz E, Samaniego R, Terol MJ, García-Marco JA, García-Pardo A. MMP-9 in B-cell chronic lymphocytic leukemia is up-regulated by alpha4beta1 integrin or CXCR4 engagement via distinct signaling pathways, ,localizes to podosomes, and is involved in cell invasion and migration. Blood. 2006 Nov 1;108(9):3143-51.

164. Buommino E, Baroni A, Canozo N, Petrazzuolo M, Nicoletti R, Vozza A, Tufano MA. Artemisinin reduces human melanoma cell migration by down-regulating alphaVbeta3 integrin and reducing metalloproteinase 2 production. Invest New Drugs. 2008 Oct 28.

165. Kurschat P, Zigrino P, Nischt R, Breitkopf K, Steurer P, Klein CE, Krieg T, Mauch C.Tissue inhibitor of matrix metalloproteinase-2 regulates matrix metalloproteinase-2 activation by modulation of membrane-type 1 matrix metalloproteinase activity in high and low invasive melanoma cell lines. J Biol Chem. 1999 Jul 23;274(30):21056-62.

166. Buckingham M, Meilhac S, Zaffran S. Building the mammalian heart from two sources of myocardial cells. Nat Rev Genet. 2005 Nov;6(11):826-35.

167. Nakamura A, Manasek FJ.An experimental study of the relation of cardiac jelly to the shape of the early chick embryonic heart. J Embryol Exp Morphol. 1981 Oct;65:235-56.

168. Simpson DG, Sharp WW, Borg TK, Price RL, Samarel AM, Terracio L. Mechanical regulation of cardiac myofibrillar structure. Ann N Y Acad Sci. 1995 Mar 27;752:131-40.

169. Price RL, Chintanowonges C, Shiraishi I, Borg TK, Terracio L.Local and regional variations in myofibrillar patterns in looping rat hearts.Anat Rec. 1996 May;245(1):83-93.

170. Linask KK, Han M, Cai DH, Brauer PR, Maisastry SM. Cardiac morphogenesis: matrix metalloproteinase coordination of cellular mechanisms underlying heart tube formation and directionality of looping. Dev Dyn. 2005 Jul;233(3):739-53.

171. Alexander SM, Jackson KJ, Bushnell KM, McGuire PG. Spatial and temporal expression of the 72-kDa type IV collagenase (MMP-2) correlates with development and differentiation of valves in the embryonic avian heart. Dev Dyn. 1997 Jul;209(3):261-8.

172. Cai DH, Brauer PR. Synthetic matrix metalloproteinase inhibitor decreases early cardiac neural crest migration in chicken embryos. Dev Dyn. 2002 Aug;224(4):441-9.

173. Weber KT, Sun Y, Guarda E. Structural remodeling in hypertensive heart disease and the role of hormones. Hypertension. 1994 Jun;23(6 Pt 2):869-77.

174. Weber KT. Fibrosis and hypertensive heart disease. Curr Opin Cardiol. 2000 Jul;15(4):264-72.

175. Pearlman ES, Weber KT, Janicki JS, Pietra GG, Fishman AP.Muscle fiber orientation and connective tissue content in the hypertrophied human heart. Lab Invest. 1982 Feb;46(2):158-64.

176. Peterson JT, Hallak H, Johnson L, Li H, O'Brien PM, Sliskovic DR, Bocan TM, Coker ML, Etoh T, Spinale FG. Matrix metalloproteinase inhibition attenuates left ventricular remodeling and dysfunction in a rat model of progressive heart failure. Circulation. 2001 May 8;103(18):2303-9.

177. Bergman MR, Teerlink JR, Mahimkar R, Li L, Zhu BQ, Nguyen A, Dahi S, Karliner JS, Lovett DH. Cardiac matrix metalloproteinase-2 expression

independently induces marked ventricular remodeling and systolic dysfunction. Am J Physiol Heart Circ Physiol. 2007 Apr;292(4):H1847-60.

178. Seeland U, Kouchi I, Zolk O, Itter G, Linz W, Böhm M. Effect of ramipril and furosemide treatment on interstitial remodeling in post-infarction heart failure rat hearts. J Mol Cell Cardiol. 2002 Feb;34(2):151-63.

179. Brower GL, Levick SP, Janicki JS. Inhibition of matrix metalloproteinase activity by ACE inhibitors prevents left ventricular remodeling in a rat model of heart failure. Am J Physiol Heart Circ Physiol. 2007 Jun;292(6):H3057-64.

180. Ahmed SH, Clark LL, Pennington WR, Webb CS, Bonnema DD, Leonardi AH, McClure CD, Spinale FG, Zile MR. Matrix metalloproteinases/tissue inhibitors of metalloproteinases: relationship between changes in proteolytic determinants of matrix composition and structural, functional, and clinical manifestations of hypertensive heart disease. Circulation. 2006 May 2;113(17):2089-96.

181. Usui ML, Mansbridge JN, Carter WG, Fujita M, Olerud JE. Keratinocyte migration, proliferation, and differentiation in chronic ulcers from patients with diabetes and normal wounds. J Histochem Cytochem. 2008 Jul;56(7):687-96.

182. Saarialho-Kere UK, Pentland AP, Birkedal-Hansen H, Parks WC, Welgus HG. Distinct populations of basal keratinocytes express stromelysin-1 and stromelysin-2 in chronic wounds. J Clin Invest. 1994 Jul;94(1):79-88.

183. Grzesiak JJ, Pierschbacher MD. Changes in the concentrations of extracellular Mg++ and Ca++ down-regulate E-cadherin and up-regulate alpha 2 beta 1 integrin function, activating keratinocyte migration on type I collagen. J Invest Dermatol. 1995 May;104(5):768-74.

184. Dumin JA, Dickeson SK, Stricker TP, Bhattacharyya-Pakrasi M, Roby JD, Santoro SA, Parks WC. Pro-collagenase-1 (matrix metalloproteinase-1) binds the alpha(2)beta(1) integrin upon release from keratinocytes migrating on type I collagen. J Biol Chem. 2001 Aug 3;276(31):29368-74.

185. Stricker TP, Dumin JA, Dickeson SK, Chung L, Nagase H, Parks WC, Santoro SA. Structural analysis of the alpha(2) integrin I domain/procollagenase-1 (matrix metalloproteinase-1) interaction. Biol Chem. 3;276(31):29375-81. (2001).

186. Brooks PC, Strömblad S, Sanders LC, von Schalscha TL, Aimes RT, Stetler-Stevenson WG, Quigley JP, Cheresh DA. Localization of matrix metalloproteinase MMP-2 to the surface of invasive cells by interaction with integrin alpha v beta 3. Cell. 1996 May 31;85(5):683-93.

187. Steffensen B, Bigg HF, Overall CM. The involvement of the fibronectin type II-like modules of human gelatinase A in cell surface localization and activation. J Biol Chem. 1998 Aug 7;273(32):20622-8.

188. Stefanidakis M, Koivunen E.Cell-surface association between matrix metalloproteinases and integrins: role of the complexes in leukocyte migration and cancer progression. Blood. 2006 Sep 1;108(5):1441-50.

189. Scragg MA, Ferreira LR.Evaluation of different staining procedures for the quantification of fibroblasts cultured in 96-well plates. Anal Biochem. 1991 Oct;198(1):80-5.

190. Reyes CD and García AJ. A centrifugation cell adhesion assay for high-throughput screening of biomaterial surfaces. J Biomed Mater Res A. 1;67(1):328-33 (2003).

191. Mirastschijski U, Haaksma CJ, Tomasek JJ, Agren MS.Matrix metalloproteinase inhibitor GM 6001 attenuates keratinocyte migration, contraction and myofibroblast formation in skin wounds. Exp Cell Res. 2004 Oct 1;299(2):465-75.

192. Almholt K, Juncker-Jensen A, Laerum OD, Danø K, Johnsen M, Lund LR, Rømer J.Metastasis is strongly reduced by the matrix metalloproteinase inhibitor Galardin in the MMTV-PymT transgenic breast cancer model. Mol Cancer Ther. 2008 Sep;7(9):2758-67.

193. DiMicco MA, Patwari P, Siparsky PN, Kumar S, Pratta MA, Lark MW, Kim YJ, Grodzinsky AJ. Mechanisms and kinetics of glycosaminoglycan release following in vitro cartilage injury. Arthritis Rheum. 2004 Mar;50(3):840-8.

194. Toth M, Sohail A, Mobashery S, Fridman R. MT1-MMP shedding involves an ADAM and is independent of its localization in lipid rafts. Biochem Biophys Res Commun. 2006 Nov 17;350(2):377-84.

195. Krüger A, Arlt MJ, Gerg M, Kopitz C, Bernardo MM, Chang M, Mobashery S, Fridman R.Antimetastatic activity of a novel mechanism-based gelatinase inhibitor. Cancer Res. 2005 May 1;65(9):3523-6.

196. Toth M, Bernardo MM, Gervasi DC, Soloway PD, Wang Z, Bigg HF, Overall CM, DeClerck YA, Tschesche H, Cher ML, Brown S, Mobashery S, Fridman R.Tissue inhibitor of metalloproteinase (TIMP)-2 acts synergistically with synthetic matrix metalloproteinase (MMP) inhibitors but not with TIMP-4 to enhance the

(Membrane type 1)-MMP-dependent activation of pro-MMP-2. J Biol Chem. 2000 Dec 29;275(52):41415-23.

197. Galardy RE, Grobelny D, Foellmer HG, Fernandez LA.Inhibition of angiogenesis by the matrix metalloprotease inhibitor N-[2R-2-(hydroxamidocarbonymethyl)-4-methylpentanoyl)]-L-tryptophan methylamide.Cancer Res. 1994 Sep 1;54(17):4715-8.

198. Brown S, Bernardo M., Li Z-H, Kotra LP, Tanaka Y, Fridman R, and Mobashery S Potent and Selective Mechanism-Based Inhibition of Gelatinases J. Am. Chem. Soc., 2000, 122 (28) 6799–6800

199. Ward RV, Atkinson SJ, Slocombe PM, Docherty AJ, Reynolds JJ, Murphy G.Tissue inhibitor of metalloproteinases-2 inhibits the activation of 72 kDa progelatinase by fibroblast membranes. Biochim Biophys Acta. 1991 Aug 30;1079(2):242-6.

200. Seo DW, Li H, Guedez L, Wingfield PT, Diaz T, Salloum R, Wei BY, Stetler-Stevenson WG. TIMP-2 mediated inhibition of angiogenesis: an MMP-independent mechanism. Cell. 2003 Jul 25;114(2):171-80.

201. Choi WS, Jeon OH, Kim HH, Kim DS. MMP-2 regulates human platelet activation by interacting with integrin aIIbb3. J Thromb Haemost 2008; 6: 517–23.

202. Frisch SM, Francis H. Disruption of epithelial cell-matrix interactions induces apoptosis. J Cell Biol. 1994 Feb;124(4):619-26.

203. Grenz H, Carbonetto S, Goodman SL. Alpha 3 beta 1 integrin is moved into focal contacts in kidney mesangial cells. J Cell Sci. 1993 Jul;105 (Pt 3):739-51.

204. Terracio L, Rubin K, Gullberg D, Balog E, Carver W, Jyring R, Borg TK.Expression of collagen binding integrins during cardiac development and hypertrophy. Circ Res. 1991 Mar;68(3):734-44.

205. Carver W, Molano I, Reaves TA, Borg TK, Terracio L.Role of the alpha 1 beta 1 integrin complex in collagen gel contraction in vitro by fibroblasts. Circ Res. 1991 Mar;68(3):734-44

206. Perris R, Syfrig J, Paulsson M, Bronner-Fraser M. Molecular mechanisms of neural crest cell attachment and migration on types I and IV collagen. J Cell Sci. 1993 Dec;106 (Pt 4):1357-68.

207. Schenk S and Quaranta V. Tales from the crypt[ic] sites of the extracellular matrix. Trends Cell Biol. 2003 Jul; 13(7):366-75.

208. Pfaff M, Göhring W, Brown JC, Timpl R. Binding of purified collagen receptors (alpha 1 beta 1, alpha 2 beta 1) and RGD-dependent integrins to laminins and laminin fragments. Eur J Biochem. 1994 Nov 1;225(3):975-84.

209. Sun M, Opavsky MA, Stewart DJ, Rabinovitch M, Dawood F, Wen WH, Liu PP. Temporal response and localization of integrins beta1 and beta3 in the heart after myocardial infarction: regulation by cytokines. Circulation. 2003 Feb 25;107(7):1046-52.

210. Ray JM, Stetler-Stevenson WG. Gelatinase A activity directly modulates melanoma cell adhesion and spreading. EMBO J. 1995 Mar 1;14(5):908-17.

211. Simpson DG, Decker ML, Clark WA, Decker RS. Contractile activity and cell-cell contact regulate myofibrillar organization in cultured cardiac myocytes. J Cell Biol. 1993 Oct;123(2):323-36.

212. Goldsmith EC, Carver W, McFadden A, Goldsmith JG, Price RL, Sussman M, Lorell BH, Cooper G, Borg TK. Integrin shedding as a mechanism of cellular adaptation during cardiac growth. Am J Physiol Heart Circ Physiol. 284(6):H2227-34. 2003

213. Bernardo MM, Brown S, Li ZH, Fridman R, Mobashery S. Design, synthesis, and characterization of potent, slow-binding inhibitors that are selective for gelatinases. J Biol Chem. 2002 Mar 29;277(13):11201-7.

214. Rosenblum G, Meroueh SO, Kleifeld O, Brown S, Singson SP, Fridman R, Mobashery S, Sagi I.Structural basis for potent slow binding inhibition of human matrix metalloproteinase-2 (MMP-2). J Biol Chem. 2003 Jul 18;278(29):27009-15.

215. Manis AE, Bowman JR, Bowlin GL, Simpson DG.Electrospun nitrocellulose and nylon: Design and fabrication of novel high performance platforms for protein blotting applications. J Biol Eng. 2007 Oct 10;1:2.

APPENDIX 1

Introduction. The principle limitation of conventional IPs is the possible contamination of the recovered material with the antibodies used to precipitate the antigen of interest. Conventional IP relies on the capture of the primary antibody/ antigen complex on to the surface of beads functionalized with protein A or protein G or a combination of proteins A/G depending on the species of origin for the primary antibody. For example, in a pull down assay for β_1 integrin the starting cell lysate is incubated with a known concentration of primary antibody. Once captured, the complexes are rinsed several times and the antigen is eluted using conditions that disrupt the binding of the primary antibody to the antigen. This may be achieved by changing the ionic strength of rinse buffers, a change in the pH of the buffers, dissociation induced by boiling of the sample, and/or by a combination of these conditions. Antigen recovery also can be achieved by exposing the recovered material to reducing conditions (very harsh by comparison to the other methods).

Ideally, the antibody is retained on the beads and only the antigen is released; however, this result is highly dependent upon the starting antibody. More typically the antigen and antibody complex and the antibody bead complex are broken down, liberating the primary antibody from the carrier beads. Under these conditions the primary antibody will "travel" with the antigen in the subsequent analysis. If the recovered material is processed for Western blot analysis this contaminating primary antibody may be recognized by the secondary antibodies used to probe the blot. The use of the Seize IP kit

largely eliminates these cross-reactivity concerns because the primary antibodies used in the initial recovery are chemically linked to a solid phase support.

Methods

Immunodetection in the infrared range using Odyssey Scanner (LiCor) was utilized to confirm the source of contaminating signal that was variably present in the evaluation of samples recovered by routine, conventional IP (See Methods section for *Routine IP* and *IP of plated CF*). Following chemiluminescent detection, PVDF membranes were stripped, blocked (Li-Cor, 927-40000) and probed at 1:1000 with Mouse anti-MMP-2 antibody. For infrared imaging, the blot was counterstained at a rate of 1:10,000 with Goat anti-Mouse 700 nM IR Conjugate (Rockland, 610-430-002) and with Goat anti-Rabbit 800 nM IR (LiCor, 926-32211) conjugate. Blot was pre-scanned for adjustment of signal to background in the 700 nM and 800 nM channels. Final scan of blot captured at a resolution of 84.7μm with an intensity setting of "4" in both channels.

Results

Appendix 1 Figure 1

Routine IP. A suspension of cardiac fibroblast were divided into two groups; lysed with RIPA buffer that was either supplemented or not supplemented with Complete protease inhibitor cocktail (Roche, 11 697 498 001) and processed for routine IP against β_1 integrin. MMP-2 was detected at a number of molecular weights in the samples recovered by IP to β_1 integrin (Lane 3 and Lane 4), in the raw unprocessed cell lysate (Lane 5), and in

lanes used to separate a recombinant MMP-2 protein standard (Lane 6). This antigen was not detected in the null IP (Lane 1) or in the β_1 antibody lane (primary antibody diluted in Laemmli buffer and run directly on the blot) (Lane2). The application of broad spectrum protease inhibitors did not disrupt the association of MMP-2 and β_1 integrin in this assay (compare lane 3 with lane 4). In this particular isolation no cross-reactivity of the primary Rabbit IP antibody was detected when the Western blots were probed for the detection of the Mouse MMP-2 primary antibody (using Horse anti-Mouse).

Figure 1, appendix 1

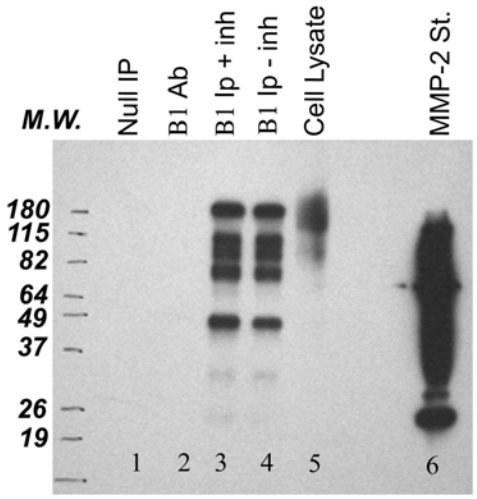

Appendix 1 Figure 2

In a second representative series of experiments Western blots were generated from a routine IP against β_1 integrin from lysates generated from suspended cells, or cells plated out for 1 hour on collagen, laminin, fibronectin, and poly-l-lysine (Panel A, Lanes 3-7, respectively). Recovered material was processed for Western blot analysis for the detection of MMP-2. Secondary Horse anti-Mouse antibody was applied and the blot was developed. MMP-2 was detected in whole cell lysate (Lane 1). In the null IP (Lane 2) bands were detected that match the molecular weight expected for intact immunoglobulin (150kDa), heavy chain (50kDa), and light chain (25kDa). The presence of these bands indicates that the precipitating antibody is being carried forward in the analysis. This contaminate interferes with the unambiguous identification of MMP-2 co-precipitated with a β_1 immunoprecipitation from lysate of suspended and plated cells (Panel A, Lanes 3-7).

The original PVDF was stripped, re-blocked, and re-probed with Mouse anti-MMP-2 antibody (Panels B-D). For infrared imaging, the blot was counterstained with Goat anti-Mouse 700 nM IR conjugate (Rockland) and with Goat anti-Rabbit 800 nM IR (LiCor) conjugate. In this assay immunoreactivity was present in the Null IP, indicating that primary anti-β_1 (Rabbit) antibodies used to conduct the original IP cross reacts with either the anti-MMP-2 (MaB, unlikely) primary, the secondary Horse anti-Mouse HRP antibody used to probe for the MMP-2 antibody, or both (Panel A, Lane 2). Staining the resulting blot using an IR tagged antibody demonstrates the spurious signal originates from the Rabbit anti-β_1 integrin antibodies used to conduct the IP (Panel D, Lane 2). Cross reactivity from the carryover of anti-β_1 integrin antibody is likely a product of different lots

of secondary antibodies used to probe the Western blots. This cross-reactivity occurred in some experiments and not others, necessitating the use of the Seize IP approach documented in the main section of this study.

Appendix 1, Figure 2

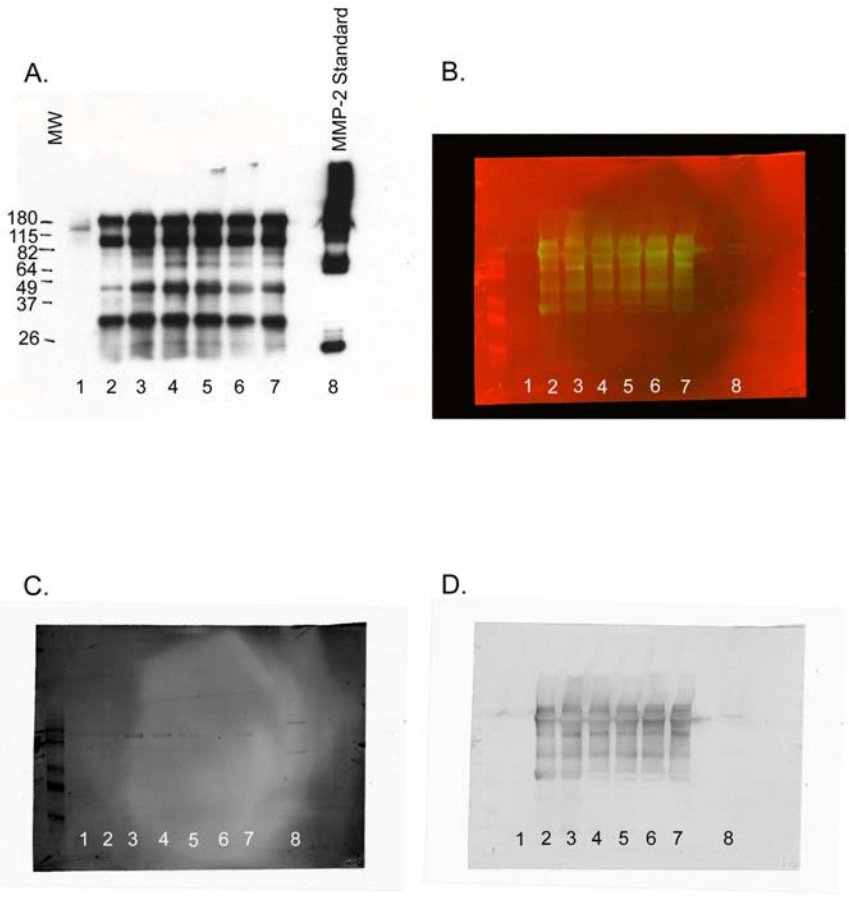

Appendix 1, Figure 2

Utilization of IR dyes to demonstrate carryover of primary antibody in traditional IP.

The panels represent a single traditional IP experiment against β_1 integrin (Anti-Rabbit) and processed for detection of MMP-2 (Anti-Mouse) using conventional chemiluminescence (A) and infrared detection as an overlay (B) or in separate detection channels; 700nM anti-Mouse(C) and 800nM anti- Rabbit. The IR system separates the contribution of the primary detection of MMP-2 (C) from the background contribution of Anti-β_1 (D), which constrains interpretation of traditional development (A). The initial design for this experiment was to address the question of is there changes in the amount of MMP-2 in association with β_1 integrin when CF are plated on specific surfaces. Lane 1, Cell lysate(Input); Lane 2, Null IP(no lysate); Lane 3, CF processed directly from culture plate; Lanes 4-7, CF plated for 1hr onto Collagen, Laminin, Fibronectin, and Poly-L-Lysine, respectively; Lane 8, MMP-2 Standard.

APPENDIX 2

Introduction. The IP experiments in this study were conducted with cells that have been maintained in culture flasks for varying lengths of time, trypsinized, rinsed several times and then allowed to recover for 15 minutes in suspension culture. In selected experiments cells were trypsinized, allowed to recover for 15 minutes and then plated for 1 hour on various substrates prior to processing. Under either condition clear evidence of MMP-9 was not detectable in cell pellet fractions (as judged by zymography and Western blot analysis). However, in conditioned media recovered from cultures of CF that had been plated for 1 hour or for more extended periods of time this protease was readily detected by gelatin zymography. Unlike MMP-2, it appears that MMP-9 is detectable only in the conditioned media compartment at the 1 hour time interval.

Methods

Culture plates (Corning, 6 well) were coated with 10 μg/ml fibronectin or poly-l-lysine overnight at 4˚C. Plates were rinsed 3X with PBS and blocked with 1% BSA at room temperature for 1 hour. CF were tryspsinized and counted as described, 50 K cells were delivered in 2 ml of ITS supplemented DMEM per well for each of the time points to be assessed and incubated from 1 hour to 48 hours. Media samples were collected from the individual cultures at the appropriate time, mixed 1:1 with Laemmeli Buffer and frozen at -70˚C.

With the expectation that the absolute concentration of gelatinases would be low in 2 ml of conditioned media from 50K cells, and to avoid the sometimes negative effects from concentration steps (such as Trichloroacetic acid precipitation), the large format Protean II XI gel electrophoresis system was used to conduct this specific zymography. The 20 cm x 20 cm x 0.15 cm format gel with a 20 well comb accommodates a large loading volume (max 187 µl). In this assay 150 µl of sample from each culture condition was assayed. Positive control of Gelatinase activity was established with Zymography Standard (Millipore CC023). From stock, a 1:100 dilution in Laemmeli buffer was made (Labelled "A"); from this dilution four serial dilutions were made at 1:10 (Labelled B-E). In each lane 20 µl of each standard sample A-E was loaded. Non-conditioned media was prepared identical to experimental groups and run as a negative control. Electrophoresis and subsequent processing for gelatin zymography were conducted as described.

Results

CF plated onto fibronectin and poly-l-lysine exhibit gelatinolytic activity of MMP-2 and MMP-9 in the conditioned media fractions as early as 1 hour following plating and this activity was detected out to at least 48 hours post plating. We can assume that the continued presence of the pro-MMP-9 results from continued deposition as the pro-form would otherwise be depleted by the activation cascade of this protease. On the other hand, levels of pro-MMP-2 seem to accumulate without obvious processing of this enzyme to the active form in the media fractions. MMP-9 activity in conditioned media at 1 hour is not

accompanied by any detectable activity in the cell pellet fractions at this time point (See Appendix 3).

Appendix 2, Figure 1

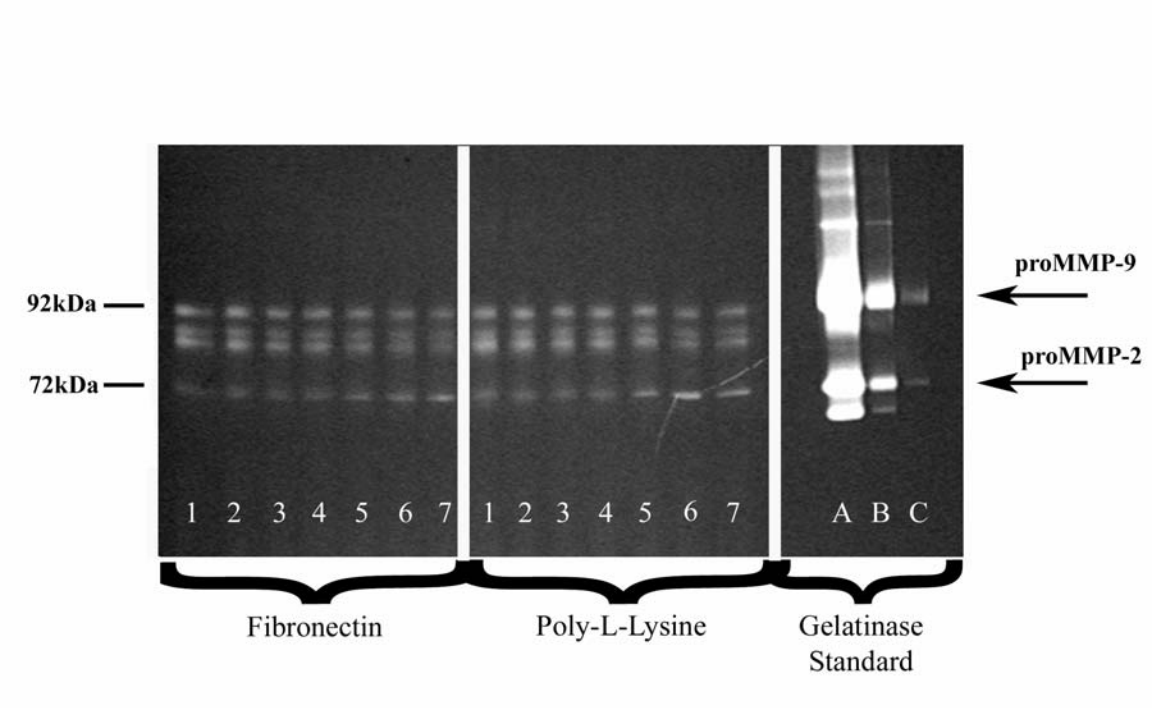

Gelatin Zymography. Accumulation of Gelatinases in media conditioned by Cardiac Fibroblast plated onto fibronectin or poly-l-lysine for 1, 4, 6, 12, 24, and 48 hours, Lanes 1-7 respectively. Dilutions of gelatinase standard (Lanes A-C) run as positive control indicate the sensitivity of zymography for small amounts of gelatinase and identify along with apparent molecular weight the proteases in conditioned media as proMMP-9 and proMMP-2.

APPENDIX 3

Introduction. SB-3CT is a highly specific inhibitor of MMP mediated protease activity [213]. It has known inhibitory effects on the gelatinases, MMP-2 and MMP-9. This reagent binds to the active site in the enzyme and functions as a competitive inhibitor [214]. To demonstrate the efficacy of this agent for this use, cultures were mixed with 10 μM SB-3CT and plated for 1 hour. Cell pellet fractions were separated by SDS gel electrophoresis and processed for zymography.

Methods

Culture plates were coated with 0.07μg/mm^2 fibronectin, cells were cultured as naïve, vehicle treated (Buffer R) (50 mM HEPES (pH 7.5), 150 mM NaCl, 5 mM $CaCl_2$, 0.01% Brij-35 and 50%DMSO) or 10μM SB-3CT treated. "Buffer R" is the diluent for an intermediate dilution of stock SB-3CT conducted prior to final dilutions in aqueous media. Cells were suspended in ITS media, or ITS media supplemented with vehicle or SB-3CT and incubated 15 minutes prior to plating. Groups plated in triplicate of 40 K cells/well in a final volume of 2 ml of media. Following a 1 hour incubation media was aspirated carefully and cultures rinsed 3X with cold PBS; excess PBS was wicked by inverting culture plates and placing them on top of lint free towels. Plates were placed on ice and 50 μl RIPA was applied per well. Lysates were collected with cell scrapers. Samples were centrifuged at 10,000 X G at 4˚C for 15 minutes. Supernatant was assayed by Bradford

Protein assay mixed with Laemmeli buffer at a concentration of 10 µg/30 µl total volume, heated for 3 minutes at 60˚C, and processed for gelatin zymography.

In a separate parallel experiment cells were treated with GM-6001 at 5µM, with a matched concentration of DMSO as vehicle control. Following 1 hour of plating, conditioned media was collected, and centrifuged for 15 minutes at 10,000 X G at 4˚C. Cultures were rinsed 3X with cold PBS as described and cell pellets were collected as described. Conditioned Media fractions were run based on equal protein values of 15 µg per sample in a total of 30 µl volume.

Results

SB-3CT treatment decreased MMP-2 associated activity as determined by Gelatin zymography (Figure 1, A). As judged by densitometric analysis, the trace (Optical Density X mm^2) values of samples treated with SB-3CT were approximately 50% of vehicle treated controls (Figure 2, B). Data shows the feasibility of this agent in blocking MMP-2 activity in cell pellet fractions. Treatment of cultures with GM6001 promoted an increase in pro-MMP-2 that was not detected in the untreated or vehicle control cultures. As this inhibitor blocks MT1-MMP mediated activity the increase in pro-MMP-2 detected in this experiment is likely a reflection of decreased processing of pro-MMP-2 on the surface of the cell to active MMP-2 (Figure 2, A). GM6001 did not appear to impact the activity of MMP-2 in the conditioned media fraction. We note the activity of MMP-9 in conditioned

media as “presumptive” as the positive control in this zymogram is a MMP-2 standard. However, the zymograms in this appendix show clear activity of MMP-2 without the activity of MMP-9 in cell pellet fractions.

Appendix 3, Figure 1

A.

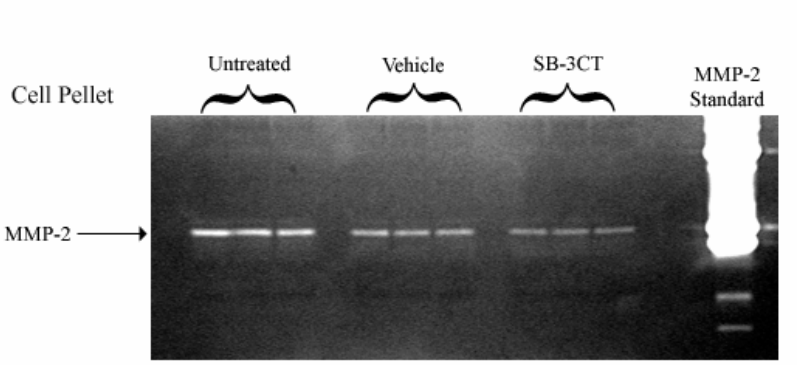

B.

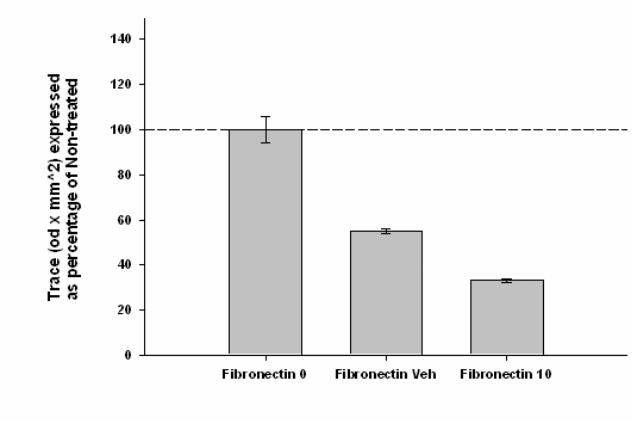

Appendix 3,Figure 2

A.

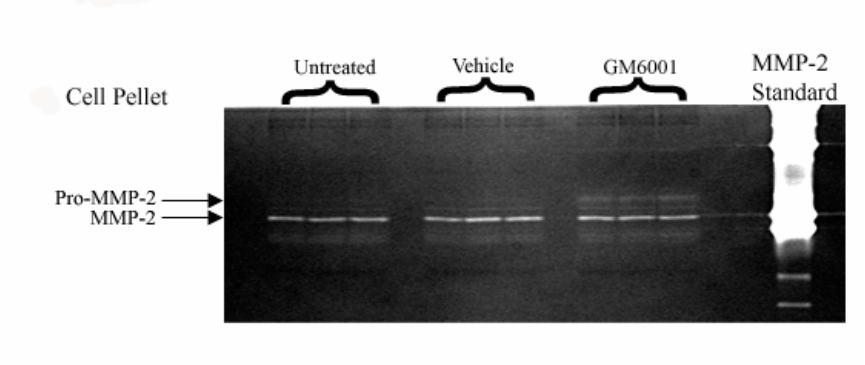

B.

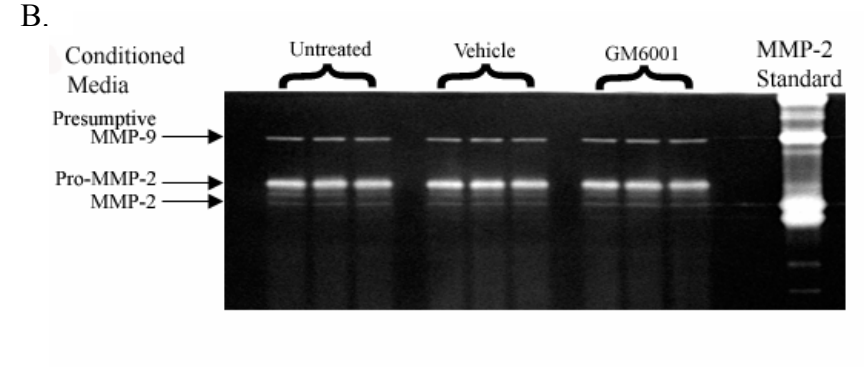

APPENDIX 4

Introduction. The running conditions used to prepare an IP for zymographic analysis are similar, but not completely identical to the conditions used to prepare this material for conventional Western Blot analysis. In early experimentation immunoreactivity against MMP-2 was present in samples recovered by IP directed at β_1 integrin. However, zymographic activity was not detectable in these early samples. Several explanations could account for this result. However, one concern of note was that the MMP-2 enzyme was not stable in the putative complex with β_1 integrin when samples were processed for zymography. Alternatively, the enzyme might be stable in the complex but not present in a form that can be activated in the zymographic gels. Integrin associated proteases have been reported to be difficult to activate under some circumstances [187]. To verify that IPs against β_1 integrin that have been processed for zymography retain MMP-2 selected samples were processed by IP against β_1 integrin, processed for zymography and then processed directly from the zymographic gels for Western blot analysis. In parallel with zymographic processing, samples were directly assessed for MMP-2 by Western blot analysis. These experiments demonstrate that MMP-2 immunoreactivity is present in the material processed for zymography and at a MW that appears to be consistent with the MW of the complex identified in the main body of this study. The underlying reasons that no protease activity was detectable in the IP recovered samples remain unclear. These results ultimately led to processing the material recovered by IP against β_1 integrin in the presence of SB-3CT. Under these circumstances protease activity was detectable when the

samples were processed for zymography. Possible reasons for why MMP-2 activity might be preserved in these experiments include:

- In the purification of the complex by IP the resultant elution is of sufficiently high enrichment for the auto-activation and catalysis of MMP-2 to occur and the inhibitor prevents the processing of a fraction of this population.

- As described by [187] (who identified collagen mediated binding of MMP-2 to β_1 integrin) cell surface bound MMP-2 may be resistant activation.

- In some instances, there is a cooperative interaction between TIMP-2 and MMP inhibitors in MT1-MMP mediated activation of MMP-2 [196]. SB-3CT could be acting to selectively activate MMP-2 in the immunoprecipitated complex.

- Alternatively, elution from routine IP was conducted by heating the antigen off the surface of the Protein A/G beads. Thermal denaturation could result in lack of enzymatic activity by while the antigenicity of the peptide is maintained. In comparison, the elution of complexes from the Seize IP is conducted with low pH buffering and a preservation of enzymatic activity only in the SB-3CT.

One consideration that has not been discussed concerns the limits of detection for the techniques used in these assays. Zymography standard at a stock concentration of

0.1mg/ml was diluted 1:100, then as a series of dilutions at 1:10 to test the approximate limit of detection for zymography. Gelatinase standard was detectable at a 1:10,000 dilution when 20 ul of the diluted samples was developed for 18 hours (Appendix 2). The starting concentration of standard is supplied as a mixed population of enzyme species. With this caveat, the total amount of protein detectable by zymography was in the range of 2 ρg. Limits of ECL Plus detection are demonstrated to be as little as 20 ρg of protein in slot blotting applications [215] (Manis 2007). With similar limits of detection, these techniques should be complimentary in the identification of MMP-2.

The most likely scenario to explain discrepancy discussed regarding the detection of MMP-2 has origin in the differences in the methods of routine and Seize IP. The latency of MMP is controlled through an interaction of the pro-peptide sequence with the Zn^{+2} of the catalytic domain. This coordination bond or "cysteine switch" stabilizes the pro-peptide and suppresses MMP-2 activation. When samples recovered by conventional IP are processed for Western blotting or zymography they were routinely boiled. Heating this type of can denature proteins and thereby prevent MMP-2 activation. In material recovered by the Seize IP methodology, the samples are eluted from the beads by a change in pH. Under these circumstances, lowering the pH can promote the activation of MMP-2. With the MMP-2 in high concentration in an IP recovered sample, the pH induced activation could result in the initiation of auto-catalytic activation and self cleavage of MMP-2. Under these conditions, the presence of an MMP-2 inhibitor such as SB-3CT could act to preserve a fraction of MMP-2 or block the activation and subsequent degradation of the isolate. This later explanation seems likely.

Methods

Immunoprecipitation and gelatin zymography. Gelatin zymography was conducted on samples recovered by IP against β_1 Integrin under conventional methods. Material recovered by IP was first separated by conventional SDS gel electrophoresis on a 10% slab gel and transferred to PVDF for Western blot analysis against β_1 and/or MMP-2 (AB1952, Chemicon; IM51, Calbiochem, respectively.) Representative fractions of IPs were then subjected to gelatin zymography.

Zymography. Equal volumes of whole cell lysate or protein fractions purified by IP from a suspension of 2 x 10^6 cells were mixed with Laemmli buffer and separated on a SDS 10% polyacrylamide gel supplemented with 1.0% gelatin. Gelatinase standards (Chemicon; 20 µl of stock solutions that had been diluted 1:200) were used as positive controls to identify MMP-9 and MMP-2 enzymatic activity. In experiments that focused on MMP-2, proMMP-2 (Calbiochem, PF037) was used as the positive control (20 µl of a 1:200 dilution of the stock solution). Following electrophoretic separation at 120V (constant voltage), gels were incubated in renaturation buffer (BioRad) for 1 hour and then transferred into development buffer (Bio-Rad) for 18 hours at 37ºC. Gels were fixed (20% Methanol, 10% Glacial Acetic Acid, 70% distilled de-ionized H_2O) and stained with Coomassie Blue, G-250 (Bio-Rad). De-stained gels were imaged (Gel Doc 2000, BioRad) and analyzed by densitometry (Quantity One, BioRad) to characterize gelatinolytic activity.

Following development and documentation, the gelatin zymograms were transferred to PVDF for Western Blot analysis against MMP-2. The preparation of these samples was done in the absence of exogenous protease inhibitors (to allow protease activity associated with IP material to function and degrade the gelatin present in the zymograms). Lanes were loaded with a whole cell lysate prepared from a cell suspension, an IP to β_1 (AB1952, Chemicon), or recombinant human MMP-2 pro-enzyme standard (PF037, Calbiochem). The anti-MMP-2 antibody used in these experiments recognizes the 72 kDa latent and 66 kDa active species of MMP-2.

In separate experiments cardiac fibroblasts (2×10^6 cells) were prepared as a suspension culture, pelleted, and lysed directly with RIPA buffer in the absence of protease inhibitors for conventional immunoprecipitation directed against β_1 integrin. Raw cell lysate and the enriched IP samples were prepared for processing by 10% SDS-PAGE (Gel 1) and for processing by 10%SDS- PAGE, 0.01% Gelatin Zymogram (Gel 2). Following electrophoresis, Gel 1 was processed for Western blotting against MMP-2. Gel 2 was processed for Zymography. Images were captured of the developed and stained zymogram. An additional interval of destaining was conducted by incubating the zymogram in Towbin buffer prior to overnight transfer (125mA) to PVDF membrane. The samples transferred from the zymograms were then processed for immunodetection of MMP-2 by conventional methods.

Results

Western blotting of cell lysate and IP of β_1 integrin confirm the presence of MMP-2 reactivity as compared to recombinant MMP-2 standard (Gel 1: A) in samples that were processed in parallel as an input for gelatin zymography (Gel 2: B). Similar patterns of immunoreactive MMP-2 are detected in (A) and (C) for whole cell lysate, IP to β_1 integrin and for MMP-2 positive control. However, the gelatinolytic activity detected (B) does not follow same this pattern. In whole cell lysate, there are a number of gelatinolytic bands that are not confirmed as MMP-2 by Western blot although the anti-MMP-2 mAB recognizes both the 72 kDa latent and 66 kDa active species of MMP-2. The lack of Zymographic activity from the IP, at the MW expected for MMP-2, is contrasted by the immunoreactive bands detected by Western blot (C).

Appendix 4, Figure 1

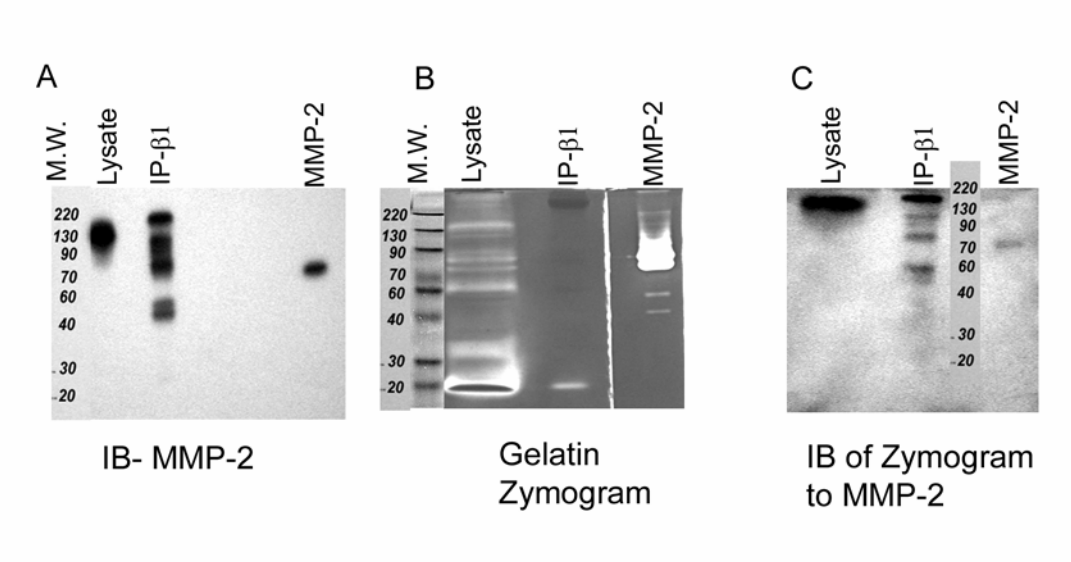

Zymography and Western Blotting. Conventional immunoprecipitation to β_1 integrin was assessed in parallel for MMP-2 by Western blot (A) and by Gelatin Zymography (B). At the conclusion of zymographic processing, the zymogram was transferred and blotted for MMP-2 (C). This experiment was conducted to verify that MMP-2 was actually retained in the complex recovered by IP and then processed for zymography. Lack of definitive zymographic activity in the IP sample is in contrast to the immunodetection of MMP-2.

APPENDIX 5

Introduction. MMP-2 is typically bound to TIMP-2; MMP-9 is typically bound to TIMP-1. However, TIMP-1 and TIMP-2 can both bind the active form of either enzyme (Ward 1991), making both peptides potential candidates as component elements of the $\alpha_3\beta_1$ integrin MMP-2 complex. Of the two molecules, TIMP-2 probably represents the more likely binding partner, a specific binding interaction between TIMP-2 and the $\alpha_3\beta_1$ integrin has been identified [200].

Methods

Following the Seize IP protocol, MMP-2 or β_1 was recovered. Next, each sample was supplemented with β-mecaptoethanol (2.5ul:100ul sample) and heated at 95˚C for 5 min. Western blotting to TIMP-1 (AB800, Chemicon) was conducted on reduced samples according to the manufacturer's literature that states that the antibody does not bind well to the non-reduced protein.

Results

In whole cell lysate immunoreactivity against TIMP-1 was detected; however, in the enriched fractions isolated by Seize IP directed against MMP-2 and β_1 no such activity was detected for TIMP-1.

Appendix 5, Figure 1.

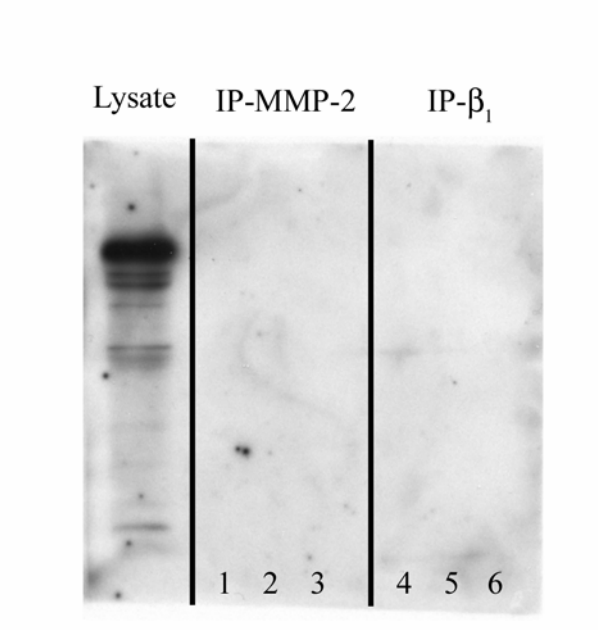

Western Blotting to TIMP-1 did not show reactivity in elution steps from IP to MMP-2 (Lanes 1-3) or from IP to β_1 integrin (Lanes 4-6). The presence of this small molecular weight inhibitor was detected in whole cell lysate.

APPENDIX 6

Introduction. To determine if MMP-2 becomes secondarily associated with the $\alpha_3\beta_1$ integrin complex when a cell lysate is prepared, live cardiac fibroblasts were pre-treated with the cross-linking agent DTSSP (21578, Pierce). This reagent will cross-link peptides that are within 12 angstroms of one another on the cell surface. Processing cross-linked cells makes it possible to determine the spatial relationships that might exist within the radius of the reagent used to prepare the samples for IP analysis or Western blot analysis.

Methods

Cell surface associated proteins were crosslinked to stabilize protein-protein interactions using DTSSP (21578, Pierce). This reagent has an effective cross linking distance of 12 Å and solubility properties limits this crosslinker to the cell surface. In these experiments cardiac fibroblasts were plated out onto poly-l-lysine coated 6 well dishes in ITS media supplemented with 5ul:20ml Gelatinase standard (CC073, Millipore) or plain ITS media. Following one hour of plating, cultures were rinsed 3X with PBS, cultures were then supplemented to a final concentration of crosslinker at 1 mM in PBS and allowed to incubate for 30 minutes at room temperature. The reaction was quenched with the addition of sufficient Tris (stock solution 1 M, pH 7.5) to bring the final Tris concentration to 15 mM for a 15 minute incubation interval. At this point cultures were placed on ice, treated with RIPA buffer, and scraped to collect the cell pellet fraction. Samples were centrifuged to pellet debris and the supernatant was transferred to clean

sample tubes and mixed with Laemmeli buffer in preparation for SDS-PAGE. Parallel cultures without the use of crosslinker were processed for SDS-PAGE. Samples were separated for Western blotting against MMP-2 and β_1 integrin on separate blots.

Results

Application of exogenous gelatinase did not appear to alter the staining patterns present in the crosslinked (Panels A & C) or native (Panels B & D) cell pellet fractions (these blots were run on 7.5 % PAGE instead of the 10% Gels that are typically used in this study, as a result the position of a bands are shifted downward on the gel). Similar molecular weight bands at 200-210kDa blots stained against MMP-2 in both the crosslinked and naïve cell pellet suggest that the interaction of MMP-2 and β_1 integrin occurs on the surface of cardiac fibroblast. Further, the application of exogenous gelatinase (Panel A & B) did not qualitatively increase the amount of staining for MMP-2 as compared to staining present generated from naïve cells (Panels C & D). The molecular weight band of 200-210kDa in "unpurified" cell pellets placed in the context of IP data demonstrating a complex of $\alpha_3\beta_1$: MMP-2 at this same molecular weight ***suggests*** 1) MMP-2 and β_1 may be associated on the cell surface 2) that this association is not dependant on crosslinking of the cell surface, and 3) application of exogenous gelatinase did not meaningfully increase the amount of MMP-2 in cell pellets.

Appendix 6, Figure 1

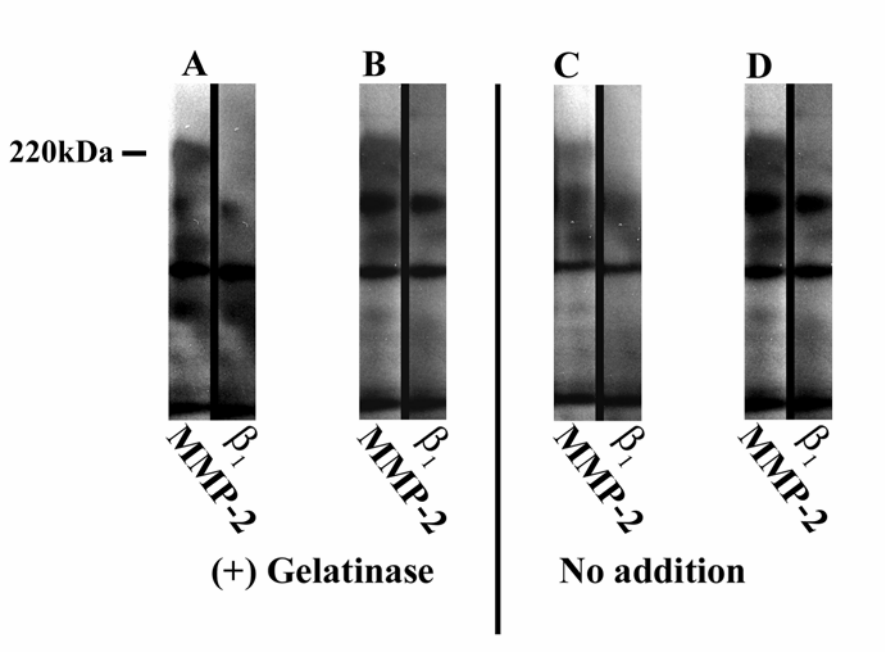

Figure 1. Crosslinking of cell surface. Cells plated on poly-l-lysine were cultured in the presence and absence of exogenous gelatinase. At the conclusion replicate cultures were surface crosslinked (Panel A & Panel C) or maintained naïve (Panel B & Panel D). Cell pellet lysates were separated by PAGE and blotted for MMP-2 and for β_1 integrin.

APPENDIX 7

Introduction. Any loss of cells due to death will artificially reduce the total number of cells observed in an adhesion assay. As a result of this potential condition cell viability was tested under a variety of culture conditions.

Methods

Assays were conducted to verify that cell viability remains constant under the conditions used to define cell adhesion. Many of these assays were conducted on cells that had been plated and allowed to adhere for a defined interval of time prior to the cultures being supplemented with drug or vehicle. This approach made it possible that each experimental condition had the same number of cells at the onset of the assay (this assumption can not be made if cells are treated in suspension with various drugs and then plated-if the drug alters adhesion or if the drug reduces viability the total number of cells will be reduced but the reason will be unknown).

These assays were designed to parallel the cell number used for plating in adhesion assays (2 K and 40 K/ per well/ 96 well plate). Viability was assessed by two metabolic based measures; the WST-1 assay and with Calcein AM. The WST-1 assay is typically used as an assay to measure cell proliferation; in this study it was used to determine the potential toxicity of the inhibitors (GM-6001 and SB-3CT) used in conventional and

centrifugal adhesion assays. This colorimetric assay relies on the conversion by mitochondrial dehydrogenases of the WST-1 tetrazolium salt to formazan. The accumulated formazan is then measured at an absorbance of ~450 nm. Calcein AM is metabolically dependant as well; however, it is the metabolic cleavage of this dye that converts Calcein AM to Calcein, the fluorescently active species of the dye. This conversion decreases the membrane permeability of the dye thereby "trapping" the dye in the cell and providing a "direct" measure of cell number. Accumulated Calcein was measured at 480ex/520em. These assays function to validate the adhesion data and suggest a cell number/density dependant response to treatment with MMP inhibitors. As the scope of adhesion assays narrowed, viability testing became more focused and was tailored to encompass conditions used to evaluate the impact of protease inhibition on cell adhesion. Viability was assessed on collagen, laminin, and fibronectin under the following sets of conditions;

Inhibitor	**Assay**	**Cells Per well**	**Dose/ Vehicle**	**Timing of dose**	**Incubation time**
GM-6001	WST-1	40 K	0, 10, 25μM	After 30min	4 hr
SB-3CT	WST-1	40 K	0,1,5,10,25μM	At plating	4 hr
SB-3CT	WST-1	40 K	0,1,5,10,25μM	At plating	24 hr
SB-3CT	WST-1	2 K	0,1,5,10,25μM	At plating	24 hrs
SB-3CT	Calcein AM	2 K	0,1,5,10,25μM	At plating	24 hrs

SB-3CT	WST-2	2 K	0,1,5,10,25μM	At 24, 26, 28 hr post plating	6 hr,4 hr,2 hr

Data from viability assays on SB-3CT was expressed as the percent of activity detected in the untreated, substrate matched control. Data from each plating substrate was screened by one-way ANOVA (P=<0.001), pairwise multiple comparisons were done using the Holm-Sidak method with an overall significance level of 0.05.

Results

General Inhibitor: GM 6001. The WST-1 assay was used in these experiments to detect overt changes in cell viability attributable to the presence of the GM6001 protease inhibitor. In this assay 40 K cardiac fibroblasts were plated in triplicate on collagen, laminin, fibronectin, poly-l-lysine or BSA coated surfaces. All experimentation was conducted with ITS media. Cells were plated for a 30 minute interval, then, the appropriate doses of inhibitor were delivered to the cultures so that the final concentration of inhibitor was 0 μM, 10 μM, and 25 μM. These doses were selected based on the manufacturer's recommended typical cell culture dose. After an additional 30 minutes (total of 1 hour post-plating), 10 μl of the WST-1 reagent was added to the cultures. The assay was allowed to develop for a total of 4 hours. Cell number was interpolated from a five point standard curve.

Substrates coated with collagen or fibronectin supported an equal metabolic rate across all administered doses of the inhibitor (Figure 1). As judged by the WST-1 assay, total cell number remained constant across all conditions tested on these 2 substrates. Cultures plated onto laminin coated surfaces showed a decrease in metabolic activity at the 25 μM dose with respect to the 10 μM dose and non-treated controls. Similarly, cultures plated onto Poly-l-lysine exhibited a decrease in metabolic activity at this same concentration of inhibitor. On BSA, total cell number, as reported by the WST-1 assay, was decreased in cultures treated with the 10 μM dose and the 25 μM dose with respect to non-treated cells. In summary, 10 μM GM6001 appears to be well tolerated by CF when the cells are plated onto collagen, laminin, fibronectin, poly-l-lysine and BSA at this time interval. N=1 of triplicates.

Specific Inhibitor: SB-3CT. The impact of the specific inhibitor SB-3CT on cell viability was also tested over a range of concentrations and culture conditions using the WST-1 assay. Initial experiments focused on the viability of cardiac fibroblast when plated in the presence of 1 μM, 5 μM, 10 μM, and 25 μM SB-3CT, or vehicle (Buffer R 25μM) for a 4 hour time interval on Collagen, Laminin, or Fibronectin coated culture surfaces. At this time point 10 μl of WST-1 reagent was added to the cultures and allowed to develop for two hours. The metabolic activity of cardiac fibroblast plated under these conditions was largely unaffected by the presence of varying doses of SB-3CT (Figure 2).

SB-3CT exhibits evidence of a density dependent effect on cell viability. At high cell density (40 K) the relative number of cells was similar on all surfaces and at all doses

of inhibitor assayed (1 μM, 5 μM, 10 μM, and 25 μM) at the 6 hour time point (Figure 2). In control experiments, cultures treated with or without vehicle (Buffer R, 25 μM) exhibited a metabolic profile that was similar to that of cultures treated with the various concentrations of the inhibitor.

After 24 hours, a cell density dependent effect of inhibitor became manifest. Cell viability in cultures treated with 0, 1, and 5 μM inhibitor was similar in low density (Appendix 7, Figure 4) and high density(Figure 3 cultures (2K vs. 40K), although there was a subjective evidence of increased metabolic activity with increasing dose of inhibitor. This pattern diverged at the 10 μM dose of inhibitor. At this dose, viability in low density cultures (2K) was markedly depressed with respect to control cultures (non-treated and vehicle matched) plated at the same density. In contrast to these results, the total metabolic activity present in cultures plated at high cell density (40 K) remained unchanged (and subjectively higher) when treated with inhibitor. A similar, albeit more pronounced trend was apparent in cultures treated with the 25 μM concentration. Total metabolic activity was depressed in cultures plated at low cell density (2 K) with respect to non-treated and vehicle matched controls. At high cell density (40 K) total metabolic activity was increased in cultures treated with this dose of inhibitor with respect to non-treated and vehicle control. The vehicle controls (DMSO matched to 25 μM dose) in these experiments exhibited a nominal effect on cultures plated at low cell density and little to no effect in cultures plated at high cell density. N=1 for 40k cells, N=2 for 2k cells at the 24 time point.

Calcein AM: Live cell analysis. A potential limitation of a metabolic based assay in assessing cell number is that changes in metabolic activity can be mistakenly interpreted as an increase or a decrease in the actual number of cells. To verify the results of the WST-1 metabolic assay Calcein AM was used to characterize cell viability/number in cultures plated at low cell density (2 K). This reagent is only taken up and retained in live cells. In these experiments CF were plated in the presence or absence of 1 μM, 5 μM, 10 μM, 25 μM SB3-CT or vehicle (Buffer R, matched concentration) prepared in ITS media for 24 hours on collagen, laminin, or fibronectin (Appendix 7, Figure 5a-c, respectively). Cell number was then determined by Calcein fluorescence derived from a standard curve of cell plated in parallel with the experimental cultures. At low doses of inhibitor (1 μM and 5 μM) the increase in metabolic activity detected by the WST-1 was not accompanied by any detectable change in cell number as measured by the Calcein Live cell assay. However, without exception, treatment with SB-3CT at the 10 μM dose, and higher, resulted in a 75% decrease in viable cells as compared to both the untreated and vehicle controls at the 24 hour time point.

In summary, the treatment of cardiac fibroblasts with the gelatinase specific inhibitor (SB-3CT) has effects that are dose and cell density dependant. At low density, and low dose (5 μM) cell number is not affected; yet, there is a slight increase in the metabolic activity detected in these cells. It can be postulated that the increased metabolic activity may be attributed to increased migration, or turnover of adhesions; yet, the reason is unknown.

Time component of viability. The specific MMP inhibitor SB-3CT induces dose dependant changes in cell viability. A time course study was conducted to more fully characterize the effects of this reagent. In preliminary studies, cells cultured in the presence of SB-3CT for 24 hours exhibited increased metabolic activity at low dose (5 μM) and decreased viability at high dose (10 μM). In these experiments cells were plated at low density (2K) in culture wells coated with collagen, laminin or fibronectin for a total of 30 hours in ITS media (Figure 6a-c). At 2 hours, 4 hours, and 6 hours prior to assessing metabolic activity, media was aspirated and replaced with media supplemented with 0, 1, 5, or 10 μM SB-3CT or vehicle (DMSO) control. The approach was used to avoid artifacts that might be induced by changes in adhesion that may occur when cells are plated in the presence of inhibitor.

The maximum dose over time tolerated by the cultures without a change in viability is 5 μM for a duration of 2 hours. At time points greater than 2 hours, there is a subjective decrease in the metabolic activity in these cultures as compared to non-treated and vehicle matched controls. At 10 μM SB-3CT, there was a detectable decrease in metabolic activity cell viability within 2 hours. With increasing time of exposure (4 hours and 6 hours) there was a more pronounced decrease in metabolic activity in cultures treated with 10 μM SB-3CT with respect to non-treated and vehicle controls. The decrease in metabolic activity as a function of dose and time of exposure was similar on all surfaces tested. (Figure 10).

Conclusions

While data indicate that there is a decrease in the metabolic activity of cardiac fibroblast following 2 hours of exposure to 10uM SB-3CT these results do not necessarily translate as a decrease in the viability of cells in the 1 hour interval used in adhesion assays or challenge the validity of adhesion results. This statement is based on equivalent data of initial cell adhesion in SB-3CT treated cultures as compared to control at 1 hour using a vital dye in conducting centrifugal adhesion assays . The following guidelines should be adhered to in the application of SB-3CT; short term experiments (1 hour in duration) a maximum dose of 10uM is tolerated, for longer durations (24 hours in duration) doses of 1uM and 5uM are appropriate. In the application of GM-6001 the maximal tolerated dose was 10uM for duration of 4 hours of culture.

Appendix 7, Figure 1

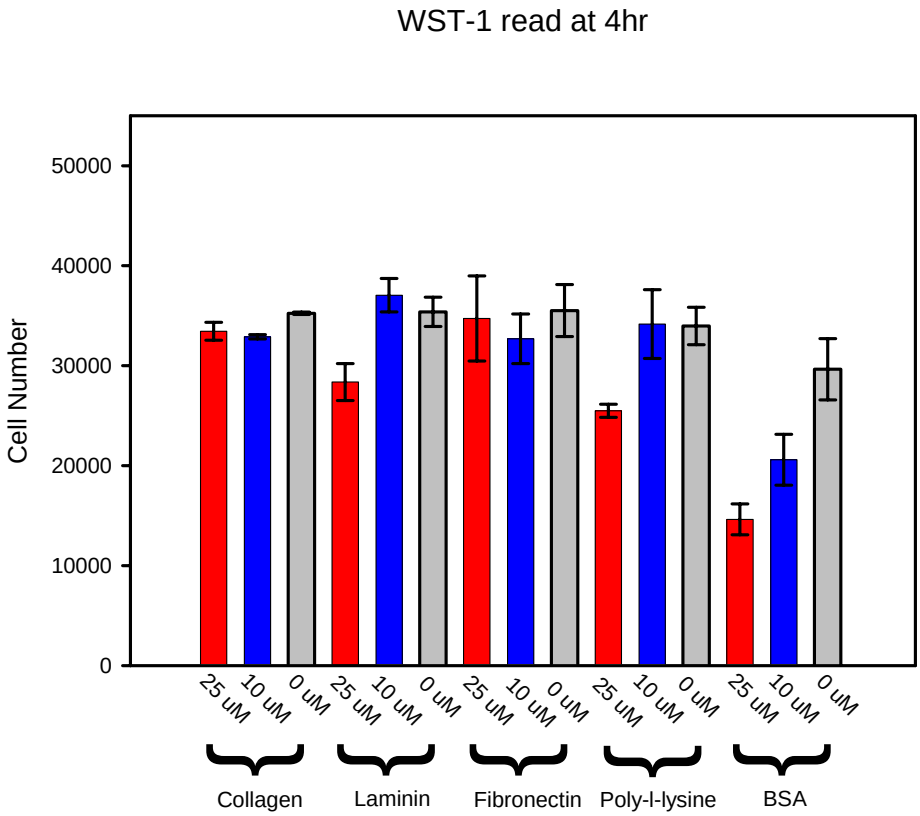

Appendix 7, Figure 2

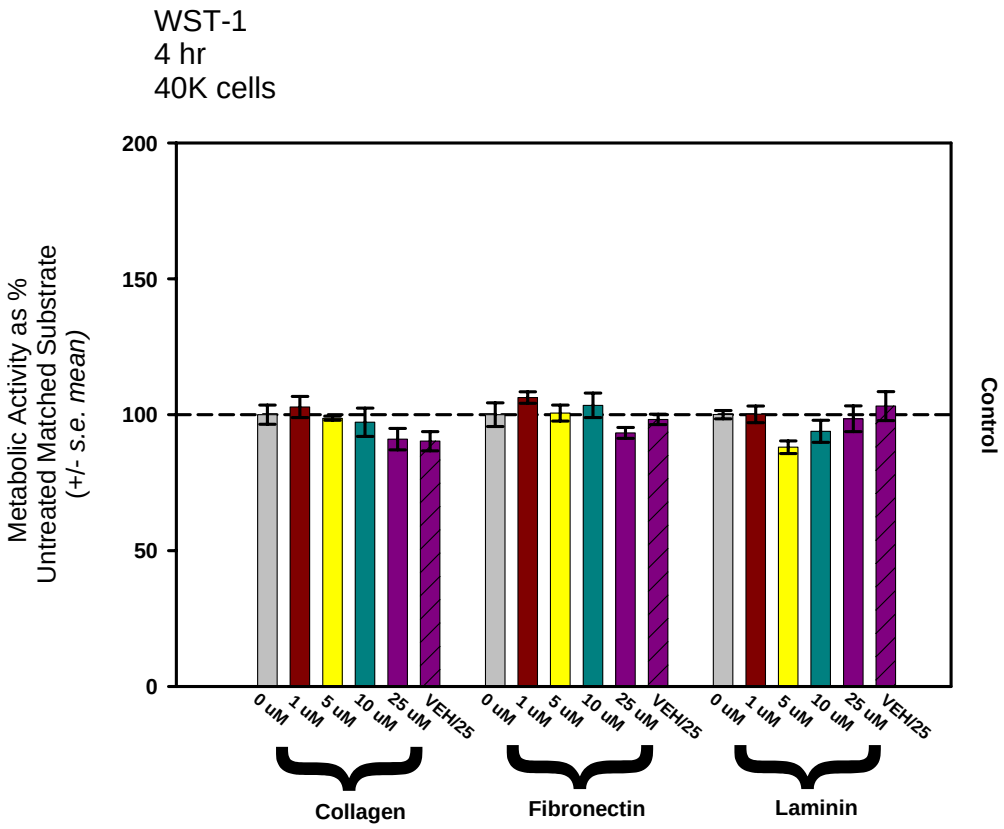

Appendix 7, Figure #3

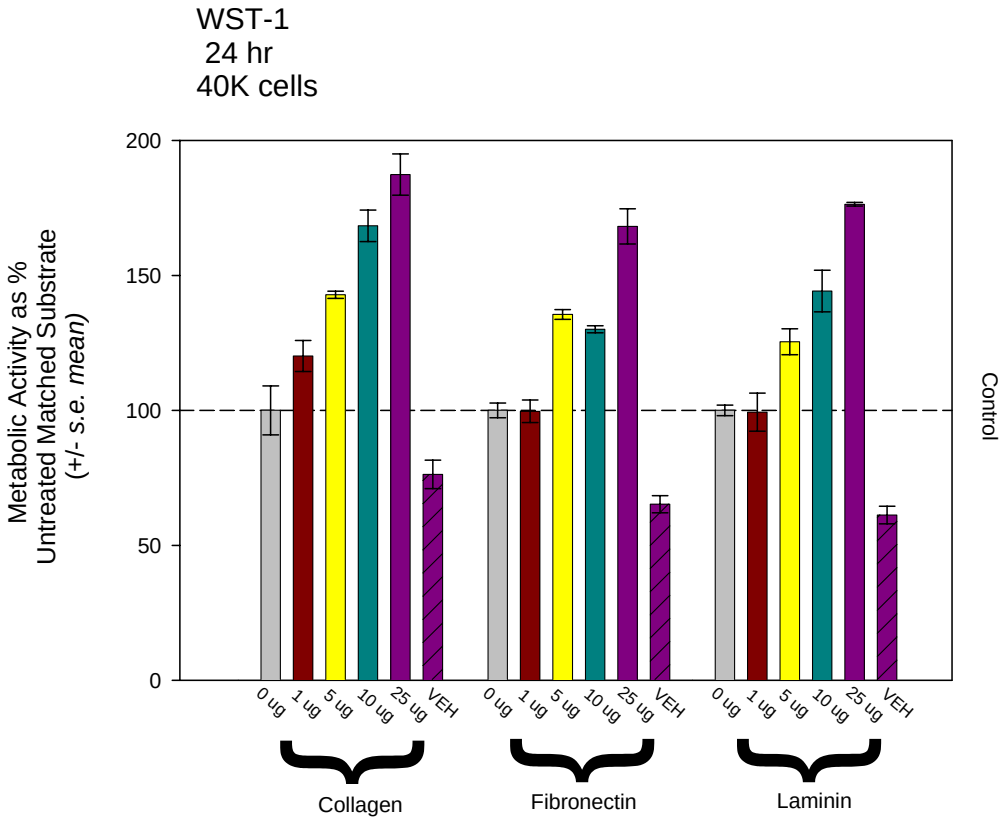

Appendix 7, Figure #4

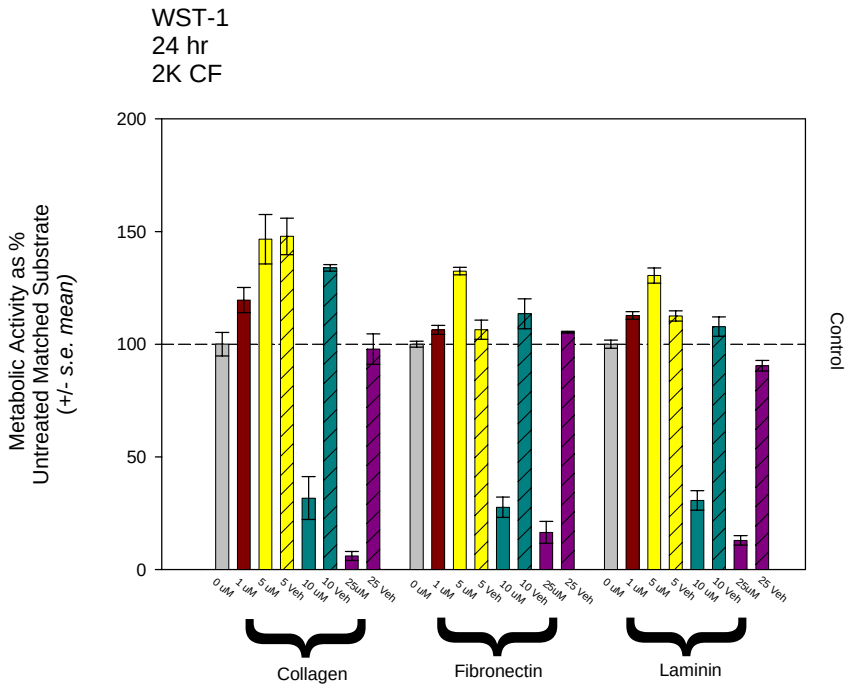

Appendix 7, Figure 5

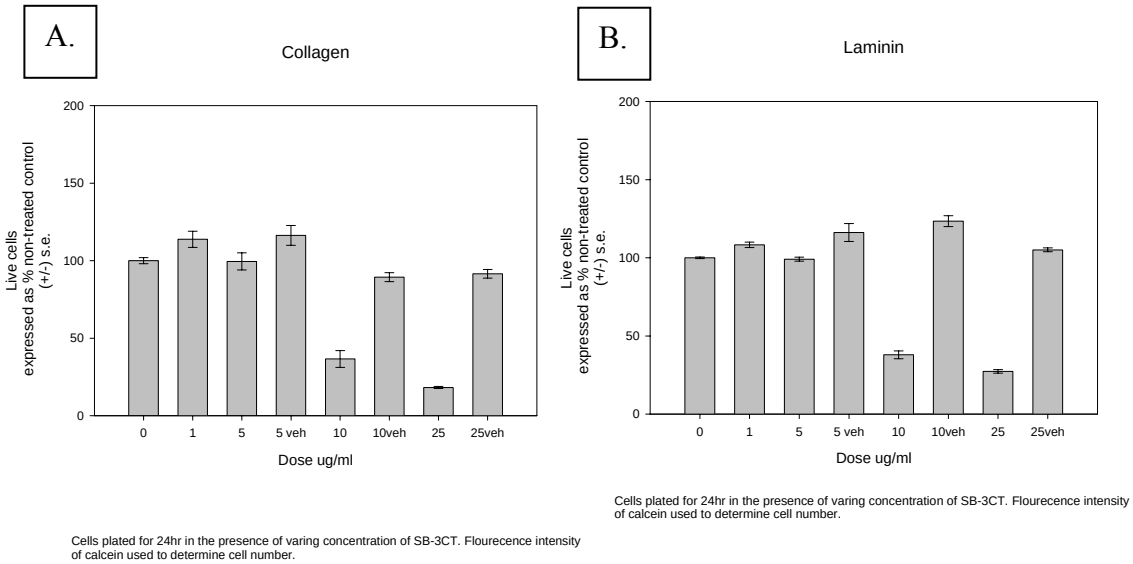

Cells plated for 24hr in the presence of varing concentration of SB-3CT. Flourecence intensity of calcein used to determine cell number.

Cells plated for 24hr in the presence of varing concentration of SB-3CT. Flourecence intensity of calcein used to determine cell number.

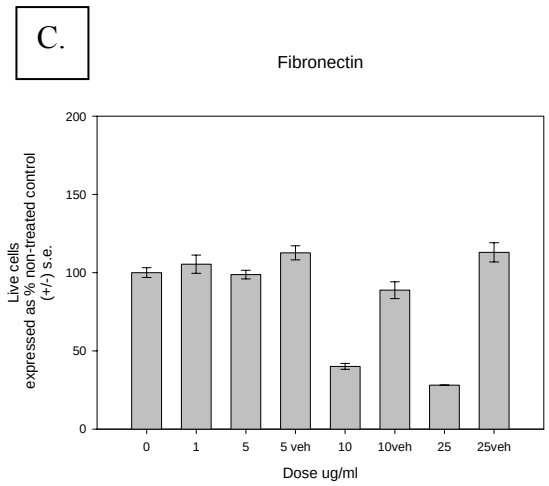

Cells plated for 24hr in the presence of varing concentration of SB-3CT. Flourecence intensity of calcein used to determine cell number.

VITA

James Russell Bowman, III born November 8, 1975 in Roanoke, Va. graduated Ravenscoft High School in 1994. In 1998, he received his Bachelor's of Science from Hampden-Sydney College, Hampden-Sydney, Va. Following a brief hiatus from being enrolled in higher education, Rusty pursued a Master's of Science in the Department of Anatomy at Virginia Commonwealth University in the laboratory of David G. Simpson. Completion of this degree in 2001 was immediately followed with matriculation in the Medical Doctorate program. Enticed by his previous research experience Rusty transferred into the combined MD/PhD program following his first semester of the medical curriculum. Both degrees are expected to be awarded in May of 2011.